

General Disclaimer

One or more of the Following Statements may affect this Document

- This document has been reproduced from the best copy furnished by the organizational source. It is being released in the interest of making available as much information as possible.
- This document may contain data, which exceeds the sheet parameters. It was furnished in this condition by the organizational source and is the best copy available.
- This document may contain tone-on-tone or color graphs, charts and/or pictures, which have been reproduced in black and white.
- This document is paginated as submitted by the original source.
- Portions of this document are not fully legible due to the historical nature of some of the material. However, it is the best reproduction available from the original submission.

GA-8705

FINAL REPORT
for
COLLISIONS OF ELECTRONS AND IONS WITH HYDROGEN ATOMS
(8 May 1967 - 7 May 1968)

Contract No. : NAS 5-11025

Prepared by
Gulf General Atomic Incorporated
P. O. Box 608, San Diego, California 92112

for
Goddard Space Flight Center
Greenbelt, Maryland

FACILITY FORM 602

N 69-16538
(ACCESSION NUMBER)

(THRU)

85
(PAGES)

1
(CODE)

CR-99265
(NASA CR OR TMX OR AD NUMBER)

24
(CATEGORY)

GA-8705

FINAL REPORT
for
COLLISIONS OF ELECTRONS AND IONS WITH HYDROGEN ATOMS
(8 May 1967 - 7 May 1968)

Contract No. : NAS 5-11025

Goddard Space Flight Center
Contracting Officer: J. L. Turner
Technical Monitor: Aaron Temkin

Work done by:

J. C. Y. Chen (Consultant)
E. M. Clarke (Summer Consultant)
E. K. Curley
R. D. Hostetler
J. William McGowan
W. Meckbach (Visiting Scientist)
W. Olson
J. F. Williams (Associated Scientist)

Report written by:

J. William McGowan

Prepared by
Gulf General Atomic Incorporated
P.O. Box 608, San Diego, California 92112

Project Manager: J. William McGowan

for

Goddard Space Flight Center
Greenbelt, Maryland

ABSTRACT

A study of 2p excitation of the hydrogen atom under electron impact is reported. The major finds have been the resonance structure just above the threshold of excitation, which was not predicted, and just below the threshold of $n = 3$, which was predicted but which for higher angular momentum states does not agree with theory. Resonance structure above $n + 3$ has also been observed.

Dissociative excitation of H_2 and D_2 has been studied under high electron energy resolution. Several new dissociation channels have been identified. Gaseous filtering techniques to be applied to radiations in the vacuum ultraviolet were studied. Some of the computer codes used on this program are given in the report, along with abstracts and papers published this year.

CONTENTS

ABSTRACT	ii
1. INTRODUCTION	1
2. NEW INSTRUMENTATION	3
3. THE 2p EXCITATION THRESHOLD	7
4. THE 2p EXCITATION IN THE VICINITY OF $n = 3$	13
5. TOTAL CROSS SECTION MEASUREMENTS	14
6. GASEOUS FILTERS	18
7. DISSOCIATIVE EXCITATION OF MOLECULAR HYDROGEN	23
8. THE THEORETICAL COMPLEMENT	27
9. DATA PROCESSING FOR ELECTRON-ATOM ELASTIC AND INELASTIC EXPERIMENTS AND A PROGRAM LISTING	29
9.1. Terminology	29
9.2. Paper Tape Format	30
9.3. Description and Instructions	30
10. OTHER COMPLEMENTARY ACTIVITIES	151
REFERENCES	156
APPENDIX I. ABSTRACTS OF PAPERS GIVEN AT SCIENTIFIC MEETINGS	I-1
APPENDIX II. PAPERS RESULTING THIS YEAR FROM THE PROGRAM	II-1

FIGURES

1. One cycle of 35 from run 39C showing the threshold region for 2p excitation. In the single cycle no feature is recognizable	5
2. The summation of 35 cycles where the sharp rise at the excitation threshold and a hint of the resonance structure just above threshold are quite evident	6
3. A sketch of the electron hydrogen atom collision region showing roughly the geometry used in the experiment	8

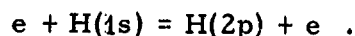
4.	The solid curve is the 2p excitation cross section calculated by Burke <u>et al.</u> for the cross section observed at 90° to the direction of the bombarding electrons. The open circles are the low resolution data (0.35 eV) of Chamberlain <u>et al.</u> for the Lyman-alpha measured at 90° to the electron path. The experimental value has been normalized to the theoretical. The data represented by the closed circles are for a resolution of 0.07 eV. They too have been normalized to the theoretical cross section but are proportional to the total cross section rather than that at 90°	9
5.	Theoretical and experimental values for the total excitation cross section in the vicinity of threshold. From threshold to 10.5 eV the statistical uncertainty is approximately ±1%. Between 11.60 and 12.20 the uncertainty is less than ±2%. For the rest of the 0.07-eV resolution data it is ~3%	10
6.	Comparison of our low resolution results with those of Long, Cox, and Smith to which our results are normalized	15
7.	A cross section for the excitation of the sum of the 3s and 3d states of atomic hydrogen. Shown for comparison are the theoretical value of Burke, Ormonde, and Whitaker and the recent experimental results of Kleinpoppin <u>et al.</u>	17
8.	A schematic diagram of the photodetector and chemical filter used in these experiments	19
9.	Relative excitation curves obtained with four different chemical filters: (a) molecular oxygen; (b) dry atomic helium; (c) dry molecular nitrogen; and (d) dry CO ₂ . The pressure in the CO ₂ filter is slightly higher than in the other filters	21
10.	The excitation curve for dissociative excitation resulting from the removal of the molecular contribution below 14 eV. This curve is generated by subtracting ~5% of the helium signal from the O ₂ curve	22
11.	A comparison of the dissociative excitation results for H ₂ and D ₂ . Also shown are a segment from the earlier Lyman-alpha excitation measurements of Fite and Brackman (FB) and a segment of the Balmer-alpha excitation curve of Burrows and Dunn (BD)	24
12.	A segment of the dissociative excitation curve near threshold, from which much of the 0.07 eV electron energy distribution is analytically removed from the curve	25

TABLE

1.	Structure in 2p excitation curve	12
----	--	----

1. INTRODUCTION

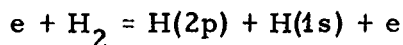
During the past year, primary attention has been focused upon the collision of highly resolved electrons with hydrogen atoms leading to the excitation of the lowest radiative state of the atom, i. e. ,



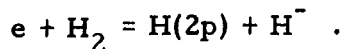
As in the case of elastic scattering of electrons from hydrogen atoms, inelastic scattering, particularly in the vicinity of the various levels of the hydrogen atom, is dominated by the formation of the temporary compound negative ion states.

In Section 3 of this report, the resonances found in the 2p channel immediately above the excitation threshold are discussed; in Section 4, those below and above the $n = 3$ level of the hydrogen atom are considered. In Section 5, a comparison is made between the measured cross section in the vicinity of threshold and the best calculated values.

Complementing the study of electrons colliding with the hydrogen atom, a study has been made of the collision of electrons with the hydrogen molecule and the subsequent dissociative excitation of the 2p state of the hydrogen atom,



in competition with



The contribution to 2p excitation from the second reaction is small. The measurements made on H_2 are unfortunately complicated by ultraviolet radiation other than Lyman-alpha which passes through the few narrow windows in the O_2 filter. In Section 6, the results of a short study of gaseous and chemical filters are discussed; in Section 7, the results of dissociative excitation are reviewed.

Since the primary purpose of the program is to test theory and to relate the results with the theory, we have been conducting under NASA's support a small theoretical program. This program is discussed in Section 8.

Because of the extreme complexity of the 2p excitation problem, we have developed a number of computer codes to process and analyze the data in next year's program. In Section 9 these codes are discussed and are thus made generally available to the scientific community. Finally, Section 10 presents a discussion of other activities that have complemented the program.

Abstracts of papers presented at scientific meetings appear in Appendix I, and articles that resulted from studies made on this program are included as Appendix II.

2. NEW INSTRUMENTATION

The apparatus used this year is essentially that used last year except for minor changes in electronics and the addition of a photo detector on a rotating table. The photo detector was designed to detect Lyman-alpha radiation. During this period two types of photon counter were used. The first was the iodine-filled Geiger counters developed some years ago in this laboratory. This was replaced by an Electromechanical Research multiplier photo tube with lithium fluoride optics. It is an 18-stage silver magnesium dynode multiplier with a potassium bromide photocathode. The geometry chosen had a side window.

The spectral sensitivity of the tube extended from 1050 Å to 1500 Å with very high sensitivity at the Lyman-alpha level (1216 Å). This new photo tube has the necessary characteristic that long wavelengths are amply rejected. The photo tube was chosen to replace the iodine-filled Geiger counter for two reasons. First, estimates indicated that the photo tube would be from a factor of 3 to 10 more sensitive than the Geiger counter. Second, since the experiments required extensive counting times, extreme reliability of all parts was necessary. It was felt that the photo tube, which has essentially infinite lifetime, would be a sensible substitute for the Geiger counter, which is unpredictable in its operating characteristics and comparatively short lived.

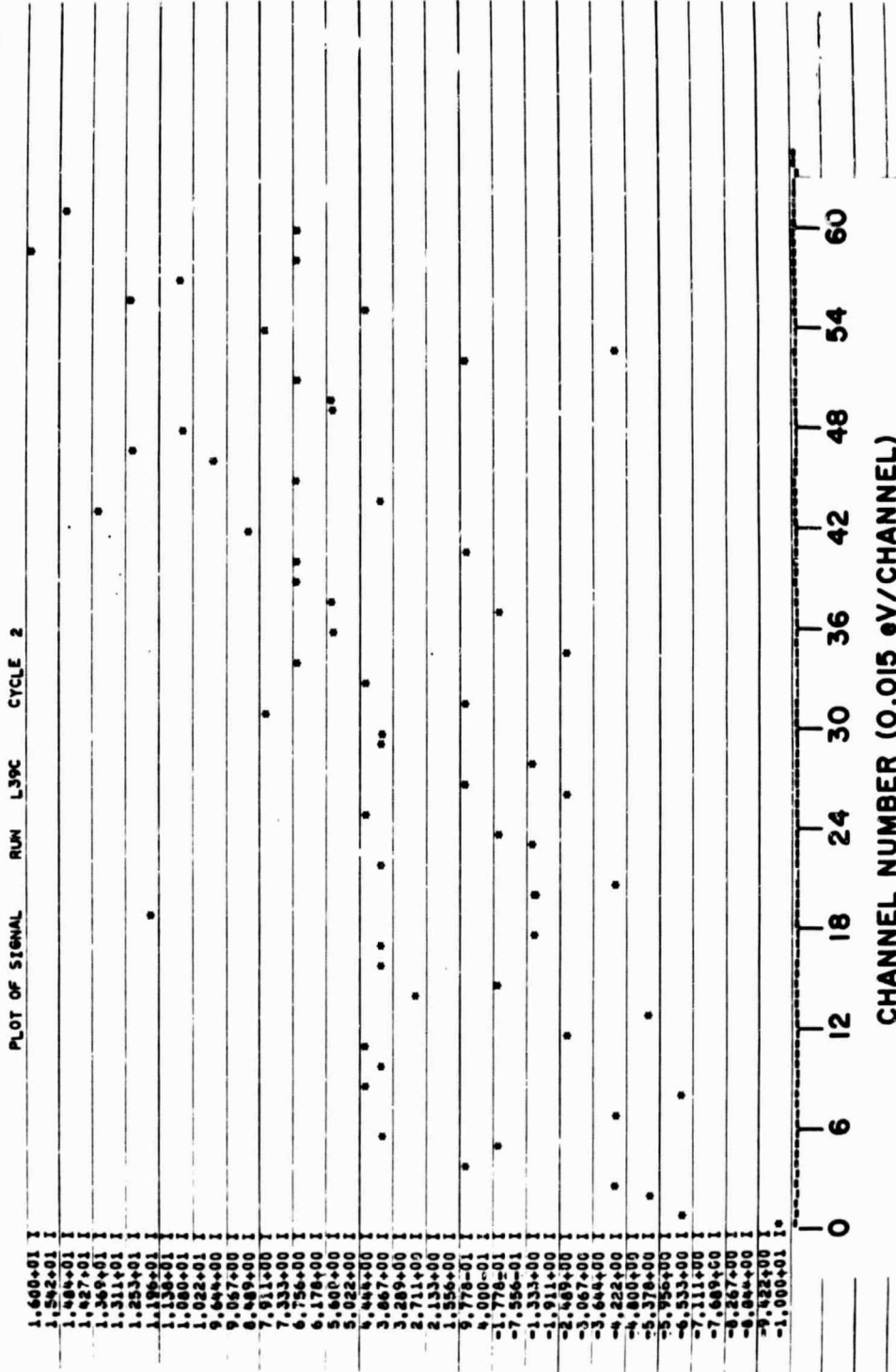
Unfortunately, the expectations for the sensitivity of this tube have not been met. At the very most, sensitivity has been increased by a factor of 2. However, since the time of its installation six months ago, the photo tube has required no service even though it has been in continuous operation for most of this time.

Between the photo detector and the interaction volume defined by the electron and hydrogen atom beams, a 1-cm-long cell with lithium fluoride windows is placed and is filled with molecular oxygen. It is a strange quirk of nature that in the absorption spectrum of molecular oxygen, one of seven very narrow windows is centered around Lyman-alpha, i. e., at 1216 Å. For the chemical (gaseous) filter to pass Lyman-alpha, the oxygen must be dry. If any moisture is present, the transmission of the cell can be greatly reduced. Consequently, dried oxygen is continuously flowed through the cell.

The experimental demands associated with the study of 2p excitation of atomic hydrogen have been excessive. The experiments have required the complete stability of the electronics, the electron beam, the hydrogen atom beam, etc., over periods well in excess of 24 hr to collect a significant number of data. In many experiments, data have been taken in 0.015-V intervals with from 60 to 100 points per cycle. For each cycle, then, the total interval is 0.9 eV for 60 data points and 1.5 eV for 100 data points. The normal counting time per data point is 1 min. If there are 60 points per cycle, the time for one cycle is 1 hr. It is interesting to compare the results that can be obtained from one cycle with those that can be obtained when a number of cycles are summed together. An example (Run 39C) is given in Figs. 1 and 2. Figure 1 shows one of 35 cycles, while in Fig. 2 all 35 cycles have been summed. In the single cycle, no feature is recognizable. In the composite Fig. 2, the 2p excitation threshold is clearly defined and the resonance near the threshold can be seen. The randomness observed below threshold gives some idea of the fluctuation of the background.

At the peak of the resonance, Fig. 2 shows approximately 300 counts for the integrated signal. One standard deviation for the (signal plus background) and background combined is approximately ± 30 counts. The resonance peak, as shown in Fig. 2 and in many of the earlier runs, was only slightly more than twice this standard deviation.

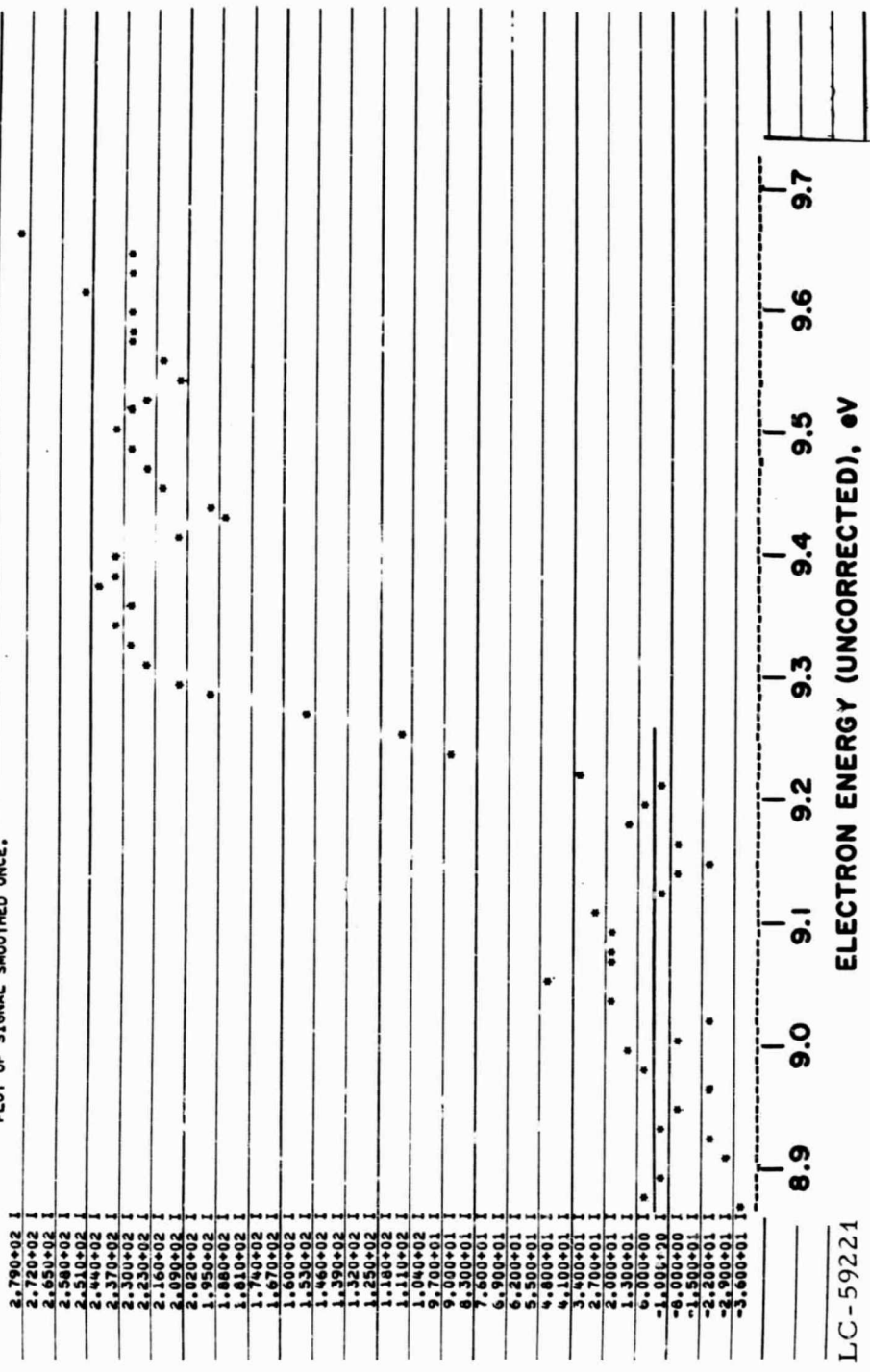
To define the first resonance above the 2p excitation threshold and to determine whether or not there are subsequent resonances, it was necessary to conduct an experiment that ran for 109 cycles. In this instance, there were 40 points per cycle. The time required for continuous running was in excess of 70 hr.



LC-59222

Fig. 1. One cycle of 35 from run 39C showing the threshold region for 2p excitation. In the single cycle no feature is recognizable.

PLOT OF SIGNAL SMOOTHED ONCE.



LC-59221

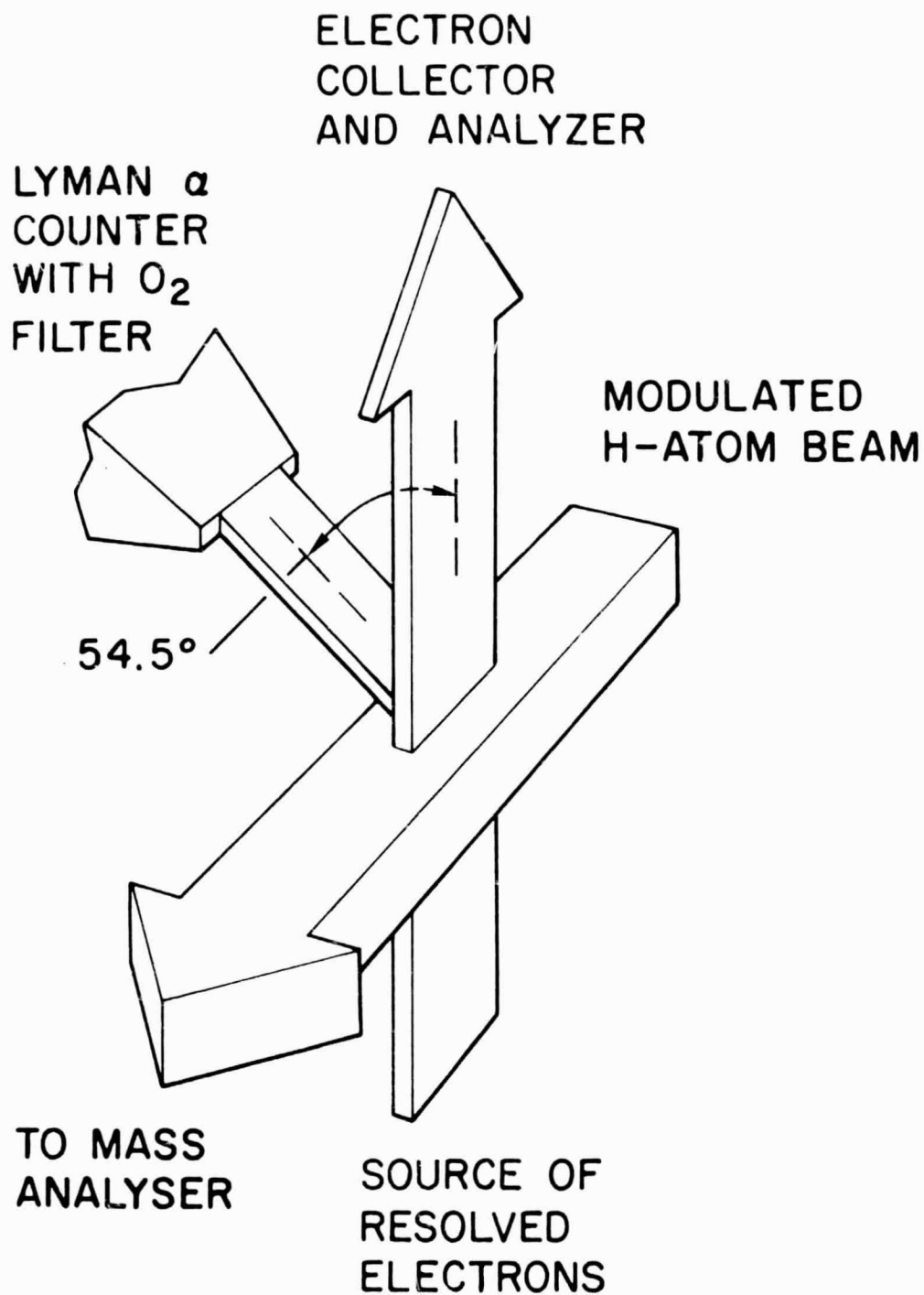
Fig. 2. The summation of 35 cycles where the sharp rise at the excitation threshold and a hint of the resonance structure just above threshold are quite evident

3. THE 2p EXCITATION THRESHOLD

In this section, we discuss the excitation of H(2p) from threshold to 0.6 eV above threshold. The collision region is shown schematically in Fig. 3. A modulated rectangular beam of hydrogen atoms nearly 90% pure is crossed with a rectangular beam of electrons with an energy distribution that ranges from 0.06 eV to 0.18 eV. Electrons from a source 127° electrostatic electron energy analyzer enter a magnetic and electric field free region, cross the modulated hydrogen atom beam from below, and pass into a collector in which a crossed electric field can be applied to collect all the electrons. When this crossed field is removed, the electrons can pass through the collector to a second electrostatic energy analyzer, where the energy distribution of the electrons is measured.

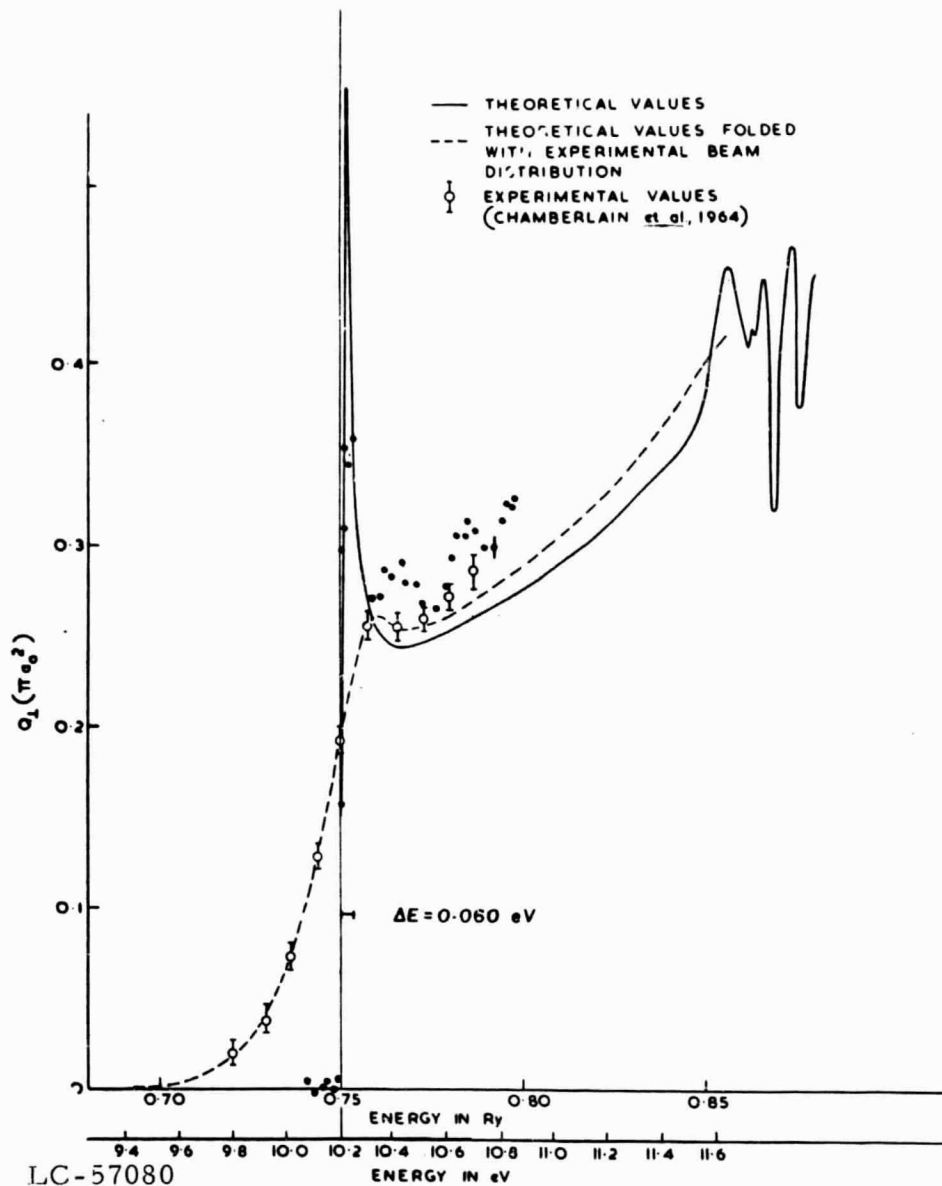
Photons from the interaction of the two beams were normally detected at an angle of 54.5° with respect to the direction of the bombarding electrons. At this angle the measured signal was proportional to the total 2p excitation cross section. (1) Ions from the interaction region were accelerated along the atomic beam axis into a Paul mass filter. As in previous experiments at this laboratory, the linear extrapolation of the ionization efficiency curve to its energy axis was used as a calibration for the electron energy scale. The data were recorded automatically over many hours, as described in Section 2. The system can be programmed to step through a prescribed energy interval. All data were collected digitally; i. e., for each energy interval, the signal plus background (S+N), the background (N), and the electron current were recorded on punched tape to be processed later by the computer. Every 8 to 12 hr, the excitation process was interrupted and an ionization efficiency curve for atomic hydrogen was taken to help fix the electron energy scale for excitation. Over more than 100 hr, in many instances the reproducibility of the onset of the ionization efficiency curves was within ± 0.015 eV.

In Fig. 4, the total cross section measurements near threshold are compared with theory⁽²⁾ and with the previously reported results of Chamberlain et al.⁽³⁾ This comparison is made primarily to show the difference between the resolutions of the two experiments and the width of the structure that one is looking for compared with what has been observed experimentally. In the left-hand portion of Fig. 5, theoretical results are compared with the theoretical predictions wherein the energy



LC-61849

Fig. 3. A sketch of the electron hydrogen atom collision region showing roughly the geometry used in the experiment



LC-57080

Fig. 4. The solid curve is the 2p excitation cross section calculated by Burke et al. for the cross section observed at 90° to the direction of the bombarding electrons. The open circles are the low resolution data (0.35 eV) of Chamberlain et al. for the Lyman-alpha measured at 90° to the electron path. The experimental value has been normalized to the theoretical. The data represented by the closed circles are for a resolution of 0.07 eV. They too have been normalized to the theoretical cross section but are proportional to the total cross section rather than that at 90° .

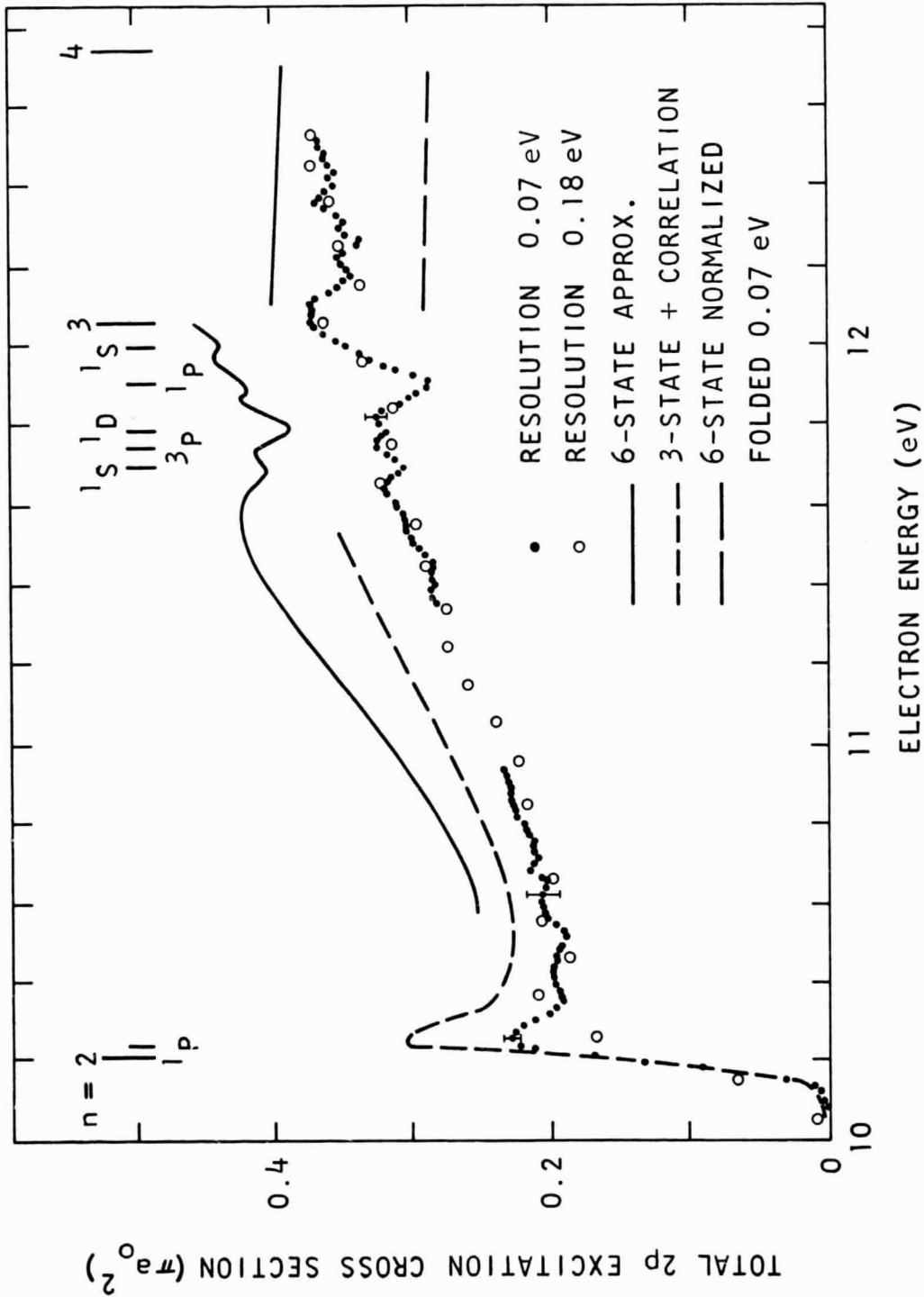


Fig. 5. Theoretical and experimental values for the total excitation cross section in the vicinity of threshold. From threshold to 10.5 eV the statistical uncertainty is approximately $\pm 1\%$. Between 11.60 and 12.20 the uncertainty is less than $\pm 2\%$. For the rest of the 0.07-eV resolution data it is $\sim 3\%$.

distribution, approximately 0.07 eV, has been folded into the theoretical curve. As can be seen, the agreement between the measured and predicted shapes of the first resonance is good. It follows, then, that the excitation cross section does consist of a sharp rise, as predicted by Damburg and Gailitis, ⁽⁴⁾ from a close-coupling approximation calculation that includes the three lowest hydrogen atom states, 1s, 2s, and 2p. It is also clear from our measurements that the sharp resonance predicted by Taylor and Burke, ⁽⁵⁾ who also used a close-coupling approximation, does really exist within 0.03 eV of threshold. Burke and his associates have shown that the total flux of this resonance is in the ¹P channel of the H⁻ compound state. This resonance unfortunately was not recognizable in the previous calculations of Damburg and Gailitis because of the coarseness of the energy grid used by them.

In the experimental results immediately following the first resonance, there appear to be at least two other broad resonance structures. Although these structures have been recognized from our earliest measurements, it was only recently that the statistics were good enough to permit us to say definitely that they exist. It was also necessary to make certain that these small structures were not due to the excitation of some countable ultraviolet from the collision of electrons with the residual H₂ in the system. Table 1 lists the positions of the most prominent structures; however, one must remember that these positions may not correspond exactly to the positions of the resonances themselves, but rather to the resonances with the electron energy distribution folded into them.

The use of the finite number of terms in the close-coupling expansion used to describe even these lowest states may be subject to some question since it is not clear how quickly the expansion converges. In the case of the elastic scattering resonances below the first inelastic threshold $n = 2$, there is every indication that the convergence is rapid. However, it is not yet clear that the ¹P "shape" resonance described by the three-state approximation above $n = 2$ is not better described by an expansion that includes the first six or more states of the hydrogen atom. Unfortunately, Burke et al. ⁽²⁾ have carried out their six-state approximation calculations only from just below the $n = 3$ level down to within 0.2 eV of the 2p excitation threshold. Over the range where the three- and six-state approximations overlap, i. e., in the region from 0.2 to 1.0 eV above the 2p threshold, the six-state calculation gives a cross section value approximately 8% lower than that given by the three-state approximation.

Another calculation reported by Taylor and Burke ⁽⁵⁾ has been carried out using the close-coupling approximation that includes the first three states of the hydrogen atom and potential terms that describe the electron-electron interaction (correlation) as a power series of terms involving r_{12} ,

the distance between the two electrons. Over the same energy range as taken above, the later calculation gives a cross section value that is approximately 20% below that given by the three-state approximation. Near threshold, the correlation terms have now shifted the calculated resonance closer to the threshold and have considerably reduced its width. This is in keeping with the experimental finding. The need for more work on the theory has recently been recognized by Damburg and Geltman, ⁽⁶⁾ who indicate that another possible source of incompleteness results from the lack of the inclusion of polarization terms of order α/r^4 . In the case of 2s excitation, the inclusion of polarization has had a marked effect on the calculated cross section.

TABLE 1
STRUCTURE IN 2p EXCITATION CURVE

Energy	Description of Structure	Comments
10.20 ± 0.02	Steep slope	Onset
10.29 ± 0.02	First max	Predicted ¹ P "shape" resonance
10.45 ± 0.03	Second max	
10.65 ± 0.03	Third max	
11.65 ± 0.03	Small min	Predicted ¹ S resonance
11.77 ± 0.02	Possible min	Predicted ¹ D resonance
11.89 ± 0.02	Large min	Predicted ¹ P resonance
12.06 ± 0.04	Broad max	"Shape" resonance at n = 3 threshold
12.16 ± 0.05	Min	
12.23 ± 0.05	Small max	
12.35 ± 0.05	Small max	

4. THE 2p EXCITATION IN THE VICINITY OF $n = 3$

Figure 5 shows details of the experimental cross section from 11.35 eV to 12.55 eV. This region overlaps the $n = 3$ threshold. Bridging the two threshold regions are low resolution measurements. Just below the $n = 3$ threshold can be seen several recognizable resonances, the most predominant of which appears near 11.88 eV. A smaller resonance appears in the vicinity of 11.65 eV. Also shown in the figure is the calculation for the six-state approximation showing a number of resonances. Folded into the calculated cross section is the experimental energy distribution, which is approximately 0.07 eV. The agreement between theory⁽²⁾ and experiment is not considered good for the 1P resonance, while for the 1S resonances the agreement is thought to be quite satisfactory.

At and above the threshold of $n = 3$ can be seen a prominent bump, which is most likely associated with a "shape" resonance just above the $n = 3$ threshold. Part of the flux for this resonance appears directly in the 2p channel. Another portion, most likely the largest part, arrives through cascade from the 3s and 3d states of the atom. The positions of the resonance structure below and above the $n = 3$ level are included in Table 1.

5. TOTAL CROSS SECTION MEASUREMENTS

Since it is impossible to measure the cross section absolutely, we have determined it from a normalization to the Borne approximation at energies in excess of 200 eV. Although this procedure is not entirely satisfactory, at present there is no simple method available for making an absolute determination. Data have been taken between the 2p excitation threshold and 200 eV; the most precise data, however, have been taken below 60 eV. In fact, continuous data have been taken every 0.1 V from 60 eV until threshold. We have found the most precise way to determine our cross section is to normalize our data to those of Long, Cox, and Smith, who in turn have normalized theirs to the Born approximation. The relative accuracy of their data is $\pm 2\%$.

Although we have not been able to assign to our data relative accuracies as small as this, we have compared our data with those of Long, Cox, and Smith (see Fig. 6). The cross sections defined by the two sets of data points are indistinguishable. It is interesting to note in our data that the finite excitation threshold is recognizable just above 10.2 eV, even though the resolution in this experiment is only 0.18 eV. Also, one can see a hint of the resonance structure in the vicinity of $n = 3$ and in the continuously taken data below $n = 4$.

To obtain an accurate estimate of the cross section in the threshold region, the high resolution data were subsequently normalized to the lowest resolution data, thus fixing the cross section scale. The values of the cross section given in Fig. 4 were fixed in this way. It is interesting to note that the cross section thus obtained is only 80% of the lowest cross section predicted. The approximation used to arrive at the cross section closest to the experimental value is the three-state close-coupling approximation, which includes 20 electron-electron correlation terms.

Quite recently, Fite *et al.* ⁽⁸⁾ have determined that the Lyman-alpha radiation emitted by hydrogen 2s atoms in a weak electric field is polarized. Consequently, all earlier measurements or estimates of the 2s excitation cross section are in error since no allowance was made for this polarization. Once the cross sections have been corrected for the polarization, at the cross section maximum, which is in the vicinity of $n = 3$, the value obtained is only 80% of the lowest predicted cross section resulting from the six-state close-coupling approximation.

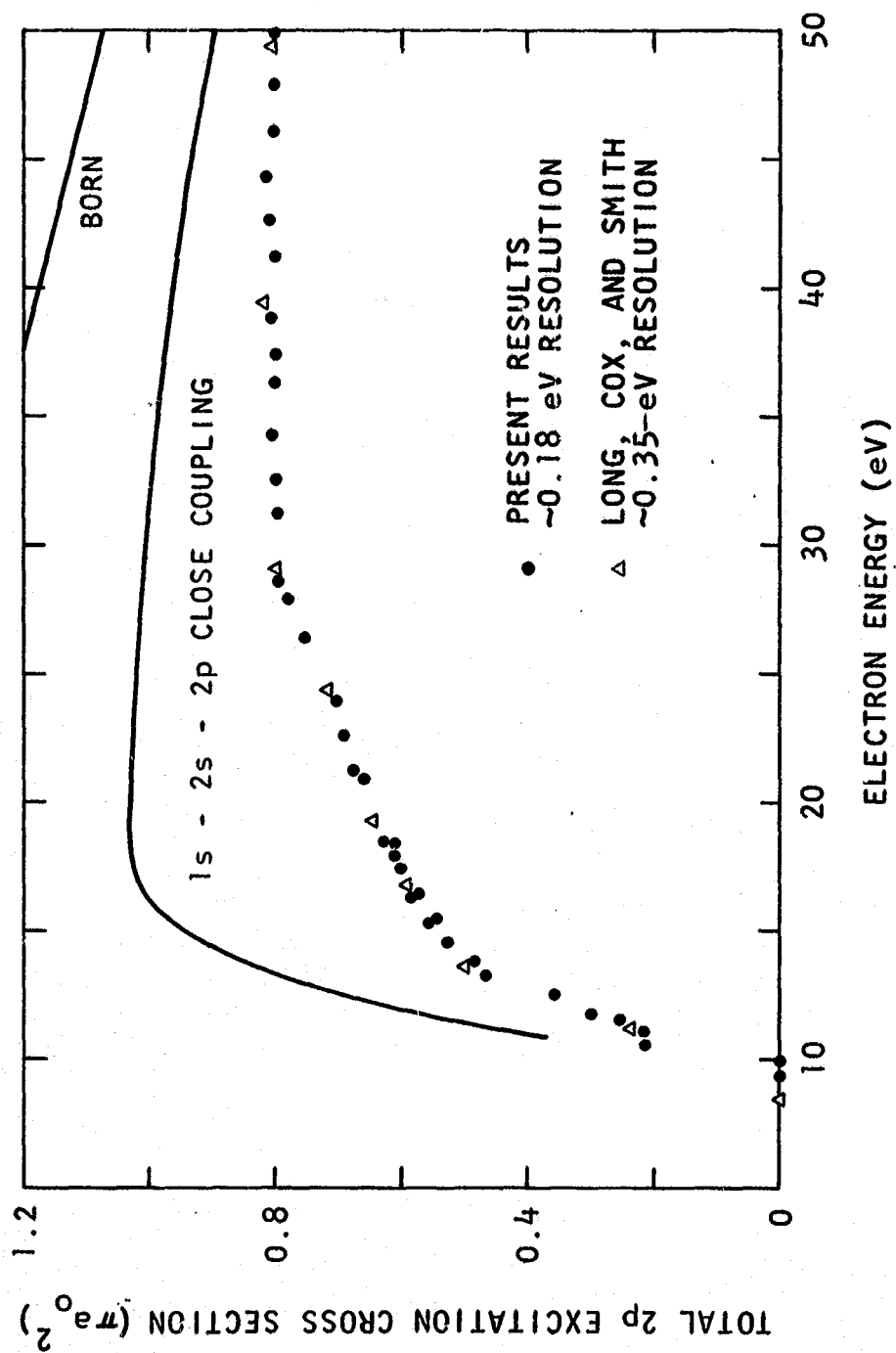


Fig. 6. Comparison of our low resolution results with those of Long, Cox, and Smith to which our results are normalized

It is an informative exercise to estimate the size of the combined excitation cross section for the 3s and 3d states of atomic hydrogen. These data are reflected in the total cross section measurements for the production of the Lyman-alpha radiation since the 3s and 3d cross sections can only couple with the ground state by passing through the 2p state. Although our total excitation cross section for the 2p state does not agree in absolute magnitude with that predicted by Burke et al., it is quite obvious that below the $n = 3$ level the general shape of the measured and calculated cross sections is the same. Consequently, there is some justification in normalizing the magnitude of the calculated cross section to that of the measured cross section in the region just above the $n = 2$ level. Having done this, we observe that the calculated portion of the cross section for the 2p state above $n = 3$ is considerably lower than the total measured cross section (Fig. 5, broken line above $n = 3$). To a first and perhaps crude approximation, the difference between the measured and normalized theoretical curves can be said to be due to cascade. This difference is shown in Fig. 7. No attempt has been made to include any contribution for the shape resonance above $n = 3$ in the calculations or to allow for the addition of states above $n = 4$ in the theory.

It is now possible to compare this difference with the predicted cross sections of Burke et al. As shown in Fig. 7, the agreement between experiment and theory is satisfactory. In fact, even with this crude approximation in which no attempt has been made to account for polarization or other factors, as in the case of 2p excitation, the value of the estimated cross section again lies slightly below that of the predicted cross section. This result is not at all in agreement with the recently published data of Kleinpoppen and Krase⁽⁹⁾ for Balmer-alpha excitation. Since our result depends upon a normalizing of the six-state approximation to the results below $n = 3$, we hesitate to say their result is in error. Furthermore, it is not clear that the six-state approximation necessarily gives an accurate description of the region above $n = 3$, although it seems reasonable that it is not in error by much.

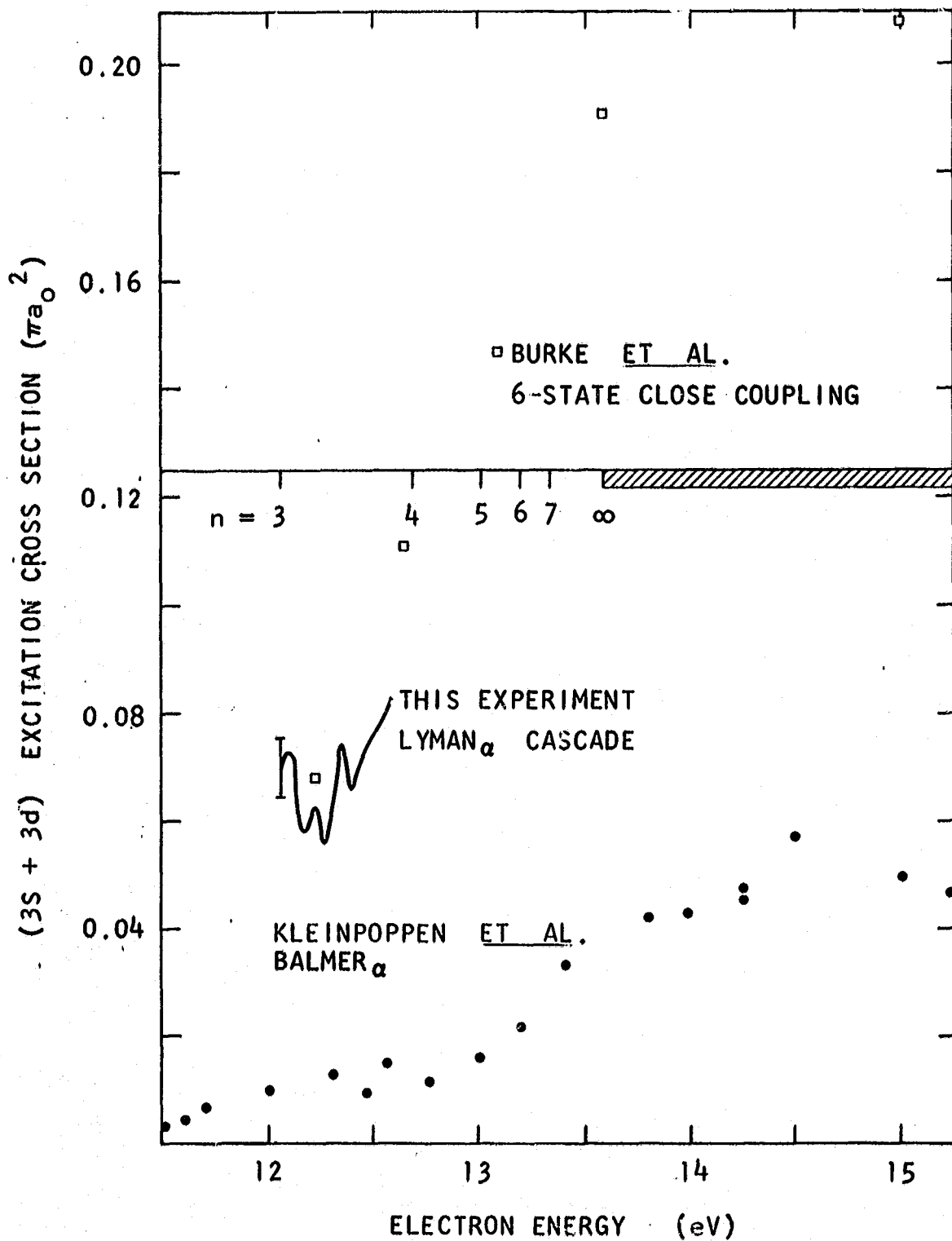


Fig. 7. A cross section for the excitation of the sum of the 3s and 3d states of atomic hydrogen. Shown for comparison are the theoretical value of Burke, Ormonde, and Whitaker and the recent experimental results of Kleinpoppen et al.

6. GASEOUS FILTERS

One of the most important problems associated with the study of the excitation of atomic hydrogen is the unequivocal detection of Lyman-alpha (1216 Å). Provided a large enough signal is available from the experiment, one can use a vacuum ultraviolet spectrometer. However, in experiments such as those performed in this laboratory where the number of photons available is very small, it becomes absolutely necessary to have the largest possible collection efficiency and reasonably large angle of acceptance. It has long been recognized that the Geiger counter, filled with either nitric oxide or iodine and with lithium fluoride optics, could be used to detect vacuum ultraviolet radiation in the vicinity of Lyman-alpha. However, to ensure the unequivocal detection of the Lyman-alpha and particularly to eliminate the molecular radiation normally associated with the bombardment of residual H₂ in the experiment, it was necessary to find a filter that would preferentially pass the 1216 Å radiation.

It was observed by Watanabe⁽¹⁰⁾ and others that in the absorption spectrum of O₂ in the vacuum ultraviolet and in the vicinity of 10 eV there are seven very deep transmission windows, one of which is centered at the Lyman-alpha. It has been the repeated observation in our laboratory that in the study of the excitation of atomic hydrogen to the $n = 2$ level, the combination of the chemical filter filled with oxygen and either a Geiger counter or a photomultiplier has been an effective detector of Lyman-alpha. However, in the study of the dissociative excitation of H₂, either by proton or electron impact, it has been recognized that there is a large contribution of molecular radiation, which passes either through the other windows or through the optically thick portion of the chemical filter.

To effectively study the dissociative excitation process it is therefore necessary to eliminate this background radiation. To do this, a series of experiments was carried out in which different gases were used as the optical filter. In Fig. 8 we show a schematic diagram of our experiment. In all cases the gases used in the chemical filter flowed through the filter continuously. However, in the case of CO₂ the rate of flow was much slower than in the cases of nitrogen, helium, and oxygen, which were virtually the same. The pressure in all filters was slightly in excess of 1 atm.

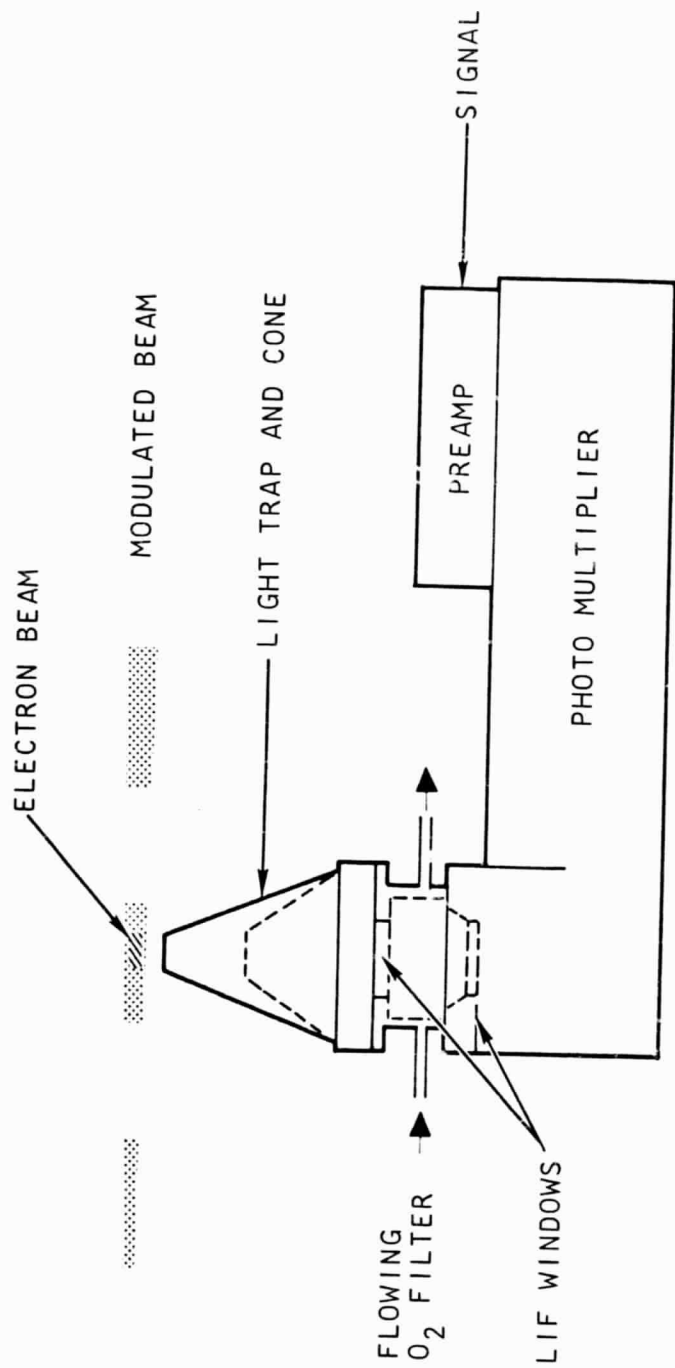


Fig. 8. A schematic diagram of the photodetector and chemical filter used in these experiments

In Fig. 9 we show the relative number of photons reaching the counter as a function of electron energy when electrons bombard H_2 . Four different gases have been used in the chemical filter. The electron energy for these experiments ranges from approximately 10 to 20 eV, an interval which embraces the onset of the molecular radiation at approximately 10.3 eV and the onset of dissociative excitation in the vicinity of 14.7 eV. Figure 9 shows the results when the O_2 filter was used. The onset of the molecular radiation is clearly visible at 10.3 eV, as is the onset of the dissociative excitation of the hydrogen atom in the $2p$ state near 14.7 eV. From this curve alone we can judge that, once we have moved a few electron volts from the threshold of dissociative excitation, the molecular contribution to the total curve is in the vicinity of 20%. Near threshold for dissociative excitation, of course, the molecular contribution is proportionately larger. Looking at Fig. 9, one can see virtually no difference in the magnitude and shape of the curves for He and N_2 (b and c, respectively), verifying what we already know, i. e., that both He and N_2 are transparent in this optical region.

Now that we recognize in curve (a) the onset of the dissociative excitation, we can use curves (b) and (c) to estimate the relative contribution of Lyman-alpha and other molecular radiation as seen by the counter. A reasonable extension of the curve, from below the dissociative excitation threshold to above, gives us this information. Above approximately 16 eV we estimate that the radiation from dissociative excitation is in the vicinity of 20% of the total radiation. This estimate, of course, is approximate, but it is reasonable. In curve (d) the complicated absorption spectrum of CO_2 is seen reflected in the structure of the curve.

To generate Fig. 10, the helium curve has been normalized to the O_2 curve in the vicinity below 14 eV and the helium curve has been subtracted from the O_2 curve in this region. The residual signal is shown in Fig. 10. The fine structure below 14.7 eV appears to be real for it is present in the curves when either helium or nitrogen is subtracted from the oxygen data. In both cases there is a sharp onset in the vicinity of the dissociative excitation threshold. It is interesting to note that above 16 eV, structure is quite pronounced in the curve.

It must be realized that by subtracting the helium (or nitrogen) data from the O_2 data, we have eliminated part of the dissociative excitation signal in the vicinity above the dissociative excitation threshold. However, this is small (20% of 20%), approximately 4% of the total signal. From this study it is clear that the estimates of the total cross section made earlier by Fite and Brackmann⁽¹⁾ are high by approximately 20%.

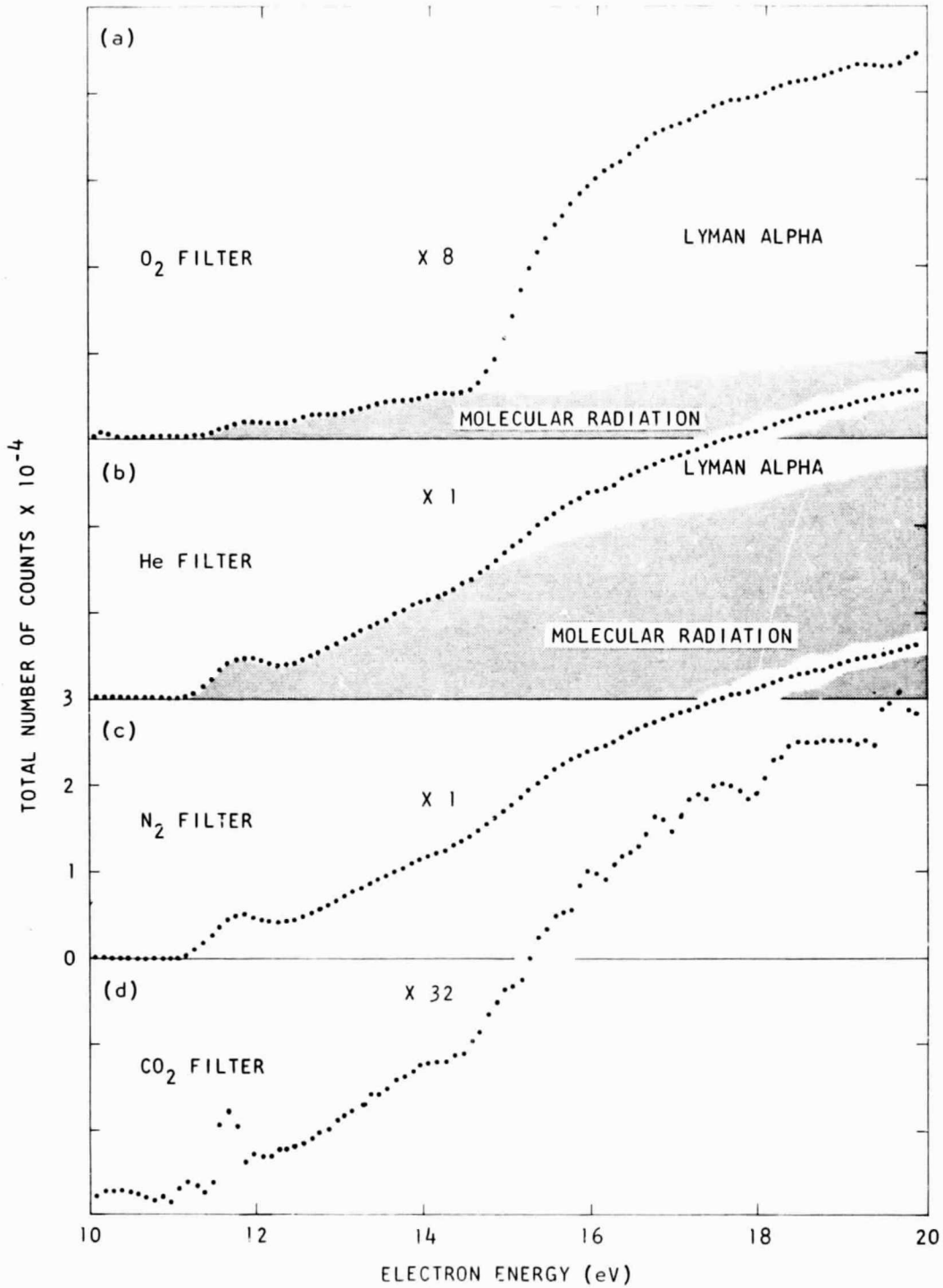


Fig. 9. Relative excitation curves obtained with four different chemical filters: (a) molecular oxygen; (b) dry atomic helium; (c) dry molecular nitrogen; and (d) dry CO₂. The pressure in the CO₂ filter is slightly higher than in the other filters

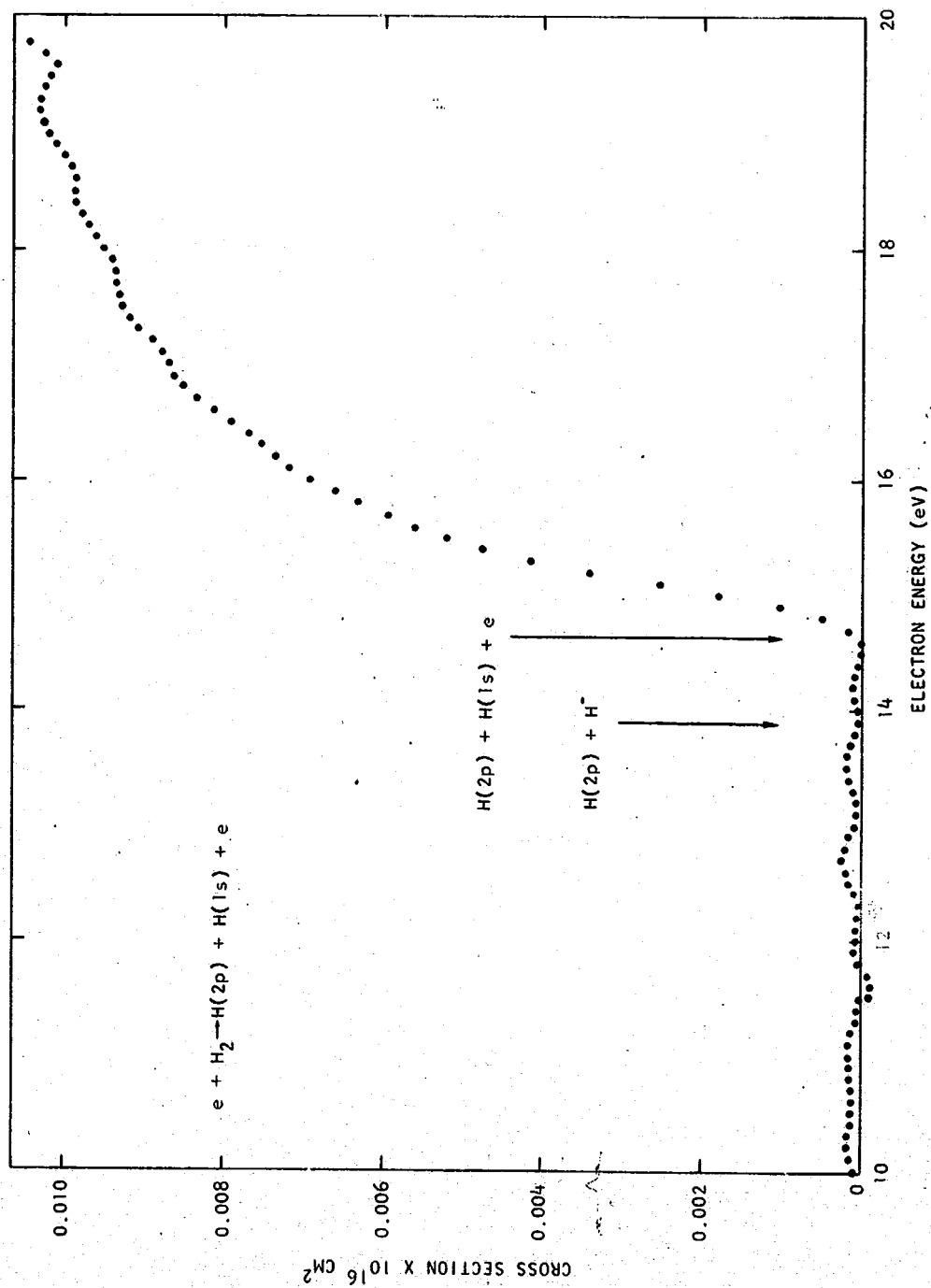


Fig. 10. The excitation curve for dissociative excitation resulting from the removal of the molecular contribution below 14 eV. This curve is generated by subtracting $\sim 5\%$ of the helium signal from the O_2 curve

7. DISSOCIATIVE EXCITATION OF MOLECULAR HYDROGEN

From the discussion in Section 6, it is clear that the originally reported value for the dissociative excitation of the 2p state of atomic hydrogen from H_2 was in error due to a large contribution of molecular radiation coming from the interaction region. As can be seen in Fig. 11, the cross section for H_2 is nearly 20% lower than the original measurements of Fite and Brackmann. (1) It is also clear from Fig. 11 that the dissociative excitation of D_2 has a cross section that is only 90% of that of H_2 . This isotope effect is in keeping with the predictions of Platzman, (11) who pointed out that there are a number of molecular states that lie above the first ionization potential. In general, there are two major deexcitation paths available for such excited states, autoionization and predissociation. The first of these processes is nearly mass independent; the time for it therefore should almost be independent of isotope substitution. The time required for dissociation depends on the velocity with which the particles separate and therefore is strongly mass dependent. A similar isotope effect has recently been reported by Burrows and Dunn (12) and by Vroom and deHeer. (13) Shown also in Fig. 11 is the maximum of the Balmer-alpha excitation curve of Burrows and Dunn. The shape of the curve is very similar to our H_2 curve.

In our preliminary data, the break in the total excitation curve in the case of H_2 is at a higher potential than in the case of D_2 . It is clear from the figure that in the case of D_2 the channel that includes excitation plus proton formation does not play a major role, whereas in the case of H_2 the onsets of both the formation of two excited states and the formation of the (2p) atom plus a proton are below the major structure that appears in our curve. No doubt this is associated with the isotope effect, details of which are not yet completely understood.

In Fig. 12 we show the excitation curve near threshold. The data shown are only relative. This curve is one from which the energy distribution of our beam has been largely removed. Three sets of data are overlapped. The structure that appears at the end of the first also appears in the beginning of the second; similarly, the structure that appears at the end of the second appears in the beginning of the third. The onset is in the vicinity of 14.7 eV. There follows a rather straight portion of the curve with very little structure. Then, in the vicinity of 15.8 eV the onset of nearly 12 small ripples, which are fairly evenly spaced, is seen. The spacing between the

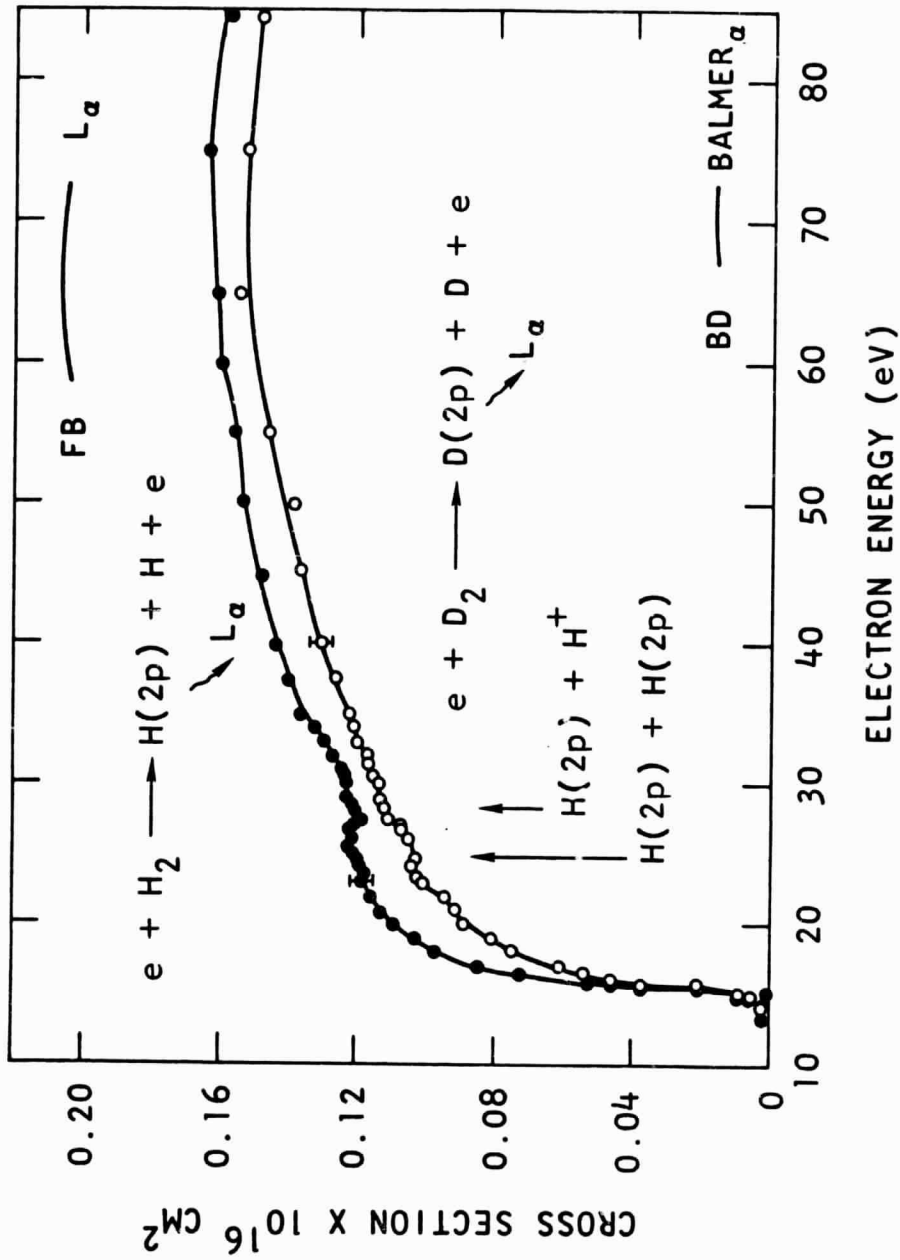


Fig. 11. A comparison of the dissociative excitation results for H₂ and D₂. Also shown are a segment from the earlier Lyman-alpha excitation measurements of Fite and Brackmann (FB) and a segment of the Balmer-alpha excitation curve of Burrows and Dunn (BD)

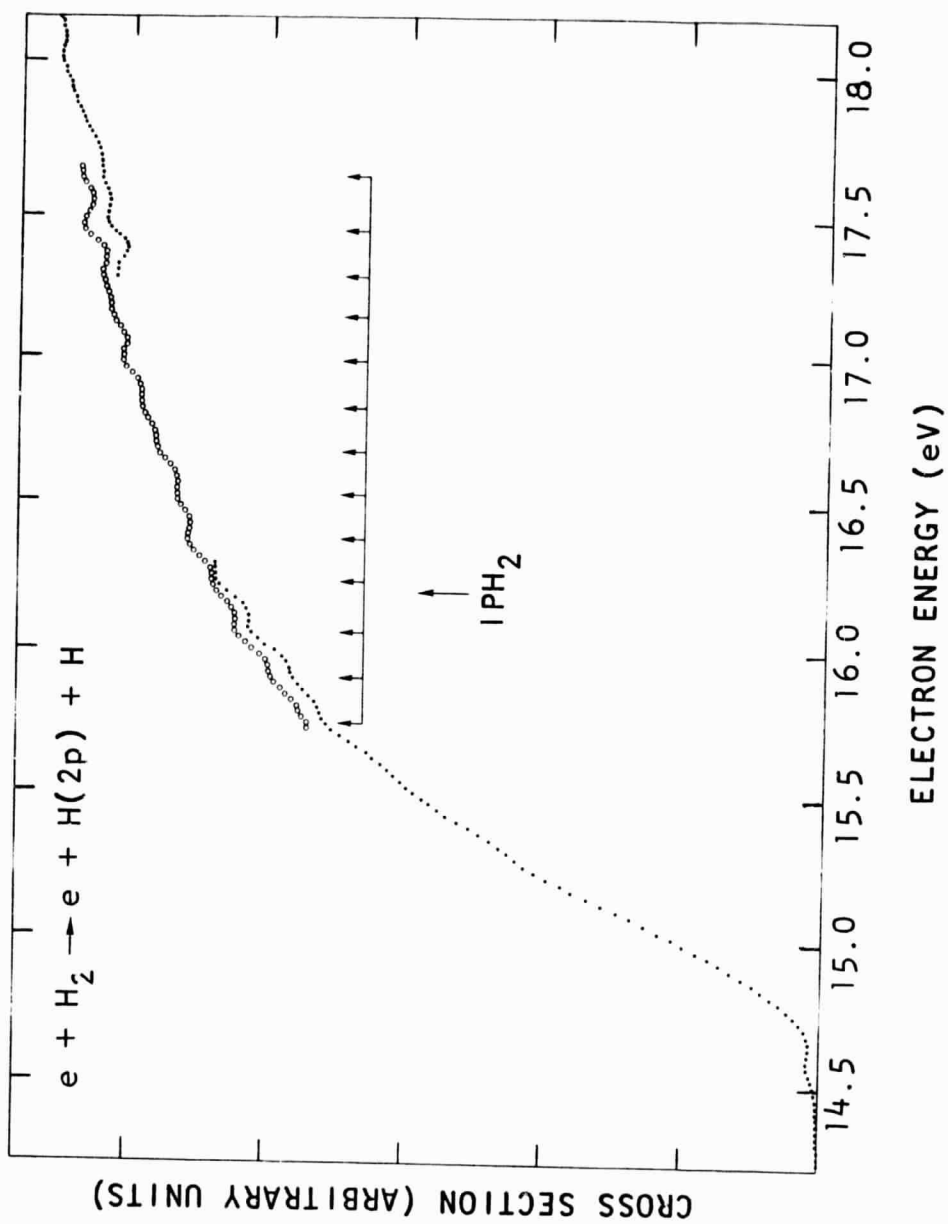
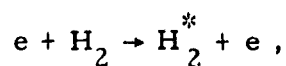
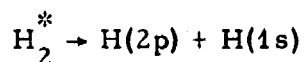


Fig. 12. A segment of the dissociative excitation curve near threshold, from which much of the 0.07-eV electron energy distribution is analytically removed from the curve

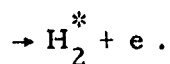
ripples is in the vicinity of 0.14 to 18 eV. This series of ripples shows a change above the ionization potential, 15.43 eV. In fact, the continuous ripple form goes on until nearly 17.8 eV, the dissociation limit of H_2^+ . Above this the nature of the structure changes, and the orderliness seems to disappear. The larger ripples which are apparent in Fig. 10 then seem to dominate. The cause of this structure is not completely understood. It is possible, although not likely, that it is due to the structure in the molecular radiation in the background of our signal, which has not been completely removed. If, however, this structure is related to the dissociative excitation of H_2 into the 2p channel, then one is prompted to suggest either that it results from a temporary formation of an H_2^* compound state, which decays into several modes, one the dissociative channel and the other the excitation of molecular levels, or that it reflects competition between predissociation and autoionization, i. e. ,



followed by



competing with



8. THE THEORETICAL COMPLEMENT

During this contract period, Professor J. C. Y. Chen, University of California, San Diego (UCSD), has participated in our study of electron hydrogen collisions. His activities at Gulf General Atomic and at the University have covered the following subjects:

1. The application of Faddeev's equation to a number of atomic problems
 - a. (e-H) elastic scattering resonances
 - b. (e-H) excitation threshold
 - c. (e⁺-H) elastic scattering and positronium formation
2. Close-coupling calculations (or the (e-H) system in momentum space)
3. Electron resonance scattering from molecules

Work is also under way at UCSD on a new variational calculation for (e-H) scattering and on the field detachment of H⁻.

Included in Appendix II is an article that resulted from these studies. In it, Ball, Chen, and Wong have investigated various solutions of the Faddeev equation for Coulomb potentials, and a practical method for solving the Faddeev equations below the three-particle breakup threshold is developed. The method is then applied to the (e, H) system in which the H⁻ bound state and the lowest members of the compound states in both the singlet and triplet series are calculated. The calculated position of the lowest ¹S resonance is in excellent agreement with the experiment, while the width of the lowest ¹S resonance is slightly less than that found experimentally.

Also during this contract year, with the support of NASA and Gulf General Atomic, a series of colloquia on atomic and molecular processes (CAMP) has been conducted. Many of the colloquia were given by people who are actively participating in electron proton and positron hydrogen atom scattering studies. A list of colloquia speakers and their topics is given in Section 10.

This spring a two-day "working session" on electron hydrogen atom collisions was held in La Jolla. The primary purpose of this session was to consider the programs presently under way and to determine what information could best be obtained from experiment to direct further theoretical studies. The program for this successful working session is also listed in Section 10.

9. DATA PROCESSING FOR ELECTRON-ATOM ELASTIC AND INELASTIC EXPERIMENTS AND A PROGRAM LISTING

The output data from the experimental devices are on punched paper tape. In order to process these data using the 1108 FORTRAN IV programs, the data first must be converted to punched cards or magnetic tape. Because of the ease in handling, storing, etc., the latter was chosen. To aid in understanding the descriptions and the instructions for the use of the various programs involved, a brief listing of terms and definitions is presented below.

9.1. TERMINOLOGY

Paper Tape

Data word: a fixed number of digits plus separator character

Data block: a block consisting of four data words--channel chamber, signal + noise, noise, and current, respectively

Data section: a section of paper tape that contains a finite number of data blocks

Leader: a section of paper tape that is comprised of feed characters

Illegal character: any punch or combination of punches that does not represent digits 0 through 9, a separator, or a feed character

Magnetic Tape

FD (Field Data Code): 2 octal digit code representation for character and digit

Floating point: the form in which a number containing an implied decimal must be before computation in FORTRAN IV can take place with meaningful results

Image tape: magnetic tape on which the image of a paper tape is written, except illegal characters, which are represented as slashes (/) (FD format)

Library tape: magnetic tape in which many data sections are stored for later retrieval

Scratch tape: tape used for one computer run only; its contents are not saved

Backup tape: a copy of any magnetic tape, used for protection purposes

9.2. PAPER TAPE FORMAT

The paper tape must contain a minimum of five feet of leader before the first data section. The leader must be marked "START" in large letters. Each data section must be separated by a minimum of 18 inches of feed characters. Five feet of leader must follow the last data section.

9.3. DESCRIPTION AND INSTRUCTIONS

This section contains a description of the function of each of the following programs used in conjunction with the electron scattering experiments, along with a detailed set of directions for use and a listing of the complete program for each.

Program Name

Program Function

- | | |
|-----------|---|
| 1. READPT | Used with the 1004 paper tape reader to read the paper tape and write the information on a magnetic tape. A slash (/) is written on the magnetic tape for any illegal character in the paper tape. |
| 2. TEDIT | Reads the magnetic tape as written by READPT, converts data from FD to floating point format, and stacks information on a library data tape. Output consists of printed tape and printer plots. Eliminates any illegal characters (slashes) by linear interpolation or direct substitution. |
| 3. TREAD | Reads the data library tape written by TEDIT and lists all runs on this tape. |
| 4. ABEAM4 | Reads the data library tape written by TEDIT and provides various calculations and printer plots as requested by user. |
| 5. COPY | Reads the data library tape and copies the information onto backup tape. |

The information in columns 1 through 7 is mandatory. The information starting in column 19 for identification of each data section is arbitrary. Below is an example READPT input deck for a paper tape containing three data sections.

1	2	3	4	5	6	7	8	9	10	11	12	13	14	15	16	17	18	19	20	21	22	23	24	25	26	27	28	29	30	31	32	33	34	35	36	37	38	39	40									
0	0	0	0	0	0	0	0	0	1	1	1	1	1	1	1	1	1	0	0	0	0	0	0	0	0	0	0	0	0	0	0	0	0	0	0	0	0	0	0	0	0							
0	0	0	1	1	1	1	1	1	1	1	1	1	1	1	1	1	1	0	0	0	0	0	0	0	0	0	0	0	0	0	0	0	0	0	0	0	0	0	0	0	0	0						
0	0	1	1	1	1	1	1	1	1	1	1	1	1	1	1	1	1	0	0	0	0	0	0	0	0	0	0	0	0	0	0	0	0	0	0	0	0	0	0	0	0	0						
0	0	1	1	1	1	1	1	1	1	1	1	1	1	1	1	1	1	0	0	0	0	0	0	0	0	0	0	0	0	0	0	0	0	0	0	0	0	0	0	0	0	0	0					

The printed output from READPT consists of three data blocks per line. Slashes are substituted for any illegal characters in the paper tape.

Prior to the start of step 2, the TEDIT program, the output listing from READPT is examined for errors. A data section is made up of one or more cycles. The channel numbers normally run sequentially, starting at 00000, to a maximum of 00099 for each cycle. In order for TEDIT to recognize the start of a new cycle it is mandatory that each starting channel number be all zeros (00000) and contain no slashes. TEDIT will correct all other channel numbers that contain slashes.

On the output listing from READPT, columns 1, 5, and 9 are the channel numbers. If errors in the paper tape have caused the channel numbers to shift from these columns, the paper tape must be corrected and step 1 repeated until all errors of this type have been eliminated.

The computer program is not included in this report since it is a standard library program held at the computer center.

STEP 2: TEDIT

TEDIT reads a data card, then reads a data section from the magnetic tape written by READPT. It converts the tape data from FD to floating point and a fixed point (integer) and writes the information on the library tape (to be used by ABEAM4 program). The printed output from TEDIT contains the following:

1. A listing of each data section by cycle
2. A printer plot of (signal + noise) - (noise) = signal
3. A printer plot of current by cycle
4. After processing each data section, a listing of Σ^* signal, $\Sigma(\text{signal} + \text{noise})$, $\Sigma \text{ noise}$, $\Sigma(\text{signal}/\text{current})$, $\Sigma((\text{signal} + \text{noise})/\text{current})$, $\Sigma(\text{noise}/\text{current})$ is given. Also, a printer plot of Σ signal and $\Sigma(\text{signal}/\text{current})$ is given.

When a blank data card is encountered, an end of file is written on the library tape and processing is completed.

The data card for each data section must be in the following format:

<u>Column</u>	<u>Name of Variables</u>	<u>FORTTRAN Format</u>
1-6	Experiment number	A6
7-12	Gas type	A6
13-18	Current variance	F6.0
19-24	Time of starting experiment	A6
25-30	Resolution	F6.0
31-36	Voltage interval	F6.0
37-42	Initial voltage	F6.0
43-48	Time interval (sec)	F6.0
49-54	Approximate minimum signal	F6.0
55-60	Approximate maximum signal	F6.0
61-66	Approximate minimum current	F6.0
67-72	Approximate maximum current	F6.0

* Σ is defined as the summing of each respective channel number over all cycles.

Q FOR TEDIT, TEDIT
UNIVAC 1108 FORTRAN IV LEVEL 2201 0029 F4614B
THIS COMPILATION WAS DONE ON 02 MAY 68 AT 10:19:07

MAIN PROGRAM ENTRY POINT 000000

1. C.. THE PURPOSE OF THIS ROUTINE IS TO READ A MAG. TAPE CONTAINING THE
2. C IMAGE OF ONE OR MORE PAPER TAPES. EDIT THIS TAPE AND WRITE THE INFO.
3. C ON A LIBRARY DATA TAPE.
4. C
5. DIMENSION CHAN(100), SPLUSN(100), NOISE(100), CURR(100), SIG(100),
6. 1 X(102), Y(102)
7. REAL NOISE
8. INTEGER CHAN
9. DIMENSION ERR1(100), ERR2(100), ERR3(100), ERR4(100), BUFF(90),
10. 1 WORD(72), ERROR(12), DATE(2)
11. DIMENSION SUM1(100), SUM2(100), SUM3(100), SUM4(100), SUM5(100),
12. 1 SUM6(100)
13. PARAMETER PTAPE = 9, LTAPE = 10
14. INTEGER BUFF, BLANK, SLASH, FIVE, ASTER, ERROR, ERR1, ERR2, ERR3,
15. 1 ERR4, TEE
16. COMMON BUFF
17. DATA BLANK/6H /, SLASH/6H /, FIVE/6H5 /, ASTER/6H *
18. 1 /, MINUS/6H- /, TEE/6HT /
19. REWIND PTAPE
20. REWIND LTAPE
21. IBEGIN = 0
22. C.. READ MAIN DATA CARD, ONE PER EACH PAPER TAPE IMAGE ON MAG. TAPE (PTAPE).
23. 10 READ(5:11) NUM, ITYPE, VAR, TIME, RES, DVOLT, VOLTST, TINT, SIGMIN

```

24. 1 , SIGMAX, CURMIN, DATE(1), DATE(2), ITIME
25. 11 FORMAT( 2A6, F6.0, A6, 8F6.0, A6, A1, I1 )
26. C.. HAS THE LAST PAPER TAPE IMAGE BEEN PROCESSED?
27. IF(NUM.NE.BLANK) 60 TO 14
28. 12 CALL REWI(LTAPE)
29. CALL REWI (PTAPE)
30. STOP
31. C.. INITIALIZE CYCLE COUNTER TO ZERO, SET LAST CYCLE FLAG TO ZERO.
32. 14 KOUNT = 0
33. DO 15 I=1,100
34. SUM1(I) = 0.0
35. SUM2(I) = 0.0
36. SUM3(I) = 0.0
37. SUM4(I) = 0.0
38. SUM5(I) = 0.0
39. 15 SUM6(I) = 0.0
40. C.. SET INDEX COUNTER FOR CHAN, SPLUSN, NOISE AND CURR ARRAYS TO ZERO.
41. L = 0
42. WRITE(6,17) NUM, ITYPE, VAR, TIME, RES
43. 17 FORMAT( 1H1, 9X 10HRUN NUMBER, 1X, A6, // 10X 3HGAS 1X A6, // 10X
44. 1 10HVARIANCE %, 1X F6.2, // 10X 4HTIME, 1X A6, // 10X 4HRES, 1X
45. 2 F6.2 / )
46. WRITE(6,18) DVOLT, VOLTST, TINT, SIGMIN, SIGMAX, CURMIN, CURMAX
47. 18 FORMAT( 10X 17HVOLTAGE INCREMENT 1X F6.2, // 10X 17HSTARTING VOLTA
48. 16E 1X F6.2, // 10X 14HTIME INTERVAL , F6.2, // 10X 12HMIN. SIGNAL
49. 2 F10.2, // 10X 12HMAX. SIGNAL ,F10.2, // 10X 13HMIN. CURRENT ,
50. 3 F10.2, // 10X 13HMAX. CURRENT , F10.2, / )

```

```

51.      WRITE(6,19) DATE(1), DATE(2)
52.      19 FORMAT( 10:I, 4HDATE, 1X 2A6, / )
53.      30 WRITE(6,31)
54.      31 FORMAT( 1H1 )
55.      C.. INCREMENT CYCLE COUNTER BY ONE.
56.      KOUNT = KOUNT + 1
57.      C.. READ ONE RECORD FROM PTAPE.
58.      40 READ(PTAPE,41) (BUFF(I), I=1,90)
59.      41 FORMAT( 90A1 )
60.      C.. TRANSLATE RECORD..
61.      CALL GINPUT ( WORD, N )
62.      DO 45 I=1,12
63.      45 ERROR(I) = BLANK
64.      C.. IF THERE WERE ILLEGAL CHARACTERS IN THE RECORD GO TO 50.
65.      IF(N.EQ.72) GO TO 50
66.      C.. WAS THIS RECORD AN END FILE, ALL BLANKS.
67.      IF(N.NE.0) GO TO 80
68.      ISWICH = 1
69.      GO TO 140
70.      C.. BEGIN TESTING THE LEGALITY OF EACH CHARACTER.
71.      50 DO 70 I=1,72
72.      IF(MOD(I,6).EQ.0) GO TO 60
73.      IF(BUFF(I).NE.SLASH.AND.BUFF(I).NE.TEE) GO TO 70
74.      BUFF(I) = FIVE
75.      K = I/6 + 1
76.      C.. FLAG K WORD IN RECORD TO BE IN ERROR.
77.      ERROR(K) = ASTER

```

```

78.      60 TO 70
79.      60 IF(BUFF(I).EQ.BLANK) GO TO 70
80.      BUFF(I) = BLANK
81.      70 CONTINUE
82.      C.. RETRANSLATE RECORD, RECORD NOW CONTAINS DIGITS AND BLANKS ONLY, NO SLASHES.
83.      CALL GINPUT ( WORD, N )
84.      C.. SEE IF A NEW CYCLE IS STARTING WITHIN LAST TRANSLATED RECORD, WORD(1),
85.      C WORD(5) OR WORD(9) WILL EQUAL ZERO.
86.      80 IF(L.EQ.0.AND.KOUNT.EQ.1) GO TO 100
87.      IF(N.GT.4) GO TO 82
88.      N = 4
89.      60 TO 85
90.      82 IF(N.GT.8) GO TO 84
91.      N = 8
92.      60 TO 85
93.      84 N = 12
94.      85 DO 90 K=4,N*4
95.      J = K-3
96.      IF(WORD(J)) 90, 120, 90
97.      90 CONTINUE
98.      C.. NO NEW CYCLE PLACE ALL WORDS INTO PROPER ARRAYS.
99.      JSAVE=0
100.     100 DO 110 J =1,N*4
101.     L = L + 1
102.     C.. TEST FOR EXCEEDING RESERVED STORAGE.
103.     IF(L.GT.100) GO TO 300
104.     CHAN(L) = WORD(J) + .5

```

```

105.      SPLUSN(L) = WORD(J+1)
106.      NOISE(L) = WORD(J+2)
107.      CURR(L) = WORD(J+3)
108.      ERR1(L) = ERROR(J)
109.      ERR2(L) = ERROR(J+1)
110.      ERR3(L) = ERROR(J+2)
111.      110 ERR4(L) = ERROR(J+3)
112.      GO TO 40
113.      C.. A NEW CYCLE STARTS WITHIN LAST RECORD.
114.      120 ISWITCH = 0
115.      JSAVE = J
116.      IF(JSAVE.EQ.1) GO TO 140
117.      K = JSAVE - 4
118.      DO 130 J=1,K,4
119.      L = L + 1
120.      C.. TEST FOR EXCEEDING RESERVED STORAGE.
121.      IF(L.GT.100) GO TO 300
122.      CHAN(L) = WORD(J) + .5
123.      SPLUSN(L) = WORD(J+1)
124.      NOISE(L) = WORD(J+2)
125.      CURR(L) = WORD(J+3)
126.      ERR1(L) = ERROR(J)
127.      ERR2(L) = ERROR(J+1)
128.      ERR3(L) = ERROR(J+2)
129.      130 ERR4(L) = ERROR(J+3)
130.      C.. TEST EACH ERROR FLAG, IF CHAN(I) IS IN ERROR SUBSTITUTE I-1.
131.      C

```

IF SPLUSN(I), NOISE(I) OR CURR(I) IS IN ERROR

```

132. C INTERPOLATE FOR ITS VALUE.
133. 140 DO 180 I=1,L
134. IF(ERR1(I).NE.BLANK) CHAN(I) = I-1
135. IF(I.NE.1) GO TO 150
136. I1 = 2
137. I2 = 3
138. GO TO 170
139. 150 IF(I.NE.L) GO TO 160
140. I1 = L-2
141. I2 = L-1
142. GO TO 170
143. 160 I1 = I-1
144. I2 = I+1
145. 170 IF(ERR2(I).EQ.BLANK) GO TO 172
146. SPLUSN(I) = (SPLUSN(I2)-SPLUSN(I1))*FLOAT(I-12)/FLOAT(I2-I1) +
147. 1 SPLUSN(I2)
148. 172 IF(ERR3(I).EQ.BLANK) GO TO 174
149. NOISE(I) = (NOISE(I2)-NOISE(I1))*FLOAT(I-12)/FLOAT(I2-I1) +
150. 1 NOISE(I2)
151. 174 IF(ERR4(I).EQ.BLANK) GO TO 180
152. CURR(I) = (CURR(I2)-CURR(I1))*FLOAT(I-12)/FLOAT(I2-I1) + CURR(I2)
153. 180 CONTINUE
154. C UPDATE LTAPE WITH THIS CYCLE DATA.
155. IF(IBEGIN.NE.0) GO TO 182
156. IBEGIN = 1
157. IF(ITIME.EQ.1) GO TO 184
158. CALL NTRAN(LTAPE, 8, 1, 0, -1)

```

```

159.      BACKSPACE LTAPE
160.      GO TO 183
161.      182 CALL NTRAN(LTAPE, 8, -1)
162.      BACKSPACE LTAPE
163.      IF (KOUNT.GT.1) GO TO 185
164.      183 LAST = 1
165.      WRITE(LTAPE) LAST
166.      184 WRITE(LTAPE) NUM, ITYPE, VAR, TIME, RES, DVOLT, VOLTST, TINT,
167.      * SIGMIN, SIGMAX, CURMIN, CURMAX, DATE(1), DATE(2)
168.      GO TO 186
169.      185 LAST = 0
170.      WRITE(LTAPE) LAST
171.      186 WRITE(LTAPE) KOUNT, L
172.      WRITE(LTAPE) (CHAN(I), SPLUSN(I), NOISE(I), CURR(I), I=1,L)
173.      LAST = 2
174.      WRITE(LTAPE) LAST
175.      END FILE LTAPE
176.      C.. CALCULATE SIGNAL VALUE FOR PLOTTING.
177.      X(1) = VOLTST
178.      X(L+2) = VOLTST + FLOAT(L-1)*DVOLT
179.      Y(1) = SIGMIN
180.      Y(L+2) = SIGMAX
181.      DO 190 I=1,L
182.      X(I+1) = VOLTST + FLOAT(I-1)*DVOLT
183.      SIG(I) = SPLUSN(I) - NOISE(I)
184.      SUM1(I) = SUM1(I) + SIG(I)
185.      SUM2(I) = SUM2(I) + SPLUSN(I)

```

```

186.      SUM3(I) = SUM3(I) + NOISE(I)
187.      SUM4(I) = SUM4(I) + SIG(I)/CURR(I)
188.      SUM5(I) = SUM5(I) + SPLUSN(I)/CURR(I)
189.      SUM6(I) = SUM6(I) + NOISE(I)/CURR(I)
190.      190 Y(I+1) = SIG(I)
191.      200 WRITE(6,201) NUM, KOUNT
192.      201 FORMAT( 30X, 14HPLOT OF SIGNAL  5X 4HRUN  A6, 5X 5HCYCLE, I3 )
193.      C.. PLOT VALUES OF SIGNAL.
194.      CALL PLOT( X, Y, L+2, 102, 46, 6 )
195.      C.. PLOT VALUES OF CURRENT.
196.      WRITE(6,31)
197.      WRITE(6,202) NUM, KOUNT
198.      202 FORMAT( 30X, 15HPLOT OF CURRENT 5X 4HRUN  A6, 5X 5HCYCLE, I3 )
199.      Y(1) = CURMIN
200.      Y(L+2) = CURMAX
201.      DO 203 I=1,L
202.      203 Y(I+1) = CURR(I)
203.      CALL PLOT( X, Y, L+2, 102, 46, 6 )
204.      C.. LIST ALL DATA FOR THIS CYCLE.
205.      WRITE(6,31)
206.      WRITE(6,204) NUM, KOUNT
207.      204 FORMAT( 22X, 4HRUN  A6, 5X 5HCYCLE, I3, //  16X 5HCHAN. 5X 3HS+N,
208.      1 9X 1HN, 10X, 1HI, 10X, 1HS /)
209.      WRITE(6,206) (ERR1(I), CHAN(I), ERR2(I), SPLUSN(I), ERR3(I),
210.      1 NOISE(I), ERR4(I), CURR(I), SIG(I), I=1,L )
211.      206 FORMAT( 14X, A2, I3, 2X, A2, F7.0, 2X, A2, F7.0, 2X, A2, F7.0,
212.      1 4X, F10.3 )

```



```

213.      WRITE(6,208)
214.      208 FORMAT( 6X, 66H* INDICATES THE VALUE TO THE RIGHT CONTAINED AN ILL
215.      LEGAL CHARACTER. / 8X 36THE NEW VALUE HAS BEEN INTERPOLATED. )
216.      C.. TEST FOR END OF PAPER TAPE IMAGE.
217.      IF(ISWCH.NE.0) GO TO 240
218.      C.. PREPARE FOR A NEW CYCLE ON PRESENT PAPER TAPE IMAGE.
219.      C.. RESET INDEX COUNTER FOR CHAN, SPLUSN, NOISE AND CURR ARRAYS TO ZERO.
220.      L = 0
221.      IF(JSAVE.EG.0) GO TO 30
222.      DO 210 I=JSAVE,N,4
223.      L = L + 1
224.      C.. TEST FOR EXCEEDING RESERVED STORAGE.
225.      IF(L.GT.100) GO TO 300
226.      CHAN(L) = WORD(I) + .5
227.      SPLUSN(L) = WORD(I+1)
228.      NOISE(L) = WORD(I+2)
229.      CURR(L) = WORD(I+3)
230.      ERR1(L) = ERROR(I)
231.      ERR2(L) = ERROR(I+1)
232.      ERR3(L) = ERROR(I+2)
233.      210 ERR4(L) = ERROR(I+3)
234.      GO TO 30
235.      C.. END OF THIS PAPER TAPE IMAGE.
236.      C.. PLOT VALUES FOR SUMMATION OF SIGNAL VS. VOLTS.
237.      240 WRITE(6,31)
238.      260 WRITE(6,261) NUM
239.      261 FORMAT( 30X 27HPLOT OF SUMMATION OF SIGNAL 5X 3HRUN A6 )

```

```

240. CALL PLOT ( X, SUM1, L, 100, 46, 6 )
241. WRITE(6,31)
242. C.. PLOT VALUES FOR SUMMATION OF SIGNAL/CURRENT VS. VOLTS.
243. WRITE(6,291) NUM
244. 291 FORMAT( 30X 35HPLOT OF SUMMATION OF SIGNAL/CURRENT 5X 3HRUN A6 )
245. CALL PLOT ( X, SUM4, L, 100, 46, 6 )
246. WRITE(6,31)
247. WRITE(6,292) NUM
248. 292 FORMAT( 50X 3HFUN A6, 5X 23HSUMMATION OF ALL CYCLES // 5X 5HCHAN.
249. 1 10X 5HVOLTS 12X 1HS 13X 3HS+N 13X 1HN 13X 3HS/I 9X 7H(S+N)/I
250. 2 11X 3HN/I / )
251. WRITE(6,293) (CHAN(I), X(I+1), SUM1(I), SUM2(I), SUM3(I), SUM4(I),
252. 1 SUM5(I), SUM6(I), I=1,L )
253. 293 FORMAT( 18, 4X, 1P7E15.4 )
254. GO TO 10
255. 300 WRITE(6,301) NUM, KOUNT
256. 301 FORMAT( 1H1, 14H **ERROR** RUN, A6, 3X, 5HCYCLE, I6, 33H CONTAINS
257. 1MORE THAN 100 CHANNELS. / 27H REMAINDER OF DATA IGNORED. )
258. GO TO 12
259. 4 END
END OF LISTING. 0 *DIAGNOSTIC* MESSAGE(S).

```

Q FOR GINPUT,GINPUT
UNIVAC 1108 FORTRAN IV LEVEL 2201 0029 F4614B
THIS COMPILATION WAS DONE ON 02 MAY 68 AT 10:19:11

SUBROUTINE GINPUT ENTRY POINT 000314

1. SUBROUTINE GINPUT (WORD, N)
2. C.. THIS ROUTINE IS A MODIFIED VERSION OF GINPUT.
3. C.. THE FOLLOWING MODIFICATIONS WERE MADE,
4. C 1) COL IS NOW IN COMMON.
5. C 2) STATEMENTS 5 AND 6 ARE NOW COMMENTS.
6. C.. THE PURPOSE OF THIS ROUTINE IS TO READ 72 COLUMNS OF FREE FORMATED
7. C INFORMATION ON A CARD, DATA MUST BE SEPERATED BY A BLANK OR COMMA.
8. C.. WORD IS THE ARRAY IN WHICH THIS ROUTINE STORES THE CARD INFORMATION.
9. C IT MUST BE DIMENSION 72 IN THE MAIN PROGRAM FOR ALPHA-NUMERIC INFO.
10. C TITLE CARDS ARE THEN WRITTEN USING 72A1 FORMAT.
11. C.. N WILL INDICATE THE FOLLOWING TO THE MAIN PROGRAM...
 - 1) N = 72 , CARD WAS ALPHA-NUMERIC.
 - 2) N =-72 , CARD WAS ALL BLANK EXCEPT FOR AN EQUAL SIGN.
 - 3) 0<N<72 , CARD CONTAINED N FLOATING POINT VALUES, THE FIRST IS STORED IN WORD(1), SECOND ONE IN WORD(2), ETC.
 - 4) -72<N<0, SAME AS 3) EXCEPT AN EQUAL SIGN WAS FOUND AT LEAST ONE SPACE BEYOND THE LAST FLOATING POINT NUMBER.
 - 5) N = 0 ALL BLANK CARD.
12. C.. IF A CHARACTER OTHER THAN A PLUS OR MINUS SIGN, COMMA, BLANK, DIGIT,
13. C DECIMAL POINT OR EQUAL SIGN IS DETECTED ON A CARD THEN THE CARD IS INTERPRETED AS ALPHA-NUMERIC IMEDIATELY.
14. C THE PURPOSE OF THE EQUAL SIGN IS TO SERVE AS A FLAG FOR WHATEVER THE

```

23. C USER WISHES.
24. C.. THE FORTRAN E FORMAT IS NOT ALLOWED. THE LARGEST ALLOWABLE NUMBER IS
25. C 9999999999. OR 9X10**9.
26. INTEGER COL, TESTWD
27. DIMENSION WORD(72), TESTWD(16), COL(72), FWORD(72)
28. COMMON COL
29. EQUIVALENCE ( FWORD, COL )
30. DATA (TESTWD(I),I=1,16)/1H0, 1H1, 1H2, 1H3, 1H4, 1H5, 1H6, 1H7,
31. 1 1H8, 1H9, 1H , 1H,, 1H,, 1H=, 1H-, 1H+ /
32. C 5 READ 6, ( COL(I), I=1,72 )
33. C 6 FORMAT( 72A1 )
34. K = 0
35. N = 0
36. SUM = 0.0
37. DEC = 0.0
38. I60 = 1
39. 8 SIGN = 1.0
40. C.. FIND FIRST NON-BLANK CHARACTER.
41. DO 7 I=1,72
42. IF(COL(I).NE.TESTWD(11)) GO TO 11
43. 7 CONTINUE
44. N = 0
45. GO TO 16
46. C.. BEGIN TESTING AT START OF NEW WORD.
47. 10 IF(COL(I).EQ.TESTWD(11)) GO TO 20
48. 11 IF(COL(I).EQ.TESTWD(15)) GO TO 30
BLANK
MINUS

```

```

49. IF(COL(I).EQ.TESTWD(16)) GO TO 40 PLUS
50. IF(COL(I).EQ.TESTWD(13)) GO TO 50 DECIMAL
51. DO 12 J=1,10
52. IF(COL(I).EQ.TESTWD(J) ) GO TO 60 0 THRU 9
53. 12 CONTINUE
54. IF(COL(I).EQ.TESTWD(12)) GO TO 70 COMMA
55. 15 IF(COL(I).EQ.TESTWD(14)) GO TO 80 EQUAL
56. C.. CHARACTER WAS ALPHA-NUMERIC.
57. N = 72
58. 16 DO 17 I=1,72
59. 17 WORD(I) = FWORD(I)
60. 18 RETURN
61. 20 GO TO(22, 18),160
62. 22 I = I + 1
63. IF(I-72) 10, 10, 18
64. C
65. 30 SIGN = -1.0
66. C.. CHARACTER WAS A MINUS SIGN.
67. 60 TO 22
68. C
69. 40 SIGN = +1.0
70. C.. CHARACTER WAS A PLUS SIGN.
71. 60 TO 22
72. C
73. 50 K = -1
74. C.. CHARACTER WAS A DECIMAL POINT.

```

75. KSAVE = 0
76. C.. INDICATE DECIMAL WAS FOUND.
77. DEC = 1.0
78. 60 TO 100
79. C
80. 60 K = 10
81. C.. CHARACTER WAS A DIGIT.
82. C ASSUME WORD HAS 10 SIGNIFICANT DIGITS TO THE LEFT OF THE DECIMAL.
83. 60 TO 120
84. C
85. C.. CHARACTER WAS A COMMA PRECEDED BY BLANKS OR ANOTHER COMMA.
86. 70 N = N + 1
87. WORD(N) = 0.0
88. I = I + 1
89. 60 TO 10
90. C
91. C.. CHARACTER WAS AN EQUAL SIGN.
92. 80 IF(N) 84, 82, 84
93. 82 N = -72
94. RETURN
95. 84 N = -N
96. RETURN
97. C
98. 100 I = I + 1
99. C
100. IF(I-72) 110, 110, 105

```

101. C.. INDICATE ENTIRE RECORD HAS BEEN TRANSLATED.
102. 105 I60 =2
103. 60 TO 135
104. 110 DO 112 J=1,10
105. IF(COL(I).EQ.TESTWD(J) ) GO TO 120
106. 112 CONTINUE
107. IF(COL(I).EQ.TESTWD(13)) GO TO 130
108. IF(COL(I).EQ.TESTWD(12)) GO TO 135
109. IF(COL(I).EQ.TESTWD(11)) GO TO 135
110. 60 TO 10
111. C
112. C.. BUILD UP WORD BY ADDING ON DIGIT JUST FOUND.
113. 120 SUM = SUM + FLOAT(J-1)*10.0**K
114. K = K - 1
115. 60 TO 100
116. C
117. C.. SAVE POSITION WHERE DECIMAL WAS FOUND.
118. 130 KSAVE = K + 1
119. C.. INDICATE THAT DECIMAL WAS FOUND.
120. DEC = 1.0
121. 60 TO 100
122. C
123. C.. ALTER CHARACTERISTIC OF FLOATING POINT WORD FOR DECIMAL POINT.
124. C.. SEE IF A DECIMAL POINT WAS FOUND.
125. 135 IF(DEC) 140, 138, 140
126. 138 KSAVE = K + 1

```

0 THRU 9
DECIMAL
COMMA
BLANK

```
127. C.. UPDATE WORD COUNTER.  
128. 140 N = N + 1  
129. WORD(N) = (SUM/10.0**KSAVE)*SIGN  
130. SUM = 0.0  
131. SIGN = 1.0  
132. DEC = 0.0  
133. GO TO 20  
134. END  
END OF LISTING. 0 *DIAGNOSTIC* MESSAGE(S).
```


FOR PLOT,PLOT
 UNIVAC 1108 FORTRAN IV LEVEL 2201 0029 F46148
 THIS COMPILATION WAS DONE ON 02 MAY 68 AT 10:19:13

SUBROUTINE PLOT ENTRY POINT 000510

DIAGNOSTIC THE NAME OR APPEARS IN A DIMENSION OR TYPE STATEMENT BUT IS NEVER REFERENCED.

- 1. SUBROUTINE PLOT(X,Y,N,N1,N2,NOUT) PLOT0010
- 2. DIMENSION X(1),Y(1),IP(150),B(6),A(18),NB(6),NA(18) PLOT0020
- 3. DIMENSION B1(6),B2(6),B3(6),NB1(6),NB2(6),NB3(6) PLOT0030
- 4. EQUIVALENCE (A,NA),(B,NB),(C,NC),(D,ND) PLOT0040
- 5. EQUIVALENCE (B1,NB1),(B2,NB2),(B3,NB3) PLOT0050
- 6. C X=ABCISSA VALUES TO BE PLOTTED PLOT0060
- 7. C Y=ORDINATE VALUES TO BE PLOTTED PLOT0070
- 8. C N=NUMBER OF POINTS TO BE PLOTTED (150 OR LESS) PLOT0080
- 9. C IF N IS NEGATIVE THE Y ARRAY IS IN DESCENDING ORDER PLOT0090
- 10. C N1=NUMBER OF PRINT WHEELS TO BE USED (108 OR LESS) PLOT0100
- 11. C N2=NUMBER OF LINES TO BE USED (RECOMMEND 50) PLOT0110
- 12. C NOUT=TAPE NO. OF OUTPUT TAPE PLOT0120
- 13. C RESTORATION AND HEADING OF PAGE IS LEFT TO USER PLOT0130
- 14. C -----PLOT0140
- 15. C ALL BLANKS PLOT0150
- 16. DATA C/6H / PLOT0160
- 17. C ALL NEGATIVE SIGNS - BOTTOM LINE USE PLOT0170
- 18. DATA D/6H-----/ PLOT0180
- 19. C STARS IN VARIOUS POSITIONS - BLANKS FILLED IN (6) PLOT0190
- 20. C SUBSTITUTE OCTAL EQUIVALENT OF * IN THIS STATEMENT PLOT0200
- 21. DATA B/6H<00000,6H0<0000,6H0<0000,6H00<000,6H000<0,6H0000</ PLOT0210

```

22. C MASK FOR PICKING OUT SECTOR PLOT0220
23. DATA B1/077000000000,0007700000000,00000770000000,
24. 100000077000,0000000007700,00000000000077/ PLOT0230
25. C MASK FOR COMPARING TO BLANK PLOT0240
26. DATA B2/6H 00000,6H0 0000,6H00 000,6H000 00,6H0000 0,6H00000 / PLOT0250
27. C MASK FOR SUBTRACTING ONE PLOT0260
28. DATA B3/6H 00000,6H00000,6H000000,6H000000,6H000000,6H000000,6H000000 / PLOT0270
29. DATA LARGE/00010000000000/ PLOT0280
30. INTEGER AND/OR PLOT0290
31. C -----PLOT0300
32. IFLG=1 PLOT0310
33. IF(N.LT.0)IFLG=2 PLOT0320
34. N=IABS(N) PLOT0330
35. C INITIALIZES FORMAT PLOT0340
36. DO 9 L=1,10 PLOT0350
37. 9 A(L)=C PLOT0360
38. C SEARCHES X POINTS FOR HIGHEST AND LOWEST VALUES PLOT0370
39. XMIN=1.E+38 PLOT0380
40. XMAX=-1.E+38 PLOT0390
41. DO 10 I=1,N PLOT0400
42. XMAX=AMAX1(XMAX,X(I)) PLOT0410
43. XMIN=AMIN1(XMIN,X(I)) PLOT0420
44. DELTAX=(XMAX-XMIN)/(FLOAT(N1-1)) PLOT0430
45. C REORDERS Y INTO DESCENDING VALUES PLOT0440
46. GO TO (20,15),IFLG PLOT0450
PLOT0460

```

```

47.      15 DO 16 I=1,N
48.      IP(I)=I
49.      16 CONTINUE
50.      YMAX=Y(I)
51.      YMIN=Y(N)
52.      GO TO 25
53.      20 DO 21 I=1,N
54.      IP(I)=0
55.      21 CONTINUE
56.      DO 23 I=1,N
57.      YMAX=-1.E38
58.      DO 22 J=1,N
59.      IF(IP(J).GE.LARGE) GO TO 22
*DIAGNOSTIC* THE TEST FOR EQUALITY BETWEEN NON-INTEGERS MAY NOT BE MEANINGFUL.
60.      IF(Y(J).LE.YMAX) GO TO 22
61.      YMAX=Y(J)
62.      KK=J
63.      22 CONTINUE
64.      IP(I)=IP(I)+KK
65.      IP(KK)=IP(KK)+LARGE
66.      23 CONTINUE
67.      DO 24 I=1,N
68.      IP(I)=IP(I)-LARGE
69.      24 CONTINUE
70.      IX1=IP(1)
71.      IX2=IP(N)
PLOT0470
PLOT0480
PLOT0490
PLOT0500
PLOT0510
PLOT0520
PLOT0530
PLOT0540
PLOT0550
PLOT0560
PLOT0570
PLOT0580
PLOT0590
PLOT0600
PLOT0610
PLOT0620
PLOT0630
PLOT0640
PLOT0650
PLOT0660
PLOT0670
PLOT0680
PLOT0690
PLOT0700
PLOT0710

```

72.	YMAX=Y(IX1)	PLOT0720
73.	YMIN=Y(IX2)	PLOT0730
74.	25 DELTAY=(YMAX-YMIN)/(FLOAT(N2-1))	PLOT0740
75.	DELT=YMAX	PLOT0750
76.	C PLOTTING SECTION	PLOT0760
77.	DO 41 K=1,N	PLOT0770
78.	I=IP(K)	PLOT0780
79.	J=IP(K+1)	PLOT0790
80.	IF(K-1)33,33,30	PLOT0800
81.	30 IF(L)31,31,33	PLOT0810
82.	31 DELT=DELT-DELTAY	PLOT0820
83.	IF(Y(I)-DELT+.0001) 32, 33, 33	
84.	C PRINTS BLANK LINES	PLOT0840
85.	32 L=-1	PLOT0850
86.	60 TO 37	PLOT0860
87.	C PRINT WHEEL POSITION (0,1,2,3,...,N1-1)	PLOT0870
88.	33 NPWP=(X(I)-XMIN)/DELTAX	PLOT0880
89.	C SECTOR(1,2,3,4,5,...,N1/5+1)	PLOT0890
90.	NSECT=(NPWP/6)+1	PLOT0900
91.	C POSITION IN SECTOR(1,2,3,4,5,6)	PLOT0910
92.	NF=MOD(NPWP,6)+1	PLOT0920
93.	C PLACES * IN FORMAT	PLOT0930
94.	C -----PLOT0940	
95.	NTST=AND(NA(NSECT),NB1(NF))	PLOT0950
96.	IF(NTST.EQ.NB2(NF))60 TO 100	PLOT0960
97.	NA(NSECT)=NA(NSECT)-NB3(NF)	PLOT0970

```

98.          GO TO 101
99.      100 NA(NSECT)=NA(NSECT)+NB(NF)
100.     101 CONTINUE
101.     C-----PLOT1010
102.          IF(K-N)34,36,36
103.     C REPEATS IF Y(I) AND Y(J) ARE CLOSER THAN DELTAY
104.     34 IF(Y(J)-DELT+.0001) 36, 35, 35
105.     35 L=1
106.          GO TO 41
107.     36 L=0
108.     C PRINTING ROUTINE
109.     37 CONTINUE
110.          WRITE (NOUT,36)DELT,(A(IL),IL=1,18)
111.     38 FORMAT ( 1PE10.3, 2H I, 18A6 )
112.          IF(L)31,39,39
113.     C RESTORES FORMAT
114.     39 DO 40 IL=1,18
115.     40 A(IL)=C
116.     41 CONTINUE
117.     C DRAWS BOTTOM AXIS
118.     DO 42 I=1,18
119.     42 A(I)=D
120.          WRITE (NOUT,43)(A(I),I=1,18)
121.     43 FORMAT(12X,18A6)
122.     C RESTORES A ARRAY TO BLANKS
123.     DO 44 I=1,18

```

PLOT1240
PLOT1250
PLOT1260
PLOT1270
PLOT1280
PLOT1290
PLOT1300
PLOT1310
PLOT1320
PLOT1330
PLOT1340
PLOT1350
PLOT1360
PLOT1370
PLOT1380
PLOT1390

```
124.      44 A(I)=C
125.      C   SETS UP * EVERY 10 PLACES FOR LOWER AXIS
126.      DO 45 I=2,12,5
127.      NA(I)=NA(I)+NB(4)
128.      NA(I+2)=NA(I+2)+NB(2)
129.      45 NA(I+3)=NA(I+3)+NB(6)
130.      NA(17)=NA(17)+NB(4)
131.      NA(1)=NA(1)+NB(1)
132.      WRITE (NOUT,43)(A(I),I=1,18)
133.      DELTAX=((XMAX-XMIN)/FLOAT(N1))*10.0
134.      DO 46 I=1,11
135.      46 A(I)=XMIN+FLOAT(I-1)*DELTAX
136.      WRITE (NOUT,47)(A(I),I=2,11)
137.      47 FORMAT(16X,1P10E10.4)
138.      RETURN
139.      END
END OF LISTING.      2 *DIAGNOSTIC* MESSAGE(S).
```


Q FOR TREAD,TREAD
UNIVAC 1108 FORTRAN IV LEVEL 2201 0029 F46148
THIS COMPILATION WAS DONE ON 02 MAY 68 AT 10:19:05

MAIN PROGRAM ENTRY POINT 000000

1. C.. THE PURPOSE OF THIS ROUTINE IS TO READ THE LIBRARY TAPE AND LIST ALL
2. C DATA BY RUN NUMBER AND BY CYCLE NUMBER.
3. INTEGER CHAN
4. REAL NOISE
5. DIMENSION CHAN(100), SPLUSN(100), NOISE(100), CURR(100), DATE(2)
6. PARAMETER LTAPE = 10
7. REWIND LTAPE
8. READ(LTAPE) NUM, ITYPE, VAR, TIME, RES, DVOLT, VOLTST, TINT,
9. 1 SIGMIN, SIGMAX, CURMIN, CURMAX, DATE(1), DATE(2)
10. WRITE(6,11) NUM
11. FORMAT(10X, 10HRUN NUMBER, 1X, A6, /)
12. WRITE(6,12) ITYPE
13. FORMAT(10X, 3HGAS, 1X, A6, /)
14. WRITE(6,13) VAR
15. FORMAT(10X, 10HVARIANCE %, 1X, F6.2, /)
16. WRITE(6,14) TIME
17. FORMAT(10X, 4HTIME, 1X, A6, /)
18. WRITE(6,15) RES
19. FORMAT(10X, 4HRES, 1X, F6.2, /)
20. WRITE(6,16) DVOLT
21. FORMAT(10X, 17HVOLTAGE INCREMENT, 1X, F6.2, /)
22. WRITE(6,17) VOLTST


```

23. 17 FORMAT( 10X, 17HSTARTING VOLTAGE , 1X, F6.2, / )
24. WRITE(6,18) TINT
25. 18 FORMAT( 10X, 14HTIME INTERVAL , F6.2, / )
26. WRITE(6,19) SIGMIN
27. 19 FORMAT( 10X, 12HMIN. SIGNAL , F10.2, / )
28. WRITE(6,20) SIGMAX
29. 20 FORMAT( 10X, 12HMAX. SIGNAL , F10.2, / )
30. WRITE(6,21) CURMIN
31. 21 FORMAT( 10X, 13HMIN. CURRENT , F10.2, / )
32. WRITE(6,22) CURMAX
33. 22 FORMAT( 10X, 13HMAX. CURRENT , F10.2, / )
34. WRITE(6,23) DATE(1), DATE(2)
35. 23 FORMAT( 10X, 4HDATE, 1X, 2A6, / )
36. 10 READ(LTAPE) KOUNT, L
37. C
38. WRITE(6,24) KOUNT
39. 24 FORMAT( 1H1, 10X, 12HCYCLE NUMBER, 1X, I3, / )
40. WRITE(6,25) L
41. 25 FORMAT( 10X, 16HNUMBER OF POINTS, I5, // )
42. C
43. READ(LTAPE) (CHAN(I), SPLUSN(I), NOISE(I), CURR(I), I=1,L )
44. WRITE(6,27) (CHAN(I), SPLUSN(I), NOISE(I), CURR(I), I=1,L )
45. 27 FORMAT( I10, 3F10.1 )
46. READ(LTAPE) LAST
47. IF(LAST.EQ.0) GO TO 10
48. WRITE(6,31)

```

L. PRINT

L. PRINT

L. PRINT

```
49.      31 FORMAT( 1H1 )
50.      IF(LAST.EQ.1) GO TO 8
51.      WRITE(6,28)
52.      28 FORMAT(/ 12H END OF FILE )
53.      CALL REWI(LTAPE)
54.      CALL EXIT
55.      END

END OF LISTING.      0 *DIAGNOSTIC* MESSAGE(S).
```

STEP 4: ABEAM4

Input for this program consists of the data library tape, as written by TEDIT, and a set of data cards. The purpose of the program is to perform various calculations based on data from different cycles of the same experiment or from different experiments.

The normal output from ABEAM4 is the following (see option 3, below):

1. Σ signal
2. Σ signal smoothed once
3. Σ (signal + noise)
4. Σ (signal + noise) smoothed once
5. Σ (signal/noise)
6. Σ noise
7. Σ current

Printer plots of the following are also given:

1. Σ signal
2. Σ signal smoothed once
3. Σ (signal + noise)
4. Σ (signal + noise) smoothed once
5. Σ (signal/noise)
6. Σ noise

By the use of an option (see option 1, below), the additional information may be obtained along with a printer plot of each.

1. first derivative of Σ signal
2. first derivative of Σ signal smoothed once
3. first derivative of Σ signal smoothed twice
4. second derivative of Σ signal smoothed twice
5. first derivative of Σ (signal + noise) smoothed once

The input card formats are as follows:

Title Card: FORTRAN format is (12A6)

Column

1-72 Title (printed at top of first page)

Option Card: FORTRAN format is (3I6)

Column

6 Option 1 = 0 or blank: derivative output not desired
= 1: desire derivative output

12 Option 2 = 0 or blank: parabolic least squares fit
for smoothing
= 1: Fourier series smoothing

18 Option 3 = 0 or blank: all output is calculated as
shown below
= 1: each term in the summation is divided by
its respective value of current (i. e. ,
 Σ (signal/current) etc.)

Run No. Card: FORTRAN format is (A6, 2I6)

Column

1-6 Experiment number (IRUN)

7-12 Number of cycles (NCYC) requested from this experiment

18 ILAST = 0 or blank: another Run No. card follows the
Cycle No. card
= 1: another title card follows the next Cycle
No. card
= 2: no more cards follow the next Cycle No. card.
The next Cycle No. card is the last to be
summed and all processing is complete

Cycle No. Card: FORTRAN format is (12I6)

Column

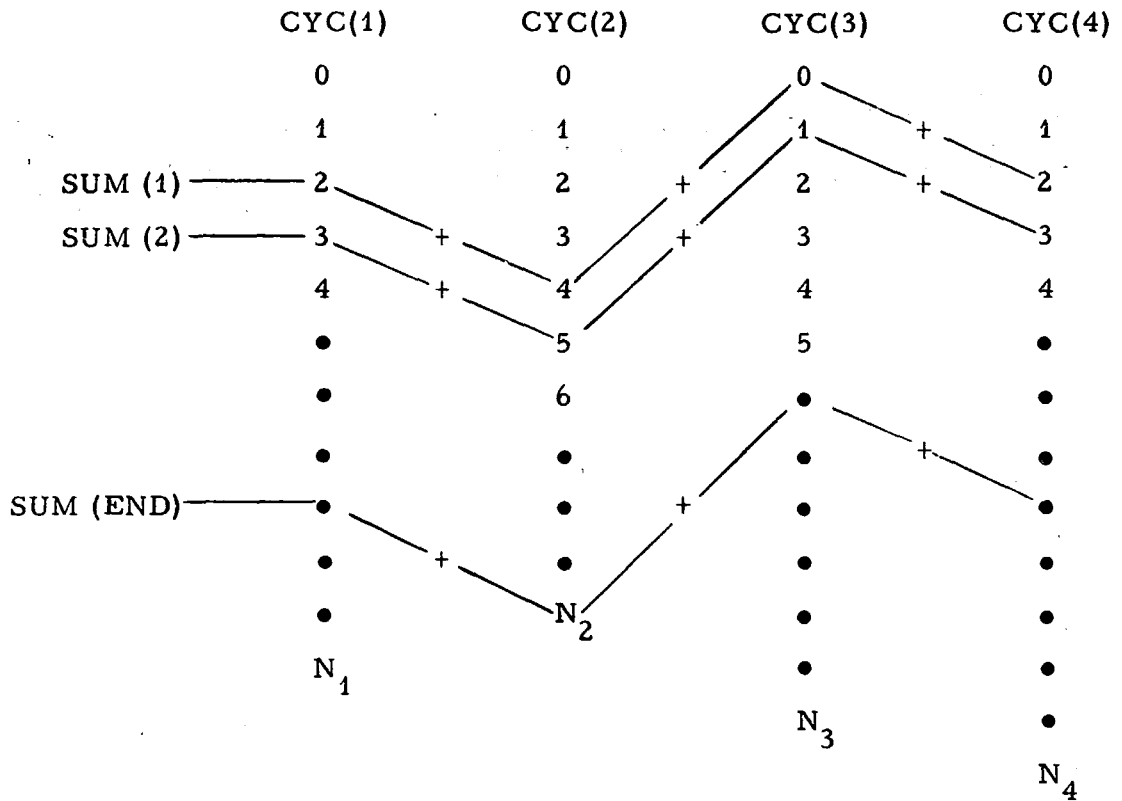
- 1-6 Cyc (1) = first requested cycle number
- 7-12 REFPNT (1)
- 13-18 Cyc (2) = second requested cycle number
- 19-24 REFPNT (2)
- . .
- . .
- . .
- 25-66 Cyc (6) = sixth requested cycle number
- 67-72 REFPNT (6)

Two or more cards of this type may be used if the number of cycles (NCYC) requested exceeds six.

Below is an example deck setup for summing together cycles 3, 5, and 6 from experiment I15; cycles 1 through 10 of experiment L25; and cycles 4 through 9 from experiment I45.

FLASG	B-DATA	LIBRARY	TAPE NUMBER												
(INSERT ABEAMA PROGRAM DECK HERE)															
7	KAT	ABEAMA													
	SUMMING OF I15, L25, I45			DATE 4/11/68											
I15	3	0													
I15	5	0													
L25	10	0													
I45	4	0		1	4	2	11	10	2	1	6	3			
I45	8	0													
I45	9	0													

Below is a diagram showing how the summing, Σ, takes place with reference to the channel numbers.



In the diagram, CYC(1) through CYC(4) are arbitrary cycles. The reference points, REFPNT(1) through REFPNT(4), are 3, 5, 1, 3, respectively. In this particular case $N_2 < N_1 < N_3 < N_4$; therefore, it is meaningless to sum past N_2 . The total number of sums that would be printed is $(N_2 - 4) + 1$.

A program listing follows.

GP FOR ABEAM4, ABEAM4
UNIVAL 1108 FORTRAN IV LEVEL 2201 0029 F4G148
THIS COMPILATION WAS DONE ON 29 MAY 68 AT 13:59:52

```
MAIN PROGRAM      ENTRY POINT 000000

1.  PARAMETER LTAPE = 10
2.  PARAMETER ID=200
3.  INTEGER PCHAR, SLI
4.  INTEGER BLANK, CYC, REFPNT, OPT1, OPT2, OPT3, RFPNT1, OPT4
5.  REAL NOISE
6.  DIMENSION SPLUSN(100), NOISE(100), SIG(100), SIG1(100), SIG2(100),
7.  1 SPN(100), SPN1(100), SIGDN(100), DSPN1(100), DSIG(100), IP(100),
8.  2 DSIG1(100), DSIG2(100), D2SIG2(100), NUMTAB(ID), TITLE(I2),
9.  3 CYC(ID), REFPNT(ID), CURR(100), SNOISE(100), VOLT(100),
10. 4 SUMCUR(100)
11. DATA BLANK/6H /,SLI/2H/I/
12. COMMON DVOLT, KEY
13. REWIND LTAPE
14. DO 5 I=1,ID
15. 5 NUMTAB(I) = 0
16. 10 IGB = 1
17. 1GE = 100
18. ITIME = 0
19. ILAST = 0
20. READ(5,11) (TITLE(I), I=1,12)
```

```

21. 11 FORMAT( 12A6)
22. WRITE(6,13) (TITLE(I), I=1,12)
23. 13 FORMAT( 1H1, 30X, 12A6, // 40X 32HREQUESTED DATA FROM LIBRARY TAPE
24. 1 )
25. DO 14 I=1,100
26. SPN(I) = 0.0
27. SIG(I) = 0
28. SIGUN(I) = 0
29. SUMCUR(I) = 0.0
30. 14 SNOISE(I) = 0.0
31. READ(5,15) OPT1, OPT2, OPT3, OPT4
32. 15 FORMAT( 12I6 )
33. 16 IF(ILAST) 150, 20, 150
34. 20 READ(5,21) IRUN, NCYC, ILAST
35. 21 FORMAT( A6, 11I6 )
36. READ(5,22) (CYC(I), REFPNT(I), I=1,NCYC )
37. 22 FORMAT( 12I6 )
38. WRITE(6,24) (IRUN, CYC(I), REFPNT(I), I=1,NCYC)
39. 24 FORMAT( / 40X, 4HRUN , A6, 2X, 5HCYCLE, I3, 2X, 10HREF. POINT I3)
40. IF(ETIME.NE.0) GO TO 28
41. RFPNT1 = REFPNT(1)
42. IGB = REFPNT(1)
43. ITIME = 1
44. C.. CHECK RUN NUMBER TABLE TO SEE TAPE DATA CAN BE FOUND BY FORWARD READING.
45. 28 DO 30 I=1,ID
46. IF(IRUN.EQ.NUMTAB(I) ) GO TO 40
47. IF(NUMTAB(I).NE.0) GO TO 30

```



```

48.      IPOS = I - 1
49.      GO TO 50
50.      30 CONTINUE
51.      40 REWIND LTAPE
52.      DO 45 I=1,10
53.      45 NUMTAB(I) = 0
54.      IPOS = 0
55.      50 READ(LTAPE) NUM, DUMMY, DUMMY,DUMMY, DUMMY, DVOLT, VOLTST
56.      IPOS = IPOS + 1
57.      NUMTAB(IPOS) = NUM
58.      IF(NUM.EQ.IRUN) GO TO 70
59.      C.. POSITION TAPE TO READ NEXT RUN NUMBER ON TAPE.
60.      55 READ(LTAPE) DUMMY, L
61.      READ(LTAPE) (DUMMY, DUMMY, DUMMY, DUMMY, I=1,L )
62.      READ(LTAPE) LAST
63.      IF(LAST-1) 55, 50, 60
64.      60 WRITE(6,61) IRUN
65.      61 FORMAT( 4H RUN A6, 28H IS NOT ON THE LIBRARY TAPE. )
66.      CALL REWI(LTAPE)
67.      CALL EXIT
68.      C.. REQUESTED RUN HAS BEEN FOUND. PICK OUT REQUESTED CYCLES.
69.      70 DO 140 J=1,NCYC
70.      72 READ(LTAPE) ICYC, L
71.      READ(LTAPE) ( DUMMY, SPLUSN(I), NOISE(I), CURR(I), I=1,L )
72.      READ(LTAPE) LAST
73.      IF(ICYC.NE.CYC(J)) 60 TO 130
74.      C.. CALC. BEGINNING AND ENDING SUBSCRIPTS BASED UPON REF. POINT NUMBER.

```

```

75. NDIF = REFPNT(J) - RFPNT1
76. IF(NDIF) 80, 90, 100
77. 80 IGB = MAX0(IGB,1-NDIF)
78. IGE = MIN0(IGE,IGB+(L-REFPNT(J)) )
79. 60 TO 110
80. 90 IGB = IGB
81. IGE = MIN0(IGE,L)
82. 60 TO 110
83. 100 IGB = IGB
84. IGE = MIN0(IGE,L-NDIF)
85. 110 DO 120 I=IGB,IGE
86. NA = 1 + NDIF
87. D = 1.0
88. IF(OPT3.NE.0) D = CURR(NA)
89. SPN(I) = SPN(I) + SPLUSN(NA)/D
90. SIG(I) = SIG(I) + (SPLUSN(NA)-NOISE(NA))/D
91. SNOISE(I) = SNOISE(I) + NOISE(NA)/D
92. SIGDN(I) = SIGDN(I) + (SPLUSN(NA)-NOISE(NA))/(NOISE(NA)*D)
93. SUMCUR(I) = SUMCUR(I) + CURR(NA)
94. 120 CONTINUE
95. 60 TO 140
96. 130 IF(LAST.EQ.0) GO TO 72
97. WRITE(6,131) CYC(J)
98. 131 FORMAT( 13H CYCLE NUMBER 16,28H IS NOT ON THE LIBRARY TAPE. )
99. CALL REWI (LTAPE)
100. CALL EXIT
101. 140 CONTINUE

```

```

102. C.. POSITION TAPE AT THE BEGINNING OF THE NEXT LOGICAL RECORD CONTAINING
103. C THE NEXT RUN NUMBER.
104. C
105. C.. CHECK FOR END OF FILE FIRST.
106. 142 IF(LAST.NE.2) GO TO 146
107. REWIND LTAPE
108. DO 144 I=1,10
109. 144 NUMTAB(I) = 0
110. GO TO 16
111. C.. IF LAST EQUALS ONE TAPE IS POSITION ALREADY.
112. 146 IF(LAST.EQ.1) GO TO 16
113. C.. THERE STILL REMAINS SOME CYCLES.
114. READ(LTAPE) DUMMY, L
115. READ(LTAPE) (DUMMY, DUMMY, DUMMY, DUMMY, I=1,L)
116. READ(LTAPE) LAST
117. GO TO 142
118. C
119. 150 X = 0
120. DO 160 I=168,16E
121. X = X + 1
122. 160 VOLT(I) = VOLTST + (X-1.0)*DVOLT
123. C.. RE-ORDER ARRAYS
124. 168M1 = 168 - 1
125. DO 162 I=168,16E
126. IA = I - 168M1
127. SIG(IA) = SIG(I)
128. SPN(IA) = SPN(I)

```

```

129. SNOISE(IA) = SNOISE(I)
130. SIGDN(IA) = SIGDN(I)
131. VOLT(IA) = VOLT(I)
132. IP(IA) = I
133. SUMCUR(IA) = SUMCUR(I)
134. 162 CONTINUE
135. NUMPTS = IGE - 168M1
136. KEY = 1
137. CALL SMT (SIG, SIG1, NUMPTS, OPT2)
138. KEY = 2
139. CALL SMT (SPN, SPN1, NUMPTS, OPT2)
140. IF( OPT3.EQ.0) GO TO 169
141. WRITE(6,168)
142. 168 FORMAT( 1H1, 12X 5HVOLTS 11X 3HS/I 12X 3HS/I 2X 2(8X 7H(S+N)/I),
143. * 6X 11H S/(N*I) , 8X 3HN/I 13X 1HI )
144. GO TO 1711
145. 169 WRITE(6,170)
146. 170 FORMAT( 1H1, 12X 5HVOLTS 12X 1HS 14X 1HS 1X 2(12X 3HS+N), 12X
147. * 3HS/N 13X 1HN 14X 1HI )
148. 1711 WRITE(6,171)
149. 171 FORMAT( 20X 2(22X, 8H(SMTH 1) ) / )
150. WRITE(6,172) ( IP(I), VOLT(I), SIG(I), SIG1(I), SPN(I), SPN1(I),
151. 1 SIGDN(I), SNOISE(I), SUMCUR(I), I=1,NUMPTS )
152. 172 FORMAT( 3X, 13, 1P8E15.6 )
153. C.. PLOT ABOVE ITEMS ON PRINTER.
154. PCHAR = BLANK
155. IF( OPT3.NE.0) PCHAR = SLI

```

```

156.      WRITE(6,173) PCHAR
157.      173 FORMAT( 1H1, 20X 9HPLOT OF S, A2 )
158.      CALL PLOT ( VOLT, SIG, NUMPTS, 100, 46, 6 )
159.      WRITE(6,174) PCHAR
160.      174 FORMAT( 1H1, 20X 9HPLOT OF S, A2, 5X 13HSMOOTHED ONCE )
161.      CALL PLOT ( VOLT, SIG1, NUMPTS, 100, 46, 6 )
162.      WRITE(6,175) PCHAR
163.      175 FORMAT( 1H1, 20X 13HPLOT OF (S+N), A2 )
164.      CALL PLOT ( VOLT, SPN, NUMPTS, 100, 46, 6 )
165.      WRITE(6,176) PCHAR
166.      176 FORMAT( 1H1, 20X 13HPLOT OF (S+N), A2, 5X 13HSMOOTHED ONCE )
167.      CALL PLOT ( VOLT, SPN1, NUMPTS, 100, 46, 6 )
168.      IF(OPT3.EQ.0) GO TO 177C
169.      WRITE(6,1761)
170.      1761 FORMAT( 1H1, 20X, 15HPLOT OF S/(N*I) )
171.      GO TO 178
172.      1770 WRITE(6,177)
173.      177 FORMAT( 1H1, 20X, 11HPLOT OF S/N )
174.      178 CALL PLOT ( VOLT, SIGDN, NUMPTS, 100, 46, 6 )
175.      WRITE(6,179) PCHAR
176.      179 FORMAT( 1H1, 20X, 9HPLOT OF N, A2 )
177.      CALL PLOT (VOLT, SNOISE, NUMPTS, 100, 46, 6 )
178.      IF(OPT1.EQ.0) GO TO 260
179.      CALL DIFF( SIG, DSIG, NUMPTS )
180.      CALL DIFF( SIG1, DSIG1, NUMPTS )
181.      KEY = 3
182.      CALL SMT (SIG1, SIG2, NUMPTS, OPT2)

```

```

183. CALL DIFF( SIG2, DSIG2, NUMPTS )
184. CALL DIFF ( DSIG2, D2SIG2, NUMPTS )
185. CALL DIFF ( SPN1, DSPN1, NUMPTS )
186. DXINV = 1./DVOLT
187. DO 180 I=1,NUMPTS
188. DSIG(I) = DSIG(I)*DXINV
189. DSIG1(I) = DSIG1(I)*DXINV
190. DSIG2(I) = DSIG2(I)*DXINV
191. D2SIG2(I) = D2SIG2(I)*DXINV*DXINV
192. DSPN1(I) = DSPN1(I)*DXINV
193. C
194. WRITE(6,191) PCHAR, PCHAR, PCHAR, PCHAR, PCHAR, PCHAR
195. FORMAT( 1H1, 12X 5HVOLTS 10X 3( 8H1ST DER., 7X), 8H2ND DER. )
196. 1 7X 8H1ST DER. / 29X 2H S, A2, 7X 2H S, A2, 7H SMTH 1, 2(4X, 2H S,
197. 2 A2, 7H SMTH 2 ), 4X 5H(S+N), A2, 7H SMTH 1 / )
198. WRITE(6,201) (IP(I), VOLT(I), DSIG(I), DSIG1(I), DSIG2(I),
199. 1 D2SIG2(I), DSPN1(I), I=1,NUMPTS )
200. FORMAT( 3X, 13, 1P6E15,6 )
201. C.. PLOT ABOVE ITEMS ON PRINTER.
202. WRITE(6,211) PCHAR
203. FORMAT( 1H1, 20X 15HDERIVATIVE OF S, A2 )
204. CALL PLOT ( VOLT, DSIG, NUMPTS, 100, 46, 6 )
205. WRITE(6,221) PCHAR
206. FORMAT( 1H1, 20X 15HDERIVATIVE OF S, A2, 14H SMOOTHED ONCE )
207. CALL PLOT ( VOLT, DSIG1, NUMPTS, 100, 46, 6 )
208. WRITE(6,231) PCHAR
209. FORMAT( 1H1, 20X, 15HDERIVATIVE OF S, A2, 15H SMOOTHED TWICE )

```

```

210. CALL PLOT ( VOLT, DSIG2, NUMPTS, 100, 46, 6 )
211. WRITE(6,241) PCHAR
212. 241 FORMAT( 1H1, 20X,19H2ND DERIVATIVE OF S, A2, 15H SMOOTHED TWICE )
213. CALL PLOT ( VOLT, D2SIG2, NUMPTS, 100, 46, 6 )
214. WRITE(6,251) PCHAR
215. 251 FORMAT( 1H1, 20X,19H2ND DERIVATIVE OF (S+N), A2, 14H SMOOTHED ONCE )
216. CALL PLOT ( VOLT, DSPN1, NUMPTS, 100, 46, 6 )
217. C
218. 260 IF(OPT4.EQ.0) GO TO 280
219. DO 270 J=1,3
220. PUNCH 261, (TITLE(I),I=1,12)
221. 261 FORMAT(12A6)
222. PUNCH 262,
223. 262 FORMAT( 5X, 1H0, 5X, 1H0 )
224. PUNCH 263, VOLT(I), VOLT(NUMPTS), DVOLT
225. 263 FORMAT( 3F12.4 )
226. GO TO (264, 265, 266), J
227. 264 PUNCH 267, (SIG(I), I=1,NUMPTS)
228. GO TO 270
229. 265 PUNCH 267, (SPN(I), I=1,NUMPTS)
230. GO TO 270
231. 266 PUNCH 267, (SNOISE(I), I=1,NUMPTS)
232. 267 FORMAT( 6F12.4 )
233. 270 CONTINUE
234. 260 IF(LAST.EQ.1) GO TO 10
235. CALL REWI ( LTAPE )
236. CALL EXIT

```

237. END

END OF LISTING. 0 *DIAGNOSTIC* MESSAGE(S).

FOR SMT,SMT
 UNIVAC 1106 FORTRAN IV LEVEL 2201 0029 F46148
 THIS COMPILATION WAS DONE ON 01 MAY 68 AT 14:22:13

```

SUBROUTINE SMT      ENTRY POINT 000471
1.  SUBROUTINE SMT ( Y, YC, NP, IOPT )
2.  C  ROUTINE TO SMOOTH CURVE
3.  DIMENSION Y(1), YC(1), B(100)
4.  COMMON DX, KEY
5.  PI = 3.1415926
6.  IF (IOPT.GT.0) GO TO 200
7.  NPM1 = NP - 1
8.  NPM2 = NP - 2
9.  DO 100 I=3,NPM2
10.  YC(I)=Y(I)-8.5714286E-02*(Y(I-2)-4.0*(Y(I-1))+Y(I+1))+6.0*Y(I)+Y(I+SMT) 050
11.  12)
12.  100 CONTINUE
13.  YC(1)=Y(1)
14.  YC(2)=0.25*(Y(1)+2.0*Y(2)+Y(3))
15.  YC(NPM1)=0.25*(Y(NPM2)+2.0*Y(NPM1)+Y(NP))
16.  YC(NP)=Y(NP)
17.  RETURN
18.  200 P = NP-1
19.  HL = P*DX
20.  YMIN = 1.E+37
21.  DO 205 I=1,NP
22.  YMIN = AMIN1(YMIN,Y(I))
SMT 030
SMT 070
SMT 080
SMT 090
SMT 100
SMT 110
SMT 120
SMT 130
  
```

```

23.      205 CONTINUE
24.      IF (YMIN.LT.0) GO TO 208
25.      DO 206 I=1,NP
26.          YC(I) = Y(I)
27.      206 CONTINUE
28.          GO TO 210
29.      208 DO 209 I=1,NP
30.          YC(I) = Y(I) - YMIN
31.      209 CONTINUE
32.      210 YI = SORT( YC(1) )
33.          YF = (SORT( YC(NP) ) - YI)/HL
34.          X = 0
35.          DO 211 I=1,NP
36.              YC(I) = SORT( YC(I) ) - YI - YF*X
37.          211 X = X + DX
38.          CALL FOUR (NP, YC, B )
39.          NPM = NP-1
40.          GO TO (212, 214, 216), KEY
41.          212 WRITE(6,213)
42.          213 FORMAT( 1H1, 20X 4HF0URIER COEFFICIENTS FOR SMOOTHING SIGNAL
43.              * )
44.          GO TO 218
45.          214 WRITE(6,215)
46.          215 FORMAT( 1H1, 20X 5HF0URIER COEFFICIENTS FOR SMOOTHING SIGNAL + NO
47.              *ISE ONCE )

```

```

48.      GO TO 218
49.      WRITE(6,217)
50.      217 FORMAT( 1H1, 20X 47FOURIER COEFFICIENTS FOR SMOOTHING SIGNAL TWTC
51.      *E )
52.      218 WRITE(6,219) (B(I), I=1,NPM )
53.      219 FORMAT( 10X 10E10.3 )
54.      DO 220 I=1,NPM
55.      CI = I
56.      220 B(I) = B(I)*COS(PI*CI/(2.0*P))**2
57.      WRITE(6,221)
58.      221 FORMAT( / 20X, 40FOURIER COEFFICIENTS FILTERED BY COS**2 )
59.      WRITE(6,219) (B(I), I=1,NPM )
60.      IF(IOPT.EQ.1) GO TO 230
61.      NMAX = IOPT
62.      GO TO 300
63.      230 BT = 0.0
64.      DO 240 I=1,20
65.      NPI = NP-I
66.      240 BT = BT+B(NPI)**2
67.      K = 20
68.      245 N = NP-K
69.      BE = B(N-1)**2
70.      CK = K
71.      BET = BT/CK
72.      IF(BE/BET-16.0) 250,250, 280

```

```

73. 250 IF(N=2) 260, 260, 270
74. 260 NMAX = NP/10
75.   WRITE(6,261)
76. 261 FORMAT( 20X, 11HTEST FAILED )
77.   GO TO 300
78. 270 K = K+1
79.   BT = BT + BE
80.   GO TO 245
81. 280 IF(N=25) 290, 270, 270
82. 290 NMAX = N+2
83. 300 WRITE(6,301) NMAX
84. 301 FORMAT( / 20X, 22HSMOOTHING ROUTINE USED 13,13H COEFFICIENTS )
85.   CALL FOURI ( NMAX, NP, B, YC )
86.   X = 0
87.   DO 310 K=1, NP
88.     YK = YC(K) + YI + YF*X
89.     YC(K) = YK*YK
90.   310 X = X + DX
91.   IF(YMIN.LT.0) GO TO 320
92.   RETURN
93. 320 DO 330 I=1, NP
94.     YC(I) = YC(I) + YMIN
95. 330 CONTINUE
96.   RETURN
97.   END

```

FIND OF LISTING. 0 *DIAGNOSTIC* MESSAGE(S).

CMT 140

FOR FOUR,FOUR
UNIVAC 1105 FORTRAN IV LEVEL 2201 0029 F4614B
THIS COMPILATION WAS DONE ON 01 MAY 68 AT 14:22:16

SUBROUTINE FOUR ENTRY POINT 000127

```
1. SUBROUTINE FOUR(NP,Y,B)
2. DIMENSION Y(1), B(1)
3. PI = 3.141592653
4. CNP = NP
5. NPM = NP-1
6. CNPM = NPM
7. PION = PI/CNPM
8. COSZ = COS(PION)
9. SINZ = SIN(PION)
10. COSK = COSZ
11. SINK = SINZ
12. DO 20 K = 1,NPM
13. BK = 0.0
14. COSKI = COSK
15. SINKI = SINK
16. DO 22 I = 2,NPM
17. BK = BK + Y(I)*SINKI
18. SINI = SINKI*COSK+COSKI*SINK
19. COSI = COSKI*COSK-SINKI*SINK
20. SINKI = SINI
21. 22 COSKI = COSI
22. SINKI = SINK*COSZ+COSK*SINZ
```

23. COSKI = COSK*COSZ-SINK*SINZ

24. COSK =COSKI

25. SINK =SINKI

26. 20 B(K)=2.0*BK/CNP

27. RETURN

28. END

END OF LISTING. 0 *DIAGNOSTIC* MESSAGE(S).

0 FOR F04R1,FOURI
UNIVAC 1108 FORTRAN IV LEVEL 2201 0029 F4614B
THIS COMPILATION WAS DONE ON 01 MAY 68 AT 14:24:17

SUBROUTINE FOUR1 ENTRY POINT 000142

```
1. SUBROUTINE FOUR1 ( NMAX, NP, B, Y )
2. DIMENSION E(1), Y(1)
3. NPM = NP-1
4. CNPM = NPM
5. PI = 3.141592653
6. PIOM = PI/CNPM
7. COSZ = COS(PIOM)
8. SINZ = SIN(PIOM)
9. Y(1) = 0.0
10. COSK = COSZ
11. SINK = SINZ
12. DO 20 K = 2, NP
13. YK = 0.0
14. PIK = PIOM
15. COSKI = COSK
16. SINKI = SINK
17. DO 22 I = 1, NMAX
18. YK = YK+B(I)*SINKI
19. YDK = YDK + PIK*B(I)*COSKI
20. PIK = PIK+PIOM
21. SINI = SINKI*COSK+COSKI*SINK
22. COSI = COSKI*COSK-SINKI*SINK
```

23. COSKI = COSI
24. SINKI = SINI
25. 22 CONTINUE
26. COSKI = COSK*COZ-SINK*SINZ
27. SINKI = COSK*SINZ+SINK*COZ
28. COSK = COSKI
29. SINK = SINKI
30. 20 Y(K) = YK
31. RETURN
32. END

END OF LISTING. 0 *DIAGNOSTIC* MESSAGE(S).

MP FOR DIFF,DIFF
UNIVAC 1108 FORTRAN IV LEVEL 2201 0029 F46148
THIS COMPILATION WAS DONE ON 01 MAY 68 AT 14:22:18

SUBROUTINE DIFF ENTRY POINT 000031

```
1. SUBROUTINE DIFF(Y,YD,NP)
2. C ROUTINE TO TAKE DIFFERENCES
3. DIMENSION Y(1) ,YD(1)
4. C
5. NPM1 = NP - 1
6. DO 100 I=2,NPM1
7. YD(I)=(Y(I+1)-Y(I-1))*0.5
8. 100 CONTINUE
9. YD(1)=Y(2)-Y(1)
10. YD(NP)=Y(NP)-Y(NPM1)
11. RETURN
12. END
```

END OF LISTING. 0 *DIAGNOSTIC* MESSAGE(S).

DIFF 020
DIFF 030
DIFF 040
DIFF 050

DIFF 060
DIFF 070
DIFF 080
DIFF 090
DIFF 100
DIFF 110
DIFF 120

#P FOR PLOT,PLOT
 UNIVAC 1108 FORTRAN IV LEVEL 2201 0029 F46148
 THIS COMPILATION WAS DONE ON 01 MAY 68 AT 14:22:20

SUBROUTINE PLOT ENTRY POINT 000510

DIAGNOSTIC THE NAME OR APPEARS IN A DIMENSION OR TYPE STATEMENT BUT IS NEVER REFERENCED.

1.	SUBROUTINE PLOT(X,Y,N,N1,N2,NOUT)	PLOT010
2.	DIMENSION X(1),Y(1),IP(150),B(6),A(1A),NB(6),NA(18)	PLOT020
3.	DIMENSION B1(6),B2(6),B3(6),NB1(6),NB2(6),NB3(6)	PLOT030
4.	EQUIVALENCE (A,NA),(B,NB),(C,NC),(D,ND)	PLOT040
5.	EQUIVALENCE (B1,NB1),(B2,NB2),(B3,NB3)	PLOT050
6.	X=ABCISSA VALUES TO BE PLOTTED	PLOT060
7.	Y=ORDINATE VALUES TO BE PLOTTER	PLOT070
8.	N=NUMBER OF POINTS TO BE PLOTTED (150 OR LESS)	PLOT080
9.	IF N IS NEGATIVE THE Y ARRAY IS IN DESCENDING ORDER	PLOT090
10.	N1=NUMBER OF PRINT WHEELS TO BE USED (108 OR LESS)	PLOT100
11.	N2=NUMBER OF LINES TO BE USED (RECOMMEND 50)	PLOT110
12.	NOUT=TAPE NO. OF OUTPUT TAPE	PLOT120
13.	RESTORATION AND HEADING OF PAGE IS LEFT TO USER	PLOT130
14.	-----PLOT140	PLOT140
15.	ALL BLANKS	PLOT150
16.	ALL NEGATIVE SIGNS - BOTTOM LINE USE	PLOT170
17.	DATA C/6H /	PLOT160
18.	DATA U/6H-----/	PLOT180
19.	STARS IN VARIOUS POSITIONS - BLANKS FILLED IN (6)	PLOT190
20.	SUBSTITUTE OCTAL EQUIVALENT OF * IN THIS STATEMENT	PLOT200

```

21. DATA B/6HK00000,6H0K0000,6H00K000,6H000K00,6H0000K0,6H00000K,6H000000K/ PLOT0210
22. C MASK FOR PICKING OUT SECTOR PLOT0220
23. DATA B1/077000000000,0007700000000,000007700000000, PLOT0230
24. 1000000077000,000000007700,000000000077/ PLOT0240
25. C MASK FOR COMPARING TO BLANK PLOT0250
26. DATA B2/6H 00000,6H0 0000,6H00 000,6H000 00,6H0000 00,6H00000 0,6H000000 0, PLOT0260
27. C MASK FOR SUBTRACTING ONE PLOT0270
28. DATA B3/6H000000,6H000000,6H000000,6H000000,6H000000,6H000000,6H000000, PLOT0280
29. DATA LARGE/0001000000000/ PLOT0290
30. INTEGER AND,OR PLOT0300
31. C ----- PLOT0310
32. IFL6=1 PLOT0320
33. IF(N.LT.0)IFL6=2 PLOT0330
34. N=IABS(N) PLOT0340
35. C INITIALIZES FORMAT PLOT0350
36. DO 9 L=1,18 PLOT0360
37. 9 A(L)=C PLOT0370
38. C SEARCHES X POINTS FOR HIGHEST AND LOWEST VALUES PLOT0380
39. XMIN=1.E+38 PLOT0390
40. XMAX=-1.E+38 PLOT0400
41. DO 10 I=1,N PLOT0410
42. XMAX=AMAX1(XMAX,X(I)) PLOT0420
43. 10 XMIN=AMIN1(XMIN,X(I)) PLOT0430
44. DELTAX=(XMAX-XMIN)/(FLOAT(N1-1)) PLOT0440
45. C REORDERS Y INTO DESCENDING VALUES PLOT0450

```

```

46.          GO TO (20,15),IFLG
47.          DO 16 I=1,N
48.             IP(I)=I
49.             16 CONTINUE
50.             YMAX=Y(1)
51.             YMIN=Y(N)
52.             GO TO 25
53.             DO 21 I=1,N
54.                IP(I)=0
55.                21 CONTINUE
56.                DO 23 I=1,N
57.                   YMAX=-1.E3A
58.                   DO 22 J=1,M
59.                      IF(IP(J).GE.LARGE) GO TO 22
*DIAGNOSTIC* THE TEST FOR EQUALITY BETWEEN NON-INTEGERS MAY NOT BE MEANINGFUL.
60.                IF(Y(J).LE.YMAX) GO TO 22
61.                YMAX=Y(J)
62.                KK=J
63.                22 CONTINUE
64.                IP(I)=IP(I)+KK
65.                IP(KK)=IP(KK)+LARGE
66.                23 CONTINUE
67.                DO 24 I=1,N
68.                   IP(I)=IP(I)-LARGE
69.                   24 CONTINUE

```

```

PLOTn460
PLOTn470
PLOTn480
PLOTn490
PLOTn500
PLOTn510
PLOTn520
PLOTn530
PLOTn540
PLOTn550
PLOTn560
PLOTn570
PLOTn580
PLOTn590
PLOTn600
PLOTn610
PLOTn620
PLOTn630
PLOTn640
PLOTn650
PLOTn660
PLOTn670
PLOTn680
PLOTn690

```

```

70.      IX1=IP(1)          PLOT0700
71.      IX2=IP(N)         PLOT0710
72.      YMAX=Y(IX1)      PLOT0720
73.      YMIN=Y(IX2)      PLOT0730
74.      25 DELTAY=(YMAX-YMIN)/(FLOAT(N2-1)) PLOT0740
75.      DELT=YMAX        PLOT0750
76.      C PLOTTING SECTION PLOT0760
77.      DO 41 K=1,N      PLOT0770
78.      I=IP(K)         PLOT0780
79.      J=IP(K+1)       PLOT0790
80.      IF(K-1)33,33,30 PLOT0800
81.      30 IF(L)31,31,33 PLOT0810
82.      31 DELT=DELTAY   PLOT0820
83.      IF(Y(1)-DELT+.001) 32, 33, 33
84.      C PRINTS BLANK LINES PLOT0840
85.      32 L=-1         PLOT0850
86.      GO TO 37        PLOT0860
87.      C PRINT WHEEL POSITION (0,1,2,3,...,N1-1) PLOT0870
88.      33 NPWP=(X(I)-XMIN)/DELTAY PLOT0880
89.      C SECTOR(1,2,3,4,5,...,N1/6+1) PLOT0890
90.      NSECT=(NPWP/6)+1 PLOT0900
91.      C POSITION IN SECTOR(1,2,3,4,5,6) PLOT0910
92.      NF=MOD(NPWP,6)+1 PLOT0920
93.      C PLACES * IN FORMAT PLOT0930
94.      C ----- PLOT0940

```

```

95.      NTST=AND(NA(NSECT),NB1(NF))          PLOT0950
96.      IF(NTST.EQ.NB2(NF)) GO TO 100      PLOT0960
97.      NA(NSECT)=NA(NSECT)-NB3(NF)        PLOT0970
98.      GO TO 101                          PLOT0980
99.      100 NA(NSECT)=NA(NSECT)+NB(NF)      PLOT0990
100.     101 CONTINUE                       PLOT1000
101.     C-----PLOT1010
102.     IF(K=N)34,36,36                    PLOT1020
103.     C REPEATS IF Y(I) AND Y(J) ARE CLOSER THAN DELTAY PLOT1030
104.     34 IF(Y(J)-DELT+.001) 36, 35, 35
105.     35 L=1
106.     GO TO 41
107.     36 L=0
108.     C PRINTING ROUTINE
109.     37 CONTINUE
110.     WRITE (NOUT,38)DELT,(A(IL),IL=1,18)
111.     38 FORMAT ( 1PE10.3, 2H I, 18A6 )
112.     IF(L)31,39,39
113.     C RESTORES FORMAT          PLOT1120
114.     39 DO 40 IL=1,18          PLOT1130
115.     40 A(IL)=C                PLOT1140
116.     41 CONTINUE              PLOT1150
117.     C DRAWS BOTTOM AXIS      PLOT1160
118.     DO 42 I=1,18              PLOT1170
119.     42 A(I)=0                  PLOT1180
                                  PLOT1190

```

```

120.      WRITE (NOUT,43)(A(I),I=1,18)
121.      43 FORMAT(12X,18A6)
122.      C   RESTORES A ARRAY TO BLANKS
123.      DO 44 I=1,18
124.      44 A(I)=C
125.      C   SETS UP * EVERY 10 PLACES FOR LOWER AXIS
126.      DO 45 I=2,12*5
127.      NA(I)=NA(I)+NB(4)
128.      NA(I+2)=NA(I+2)+NB(2)
129.      45 NA(I+3)=NA(I+3)+NB(6)
130.      NA(17)=NA(17)+NB(4)
131.      NA(1)=NA(1)+NB(1)
132.      WRITE (NOUT,43)(A(I),I=1,18)
133.      DELTAX=((XMAX-XMIN)/FLOAT(N1))*10.0
134.      DO 46 I=1,11
135.      46 A(I)=XMIN+FLOAT(I-1)*DELTAX
136.      WRITE (NOUT,47)(A(I),I=2,11)
137.      47 FORMAT(15X,1P10E10.4)
138.      RETURN
139.      END
END OF LISTING.      2 *DIAGNOSTIC* MESSAGE(S).

```

SUMMATION LH21 AND LH22 TWO CYCLES RESULTS NO. 01., BY CURRENT

REQUESTED DATA FROM LIBRARY TAPE

RUN	LH21	CYCLE 1	REF. POINT 1
RUN	LH21	CYCLE 2	REF. POINT 1
RUN	LH22	CYCLE 1	REF. POINT 1
RUN	LH22	CYCLE 3	REF. POINT 1

STEP 5: COPY

The COPY program is used to make a backup tape for the data library tape. A backup tape is kept at all times. It is suggested that after every ten experiments, the library tape be copied onto the backup tape.

Below is a complete set of cards that comprise the COPY deck.

1	2	3	4	5	6	7	8	9	0	1	2	3	4	5	6	7	8	9	0	1	2	3	4	5	6	7	8	9	0	1	2	3	4	5	6	7	8	9	0
V	ASG	A=DATA	LIBRARY	TAPE	NUMBER																																		
V	ASG	B=BACKUP	TAPE	NUMBER																																			
V	XGT	MATCH																																					
.	DUP	A,B																																					
.	TEF	B																																					
.	TRW	A,B																																					
.	CMP	A,B																																					
.	TRI	A,B																																					

After the backup tape is written, a comparison is made. If the two tapes do not match, the output listing from COPY will so indicate.

No listing is given for this program.

STEP 6: UPDATE

Using the UPDATE program, five types of changes can be made to the data library tape. These five changes are described below.

<u>Type Number</u>	<u>Description of Change</u>
1	Allows the user to change any word of the data that was on the card for TEDIT
2	Allows the user to delete an entire experiment from the library tape
3	Causes an entire cycle to be deleted from an experiment and remaining cycles to be re-sequenced
4	Allows the signal + noise, noise, and current values for a particular channel number of a cycle to be changed
5	Allows any channel number, along with its signal + noise, noise, and current values, to be deleted from any cycle of an experiment

Card formats for the preceding changes are as follows:

Type 1

First Card

Column

6	Punch one (1)
7-12	Experiment number

Second Card

Identical to that used for TEDIT except for information to be changed

Type 2

Column

6	Punch two (2)
7-12	Experiment number

Type 3

Column

6	Punch three (3)
7-12	Experiment number
13-18	Cycle number

Type 4

Column

6	Punch four (4)
7-12	Experiment number
13-18	Cycle number
19-24	Channel number
25-30	Signal + noise value
31-36	Noise value
37-42	Current value

The last three items are always changed together; therefore, if no change is desired, the existing value must be entered.

Type 5

Column

6	Punch five (5)
7-12	Experimental number
13-18	Cycle number
19-24	Channel number

The different types of change cards for any one experiment should be in the following sequence: 2, 3, and 4 (in any sequence), 5, and 1. If more than one type 5 change is to be made for any one cycle in any one experiment, cards should be in descending channel-number order, the largest first. This order eliminates the necessity of later change cards that reflect the changes made by previous change cards.

If more than one experiment is to be changed, then the individual groups of change cards must be in the same order as on the library tape (excluding experiments that are not to be changed).

9 FOR UDATE.UPDATE
UNIVAC 1108 FORTRAN IV LEVEL 2201 0029 F46148
THIS COMPILATION WAS DONE ON 21 JUN 68 AT 17:09:44

MAIN PROGRAM ENTRY POINT 000000

```
1.        PARAMETER LTAPE = 9, NTAPE = 10
2.        INTEGER CHAN, CYCLE
3.        REAL NOISE
4.        COMMON IIRUN, GAS, VAR, TIME, RES, DVOLT, VOLTST, TINT, SIGMIN,
5.        *    SIGMAX, CURMIN, CURMAX, DATE(2), CHAN(100,100), SPLUSN(100,100)
6.        *    NOISE(100,100), CURR(100,100), CYCLE(100), L(100), LAST(100)
7.        *    NMAX
8.        REWIND LTAPE
9.        REWIND NTAPE
10.        CALL INRUN(LTAPE)
11.        C.. READ A CHANGE TYPE CARD..
12.        10 READ(5,11) ITYPE, NRUN, NNCYC, NCHAN, XSPN, XN, XCURR
13.        11 FORMAT( I6, A6, I6, I6, 3F6.0 )
14.        IF(ITYPE.EQ.0) GO TO 80
15.        20 IF(NRUN.EQ.IRUN) GO TO 25
16.        C.. WRITE OUT RUN THAT IS IN MEMORY..
17.        CALL OUTRUN(NTAPE)
18.        C.. WAS THIS THE LAST RUN ON LTAPE?
19.        IF(LAST(NMAX).EQ.2) GO TO 110
20.        C.. READ IN A NEW RUN..
21.        CALL INRUN (LTAPE)
```

```

22.      60 TO 20
23.      C.. DETERMINE WHICH TYPE OF CHANGE IS TO BE MADE..
24.      25 GO TO (30, 40, 50, 60, 70), ITYPE
25.      C.. MAIN DATA IS TO BE CHANGED. TYPE 1.
26.      30 READ(5,31) IRUN, GAS, VAR, TIME, RES, DVOLT, VOLTST, TINT, SIGMIN,
27.      * SIGMAX, CURMIN, CURMAX, DATE(1), DATE(2)
28.      31 FORMAT( 2A6, F6.0, A6, 8F6.0, A6, A1 )
29.      60 TO 10
30.      C
31.      C.. DELETE THE RUN NOW IN MEMORY.. TYPE 2.
32.      40 IF(LAST(NMAX),EQ,2) GO TO 100
33.      C.. READ IN ANOTHER RUN FROM TAPE.
34.      CALL INRUN(LTAPE)
35.      60 TO 10
36.      C.. DELETE CYCLE NCYC WHICH IS NOW IN MEMORY. TYPE 3.
37.      C.. CYCLE NUMBERS WILL BE RE-SEQUENCED IN OUTRUN.
38.      50 IF(NCYC.LE.0.OR.NCYC.GT.NMAX) GO TO 130
39.      CYCLE(NCYC) = 0
40.      60 TO 10
41.      C.. CHANGE DATA OF CYCLE NUMBER NCYC AND CHANNEL NUMBER NCHAN. TYPE 4.
42.      60 IF(NCYC.LE.0.OR.NCYC.GT.NMAX) GO TO 130
43.      KCHAN=NCHAN+1
44.      CHAN(KCHAN,NCYC) = NCHAN
45.      SPLUSN(KCHAN,NCYC) = XSPN
46.      NOISE(KCHAN,NCYC) = XN

```

```

47. CURR(KCHAN,NCYC) = XCURR
48. GO TO 10
49. C.. CHANNEL NUMBER NCHAN IN CYCLE NCYC IS TO BE DELETED. TYPE 5.
50. 70 IF(NCYC.LE.0.OR.NCYC.GT.NMAX) GO TO 130
51. IF(NCHAN*1.EQ.L(NCYC))GO TO 78
52. JM = L(NCYC)
53. JP1 = NCHAN + 2
54. DO 75 I=JP1,JM
55. C.. CHAN(I-1,NCYC) = CHAN(I,NCYC)
56. SPLUSN(I-1,NCYC) = SPLUSN(I,NCYC)
57. NOISE(I-1,NCYC) = NOISE(I,NCYC)
58. 75 CURR(I-1,NCYC) = CURR(I,NCYC)
59. 78 L(NCYC) = L(NCYC) - 1
60. GO TO 10
61. C.. WRITE OUT THE RUN THAT IS IN MEMORY.
62. 88 CALL OUTRUN (NTAPE)
63. C.. THERE ARE NO MORE CHANGES TO BE MADE, COPY REST OF LTAPE.
64. 90 IF(LAST(NMAX).EQ.2) GO TO 100
65. CALL INRUN(LTAPE)
66. CALL OUTRUN(NTAPE)
67. GO TO 90
68. 100 BACKSPACE NTAPE
69. LAST(NMAX) = 2
70. WRITE(NTAPE) LAST(NMAX)
71. END FILE NTAPE

```

```

72.      CALL REWI(LTAPE)
73.      REWIND NTAPE
74.      CALL EXIT
75.      110 WRITE(6,111) NRUN
76.      111 FORMAT( /, 33H REQUESTED CHANGE FOR RUN NUMBER , A6, 57H IS NOT IN
77.          * SEQUENCE OR THE RUN NUMBER ITSELF IS IN ERROR. / )
78.      GO TO 100
79.      130 WRITE(6,131) NCYC, NRUN
80.      131 FORMAT( /, 14H CYCLE NUMBER , I6,25H IS OUT OF RANGE FOR RUN A6 /)
81.      GO TO 100
82.      END
END OF LISTING.      0 *DIAGNOSTIC* MESSAGE(S).

```


2) FOR INRUN,INRUN
 UN:VAC 1108 FORTRAN IV LEVEL 2201 0029 F46148
 THIS COMPILATION WAS DONE ON 21 JUN 68 AT 17:09:46

SUBROUTINE INRUN ENTRY POINT 000204

```

1. SUBROUTINE INRUN (LTAPE)
2. INTEGER CHAN, CYCLE
3. REAL NOISE
4. COMMON IRUN, GAS, VAR, TIME, RES, DVOLT, VOLTST, TINT, SIGWIN,
5. * SIGMAX, CURMIN, CURMAX, DATE(2), CHAN(100,100), SPLUSN(100,100)
6. * , NOISE(100,100), CURR(100,100), CYCLE(100), L(100), LAST(100)
7. * , NMAX
8. READ(LTAPE) IRUN, GAS, VAR, TIME, RES, DVOLT, VOLTST, TINT, SIGWIN,
9. * SIGMAX, CURMIN, CURMAX, DATE(1), DATE(2)
10. N = 0
11. C
12. 10 N = N + 1
13. IF(N.GT.100) GO TO 20
14. READ(LTAPE) CYCLE(N), L(N)
15. IMAX = L(N)
16. READ(LTAPE) ( CHAN(I,N), SPLUSN(I,N), NOISE(I,N), CURR(I,N), I=1,
17. * IMAX )
18. READ(LTAPE) LAST(N)
19. IF(LAST(N).EQ.0) GO TO 10
20. NMAX = N
21. RETURN
  
```

```

22. C DELETE THE REMAINDER OF THIS EXPERIMENT, IT EXCEEDS 100 CYCLES.
23. 20 READ(LTAPE) DUMMY, IDUM
24. READ(LTAPE) (DUMMY, DUMMY, DUMMY, DUMMY, I=1, IDUM)
25. READ(LTAPE) ILAST
26. IF(ILAST.EQ.0) GO TO 20
27. NMAX = 100
28. LAST(NMAX) = ILAST
29. 30 WRITE(6,31) IRUN
30. 31 FORMAT( /, 5X, A6,86H EXCEEDED 100 CYCLES, THE REMAINING CYCLES WA
31. *VE BEEN DELETED *** SORRY ABOUT THAT ***. )
32. RETURN
33. END

```

END OF LISTING. 0 *DIAGNOSTIC* MESSAGE(S).

9 FOR OTRUN,OUTRUN
 UNIVAC 1108 FORTRAN IV LEVEL 2201 0029 F4G148
 THIS COMPILATION WAS DONE ON 21 JUN 68 AT 17:09:48

SUBROUTINE OTRUN ENTRY POINT 000142

```

1. SUBROUTINE OTRUN(NTAPE)
2. INTEGER CHAN, CYCLE
3. REAL NOISE
4. COMMON IRUN, GAS, VAR, TIME, RES, DVOLT, VOLTST, TINT, SIGMIN,
5. * SIGMAX, CURMIN, CURMAX, DATE(2), CHAN(100,100), SPLUSN(100,100)
6. * NOISE(100,100), CURR(100,100), CYCLE(100), L(100), LAST(100)
7. * NMAX
8. WRITE(NTAPE) IRUN, GAS, VAR, TIME, RES, DVOLT, VOLTST, TINT,
9. * SIGMIN, SIGMAX, CURMIN, CURMAX, DATE(1), DATE(2)
10. ICYC = 0
11. DO 20 N=1,NMAX
12. IF(CYCLE(N).EQ.0) GO TO 20
13. ICYC = ICYC + 1
14. WRITE(NTAPE) ICYC, L(N)
15. IMAX = L(N)
16. WRITE(NTAPE) (CHAN(I,N), SPLUSN(I,N), NOISE(I,N), CURR(I,N), I=1,
17. * IMAX )
18. WRITE(NTAPE) LAST(N)
19. DO CONTINUE
20. BACKSPACE NTAPE
21. WRITE(NTAPE) LAST(NMAX)
22. RETURN
23. END
  
```

END OF LISTING. 0 *DIAGNOSTIC* MESSAGE(S).

STEP 7: LEØF (List and End of File)

One input card, in FORTRAN format (A6, I6), is necessary for execution of this program.

Column

1-6	INUM = last valid experiment number
7-12	LCYCLE = last valid cycle number

After LEØF has encountered the last valid cycle number on the library tape, an end of file is written.

A program listing follows.

FOR LEUF,LEOP
 UNIVAC 1108 FORTRAN IV LEVEL 2201 0029 F46148
 THIS COMPILATION WAS DONE ON 07 MAY 68 AT 11:58:51

```

MAIN PROGRAM      ENTRY POINT 000000

1.  C.. THE PURPOSE OF THIS ROUTINE IS TO READ THE LIBRARY TAPE AND LIST ALL
2.  C  DATA BY RUN NUMBER AND BY CYCLE NUMBER.
3.  C  PARAMETER LTAPE = 10
4.  C  INTEGER CHAN
5.  C  REAL NOISE
6.  C  DIMENSION CHAN(100), SPLUSN(100), NOISE(100), CURR(100), DATE(2)
7.  C  REWIND LTAPE
8.  C  READ(5,7) INUM, LCYCLE
9.  C  7:FORMAT( A6, I6)
10. C  8 READ(LTAPE) NUM, ITYPE, VAR, TIME, RES, OVOLT, VOLTST, TINT,
11. C  1 SIGMIN, SIGMAX, CURMIN, CURMAX, DATE(1), DATE(2)
12. C  WRITE(6,11) NUM
13. C  11 FORMAT( 10X, 10HRUN NUMBER, 1X, A6, / )
14. C  WRITE(6,12) ITYPE
15. C  12 FORMAT( 10X, 3HGAS, 1X, A6, / )
16. C  WRITE(6,13) VAR
17. C  13 FORMAT( 10X, 10HVARIANC %, 1X, F6.2, / )
18. C  WRITE(6,14) TIME
19. C  14 FORMAT( 10X, 4HTIME, 1X, A6, / )
20. C  WRITE(6,15) RES
21. C  15 FORMAT( 10X, 4HRES, 1X, F6.2, / )
  
```

```

22.      WRITE(6,16) DVOLT
23.      16 FORMAT( 10X, 17HVOLTAGE INCREMENT, 1X, F6.2, / )
24.      WRITE(6,17) VOLTST
25.      17 FORMAT( 10X, 17HSTARTING VOLTAGE , 1X, F6.2, / )
26.      WRITE(6,18) TINT
27.      18 FORMAT( 10X, 14HTIME INTERVAL , F6.2, / )
28.      WRITE(6,19) SIGMIN
29.      19 FORMAT( 10X, 12HMIN. SIGNAL , F10.2, / )
30.      WRITE(6,20) SIGMAX
31.      20 FORMAT( 10X, 12HMAX. SIGNAL , F10.2, / )
32.      WRITE(6,21) CURMIN
33.      21 FORMAT( 10X, 13HMIN. CURRENT , F10.2, / )
34.      WRITE(6,22) CURMAX
35.      22 FORMAT( 10X, 13HMAX. CURRENT , F10.2, / )
36.      WRITE(6,23) DATE(1), DATE(2)
37.      23 FORMAT( 10X, 4HDATE, 1X, 2A6, / )
38.      10 READ(LTAPE) KOUNT, L
39.      C
40.      WRITE(6,24) KOUNT
41.      24 FORMAT( 10X, 12HCYCLE NUMBER, 1X, I3, / )
42.      WRITE(6,25) L
43.      25 FORMAT( 10X, 16HNUMBER OF POINTS, I5, // )
44.      C
45.      READ(LTAPE) (CHAN(I), SPLUSN(I), NOISE(I), CURR(I), I=1,L )
46.      IF(NUM.EQ.INUM.AND.KOUNT.EQ.LCYCLE) GO TO 40

```

```
47.      READ(LTAPE) LAST
48.      IF(LAST.EQ.0) GO TO 10
49.      WRITE(6,31)
50.      31 FORMAT( 1H1 )
51.      IF(LAST.EQ.1) GO TO 8
52.      WRITE(6,28)
53.      28 FORMAT(/ 12H END OF FILE )
54.      CALL REWI(LTAPE)
55.      CALL EXIT
56.      40 LAST = 2
57.      WRITE(LTAPE) LAST
58.      END FILE LTAPE
59.      WRITE(6,28)
60.      CALL REWI(LTAPE)
61.      CALL EXIT
62.      END
```

END OF LISTING. 0 *DIAGNOSTIC* MESSAGE(S).

STEP 8: SMOOTH

This program Fourier-smooths data, unfolds a given Gaussian electron energy distribution from the data, and gives the results for the derivative of the function in tabular form. The program is prepared to accept card input. The deck of cards needed is generated as one of the options in ABEAM4.

The normal output of this program, which in its present form was prepared for the study of autoionization in molecular gases, is:

1. Input data Fourier-smoothed
2. Derivative of Fourier-smoothed square root of the data
3. Derivative of Fourier-smoothed data
4. Derivative of Fourier-smoothed data with energy distribution unfolded for case 1
5. Derivative of Fourier-smoothed data with energy distribution unfolded for case 2
6. Derivative of Fourier-smoothed data with energy distribution unfolded for case 3

At present there is one graphic output, which gives the input data Fourier-smoothed once.

The input sequence and card formats are given below.

Title Card: FORTRAN format is (12A6)

Column

1-72 Title (printed at top of first page)

First Data Card: FORTRAN format is (3I6, 3F6.0, I6)

Column

6 IN = 0: accept Y values as input
= 1: after reading in Y values below, read YT values
and compute $Y = Y - YT$

12 ISTOP = 0: last problem
= 1: read in another title card for a new problem

18 NDEL = number of delta (Δ) values to follow

19-24 DEL (1) = Δ value(s) for unfolding

FOR SMOOTH,SMOGT;
 UNIVAC 1108 FOKTRAN IV LEVEL 2201 0029 F4614B
 THIS COMPILATION WAS DONE ON 29 APR 68 AT 13:17:09

```

MAIN PROGRAM      ENTRY POINT 000000
1.  C      PROGRAM SMOOTHS
2.  DIMENSION Y(300),YT(300),D(300),YD(300),DYS(300,3),DEL(3),YDS(300)
3.  DIMENSION LABEL(12)
4.  DIMENSION VOLT(100)
5.  12 WRITE(6,124)
6.  124 FORMAT(1H1)
7.  READ(5,15) (LABEL(I), I=1,12)
8.  15 FORMAT(12A6)
9.  READ(5,16) IN, ISTOP, NDEL, DEL(1), DEL(2), DEL(3), NMAX
10.  16 FORMAT( 3I6, 3F6.0, I6 )
11.  WRITE(6,151) (LABEL(I), I=1,12)
12.  151 FORMAT(4X, 12A6 )
13.  READ (5,17)SI,SF,JX
14.  17 FORMAT(3F12.4)
15.  HL = (SF-SI)
16.  NPM = HL/UX+.1
17.  NP = NPM+1
18.  READ(5,18) (Y(I), I=1,NP)
19.  18 FORMAT(6F12.4)
20.  IF (IN)20,20,19
21.  19 READ (5,19) (YT(I), I=1,NP)
22.  DO 14 I = 1,NP
23.  14 Y(I) = Y(1)-YT(I)
24.  20 WRITE(6,174)NP,SI,DX,SF
25.  174 FORMAT(23X,27HFOURIER SMOOTHING OF SIGNAL / 20X,30HINPUT SIGNAL F

```

```

26. 10K DATA RANGE... 14,1X,1H(F5.2,1H/F4.2,1H/F5.2,5H)E.V. )
27. WRITE(6,1B1)(Y(I),I=1,NP)
28. 1B1 FORMAT(10X,10F8.0)
29. YMIN = 1.E+37
30. DO 205 I=1,NP
31. YMIN = AMINI(YMIN, Y(I) )
32. 205 CONTINUE
*DIAGNOSTIC* THE TEST FOR EQUALITY BETWEEN NON-INTEGERS MAY NOT BE MEANINGFUL.
33. IF (YMIN.GE.0) GO TO 210
34. DO 206 I=1,NP
35. Y(I) = Y(I) - YMIN
36. 206 CONTINUE
37. 210 WRITE(6,1B2)
38. 1B2 FORMAT(/20X,42HFOURIER COEFFICIENTS OF SQUARE ROOT SIGNAL /)
39. X = 0.0
40. Y1 = SQRT(Y(1))
41. YF = (SQRT(Y(NP))-Y1)/HL
42. DO 21 I = 1,NP
43. Y(I) = SQRT(Y(I))-YI-YF*X
44. 21 X = X+DX
45. CALL FOUR(NP,Y,B)
46. WRITE(6,1B3) (3(K),K=1,NPM)
47. 1B3 FORMAT(10X,10E10.3)
48. PI = 3.141592653
49. CNPM = NPM
50. DO 186 I = 1,NPM
51. CI = I

```

```

52. 186 B(I) = B(I)*COS(PI*CI/(2.0*CNPM))**2
53. WRITE(6,135)
54. 185 FORMAT(/20X,47HFOURIER COMPONENTS FILTERED BY COS**2 ATTENUATION )
55. WRITE(6,183)(B(K),K=1,NPM)
56. IF (NMAX.NE.0) GO TO 35
57. BT = 0.0
58. DO 24 I = 1,20
59. NPI = NP-I
60. 24 BT = BT+B(NPI)**2
61. K = 20
62. 201 N = NP-K
63. BE = B(N-1)**2
64. CK = K
65. BLT = BT/CK
66. IF (BE/BET-16.)27,27,28
67. 27 IF (N-2)29,29,33
68. 29 NMAX = NP/10
69. WRITE(6,291)
70. 291 FORMAT(/20X,11HTEST FAILED /)
71. GO TO 35
72. 33 K = K+1
73. BT = BT+BE
74. GO TO 261
75. 28 IF (N-25)231,33,33
76. 261 NMAX = N+2
77. 35 CONTINUE
78. WRITE(6,36)NMAX

```

```

79. CALL FOUR4(NMAX, NP, B, Y, YD)
80. J6 FORMAT(2UX, 24HSMOOTHED SQUARE ROOT HAS I4, IX, 18HFOURIER COMPONENT
81. 15 / )
82. X=0.0
83. DO 37 K = 1, NP
84. YK = Y(K)+YI+YF*X
85. Y(K) = YK*YK
86. J7 X = X+DX
*DIAGNOSTIC* THE TEST FOR EQUALITY BETWEEN NON-INTEGERS MAY NOT BE MEANINGFUL.
87. IF (YMIN.GE.0) GO TO 44
88. DO 43 I=1, NP
89. Y(I) = Y(I) + YMIN
90. J3 CONTINUE
91. 44 NPNT = NP - 2
92. DO 45 I = 1, 2
93. 45 YUS(I) = 0.0
94. DO 46 I = 3, NPNT
95. 46 YUS(I) = 0.10*(-2.0*Y(I-2)-Y(I-1)+Y(I+1)+2.0*Y(I+2))
96. DO 465 I = NPNT, NP
97. 465 YUS(I) = 0.0
98. DO 60 J=1, NDEL
99. CALL UNFSUR(NMAX, NP, HL, DEL(J), DX, YI, YF, B, YT)
100. DO 40 I = 1, 2
101. 40 DYS(I, J) = 0.0
102. DO 41 I = 3, NPNT
103. 41 DYS(I, J) = 0.10*(-2.0*Y(I-2)-Y(I-1)+Y(I+1)+2.0*Y(I+2))
104. DO 42 I = NPNT, NP

```

```

105. 42 DYS(I,J) = 0.0
106. 60 CONTINUE
107. WRITE(6,51)
108. 51 FORMAT( / 20X 26HS = INPUT DATA (SMOOTHED). )
109. WRITE(6,52)
110. 52 FORMAT( / 20X 57HDSA = DERIVATIVE OF (SMOOTHED SQUARE ROOT OF INPU
111. *T DATA). )
112. WRITE(6,53)
113. 53 FORMAT( / 20X 26HDT(0) = DERIVATIVE OF (S). )
114. WRITE(6,54)
115. 54 FORMAT( / 20X 37HDT(.XX) = DERIVATIVE OF (UNFOLDED S). )
116. WRITE(6,61) (DEL(I), I=1,NDEL)
117. 61 FORMAT( / 18A, 1HX 13X 1HS 11X 3HDSA 9X 6H DT(0) 3(7X 3HOT(
118. 1 F4.2, 1H) ) )
119. X=SI
120. DO 70 I = 1,NP
121. WRITE(6,63) X, Y(I), YD(I), YDS(I), (DYS(I,J),J=1,NDEL)
122. 63 FORMAT( 10X, F9.2, 6F14.4 )
123. VOLT(I) = X
124. 70 X = X+DX
125. WRITE(6,901)
126. 901 FORMAT( 10I, 33HPLOT OF S SMOOTHED ONCE (FOURIER) )
127. CALL PLOT( VOLT, Y, NP, 100, 44, 6 )
128. IF(ISTOP) 72, 72, 72
129. 72 CALL EXIT 'V', 72
130. END
END OF LISTING. 2 *DIAGNOSTIC* MESSAGE(S).

```

@ FOR UNFSQR,UNFSQR
 UNIVAC 1108 FORTRAN IV LEVEL 2201 0029 F4G14B
 THIS COMPILATION WAS DONE ON 29 APR 68 AT 13:17:12

```

SUBROUTINE UNFSQR      ENTRY POINT 000440
1.  SUBROUTINE UNFSQR(NC,NP,HL,DL,DX,SI,SF,B,Y)
2.  DIMENSION Y(300), B(300),C(300),S(300),EX(300)
3.  PI = 3.141592653
4.  TLN = 0.69314716
5.  CHI = (PI*DL/HL)**2/(16.*TLN)
6.  CON = .SI*SI-(SF*DL)**2/(8.0*TLN)
7.  CLOP = 2.0*CHI*HL/PI
8.  SGN = -1.0
9.  SU1 = 0.0
10. SU2 = 0.0
11. DV 00 K = 1,NC
12. CK = K
13. SU1 = SU1 + CK*B(K)
14. SU2 = SU2 + SGN*CK*B(K)
15. 60 SGN = -SGN
16. SU1 = -2.0*SF*CLOP*SU1
17. SU2 = -2.0*SF*CLOP*SU2
18. Y(1) = CON+SU1
19. Y(NP)=(SF*HL)**2 +2.0*SI*SF*HL+CON+SU2
20. NPM = NP-1
21. X = DX
22. SINX = SIN(PI*X/HL)
  
```

23. $COSX = \cos(\pi * X / HL)$
 24. $EL = \exp(\chi)$
 25. $FC = EC * EC$
 26. $SINZ = SINX$
 27. $COSZ = COSX$
 28. $NCM = NC - 1$
 29. $NI = NC + NC$
 30. $EXPZ = 1.0$
 31. $DU \ 10 \ K = 1, NT$
 32. $EAPZ = EC * EXPZ$
 33. $EA(K) = EXPZ$
 34. $10 \ EC = FC * EC$
 35. $DU \ 50 \ M = 2, NPM$
 36. $YM = (SF * X) ** 2 + 2.0 * SF * SINX + CON$
 37. $SINK = SINX$
 38. $COSK = COSX$
 39. $DU \ 20 \ K = 1, NT$
 40. $S(K) = SINK$
 41. $C(K) = COSK$
 42. $SINKP = SINK * COSX + COSK * SINX$
 43. $COSKP = COSK * COSX - SINK * SINX$
 44. $SINK = SINKP$
 45. $20 \ COSK = COSKP$
 46. $T6 = 0.0$
 47. $DU \ 30 \ K = 1, NCM$


```

40. BK = 0.0
49. KP = K+1
50. DU 28 N = KP,NC
51. NAK = N-K
52. NPK = N+K
53. 28 BK = BK+B(N)*(EX(N,K)*C(N,K)-EX(NPK)*C(NPK))
54. 30 TG = TG + B(K)*BK
55. TH = 0.0
56. TE = 0.0
57. DU 40 K = 1,NC
58. CK = K
59. BK = B(K)
60. KI = K+K
61. TG = TG+BK*BK*(1.-EX(KT)*C(KT))/2.0
62. TH = TH +BK*EX(K)*(X*S(K)-CLOP*CK*C(K))
63. 40 TL = TE + BK*EX(K)*S(K)
64. Y(M) = TG+2.0*SF*TH+2.0*SI*TE+YM
65. X = X+DX
66. S1NK = SINX*COSZ+COSX*SINZ
67. COSK = COSX*COSZ-SINX*SINZ
68. S1NK = S1NK
69. CUSA = COSK
70. RETURN
71. END

```

END OF LISTING. 0 *DIAGNOSTIC* MESSAGE(S).

W FOR FOUR,FUCK
UNIVAC 1108 FORTRAN, IV LEVEL 2201 0029 F46148
THIS COMPILATION WAS DONE ON 25 APR 68 AT 13:17:14

SUBROUTINE FOUR ENTRY POINT 000127

```
1. SUBROUTINE FOUR(NP,Y,B)
2. DIMENSION Y(300),B(300)
3. PI = 3.141592653
4. CNP = NP
5. NPM = NP-1
6. CNPM = NPM
7. PION = PI/CNPM
8. COSZ = COS(PION)
9. SINZ = SIN(PION)
10. COSK = COSZ
11. SINK = SINZ
12. DO 20 K = 1,NPM
13. BK = 0.0
14. COSKI = COSK
15. SINKI = SINK
16. DO 22 I = 2,NPM
17. BK = BK + Y(I)*SINKI
18. SINI = SINKI*COSK+COSKI*SINK
19. COSI = COSKI*COSK-SINKI*SINK
20. SINKI = SINI
21. DO 22 COSKI = COSI
```

22. $SINKI = SINK * COSZ + COSK * SINZ$
23. $COSKI = COSK * COSZ - SINK * SINZ$
24. $COSK = COSKI$
25. $SINK = SINKI$
26. $ZO B(K) = 2.0 * BK / CNP$
27. RETURN
28. END

END OF LISTING. 0 *DIAGNOSTIC* MESSAGE(S).

FOR FOURI, FOURI
UNIVAC 1108 FORTKAM IV LEVEL 2201 0029 F46148
THIS COMPILATION WAS DONE ON 29 APR 68 AT 13:17:15

SUBROUTINE FOURI ENTRY POINT 000145

```
1. SUBROUTINE FOURI(NMAX, NP, B, Y, YC)
2. DIMENSION H(300), Y(300), YD(300)
3. NPM = NP-1
4. CNPM = NPM
5. PI = 3.141592653
6. PIOM = PI/CNPM
7. COSZ = COS(PIOM)
8. SINZ = SIN(PIOM)
9. Y(1) = 0.0
10. YD(1) = 0.0
11. COSK = COSZ
12. SINK = SINZ
13. DO 20 K = 2, NP
14. YK = 0.0
15. YDK = 0.0
16. PIK = PIOM
17. COSKI = COSK
18. SINKI = SINK
19. DO 22 I = 1, NMAX
20. YK = YK + B(I) * SINKI
21. YDK = YDK + PIK * B(I) * COSKI
```

22. $PIK = PIK + PIOM$
 23. $SINI = SINIKI * COSK + COSKI * SINK$
 24. $COSI = COSKI * COSK - SINIKI * SINK$
 25. $COSKI = CJSI$
 26. $SINKI = SINI$
 27. 22 CONTINUE
 28. $COSKI = COSK * COSZ - SINK * SINZ$
 29. $SINKI = COSK * SINZ + SINK * COSZ$
 30. $COSK = COSKI$
 31. $SINK = SINKI$
 32. $Y(K) = YK$
 33. 20 $YU(K) = YDK$
 34. RETURN
 35. END

END OF LISTING. 0 *DIAGNOSTIC* MESSAGE(S).

STEP 9: SIMCUR

The program is designed to fold into any given analytic function a Gaussian function with specified full width at half maximum, Δ , in eV units:

$$F(E) = \frac{1}{N} \int_{x_0}^{x_L} f(E') \exp\left[-\ln \frac{2}{(1/2 \Delta)^2} (E - E')^2\right] dE'$$

where the normalization function is

$$N = \int_{x_0}^{x_L} \exp\left[-\ln \frac{2}{(1/2 \Delta)^2} (E - E')^2\right] dE' .$$

In program notation the function is

$$CS(i) = \frac{\int_{x_0}^{x_L} CS(x) * \exp[-\xi(E - x)^2] dx}{\int_{x_0}^{x_L} \exp[-\xi(E - x)^2] dx} ,$$

where

$$\xi = \frac{\text{LN}(2)}{\left(\frac{1}{2} \Delta / 13.605\right)^2}$$

$$E = \frac{\text{EV}(i)}{13.605}$$

$$X_0 = E - \text{LIMITS}$$

$$X_L = E + \text{LIMITS}$$

$$\text{EV}(i) = \text{EVMIN} + (i - 1) * \text{DELEV} .$$

The output of this program is in table form giving the energy scale in eV and Rydberg units. As an option the output can be given in graphic form.

In the case considered here, the form of the ionization cross section proposed by Omidvar is in the program. This equation can be replaced by any other. In its present form it is possible to obtain as an option the ratio of Omidvar's function to any requested power function. The input card formats are as follows:

First Card: FORTRAN format is (2E12.6, 3I6)

Column

1-12	COE = coefficient of power function
13-24	POWER = power of the function
25-36	KLAST = 1: return for new run = 2: exit; all job completed

Second Card: FORTRAN format is (2E12.6, 3I6)

Column

1-12	LIMITS = integration interval
13-24	DELTA = full width at half maximum of Gaussian distribution
25-30	IFOLD = 1: do not fold data = 2: fold data
31-36	IPLOT = 1: give plot = 2: do not give plot
37-42	ILAST = 1: return here for new set of options after processing this problem = 2: do not return here

Third Card: FORTRAN format is (3E12.6, I6)

Column

1-12	EVMIN = the minimum value of the electron energy (eV) in the domain of the problem
13-24	EVMAX = the maximum value of the electron energy (eV) in the problem
25-36	DELEV = the step for output starting at EVMIN and going to EVMAX

37-42

LAST = 1: return here for new values after processing
this problem

= 2: do not return here

Below is an example of the deck setup as it stands for the Omidvar equation. In this case we are comparing Omidvar's cross section first with the 1.127 power law and then with a 1.5 power law. A plot is not requested. The energy distributions requested are 0.06 eV and 0.08 eV.

1	2	3	4	5	6	7	8	9	0	1	2	3	4	5	6	7	8	9	0	1	2	3	4	5	6	7	8	9	0	1	2	3	4	5	6	7	8	9	0		
										(INSERT SIMCUR PROGRAM HERE)																															

A program listing follows.

□ FOR SIMCUR, SIMCUR
 UNIVAC 1104 FORTRAN IV LEVEL 2201 0029 F4G14B
 THIS COMPILATION WAS DONE ON 27 MAY 68 AT 11:58:03

```

    MAJR. PROGRAM      ENTRY POINT 000000

    1.  C   PLOT SIMPLE CURVE AND FOLD SIMPLE CURVE
    2.      DIMENSION CS(1000), EV(1000), ARRAY(20)
    3.      COMMON /SIGMA/ COE, POWER
    4.      COMMON /FUN/ XSEE, XK
    5.      DATA INIT/ -1/, JPEND/1/
    6.      REAL LIMITS
    7.      IP = 2
    8.      C
    9.      C... COE IS NOT USED IN OMDVAR'S FUNCTION, INPUT CARD IS TO BE
    10.     C... LEFT BLANK IN THIS FIELD.
    11.     400 READ(5,401) COE, POWER, KLAST
    12.     401 FORMAT( 2E12.6,3I6)
    13.     410 READ(5,401) LIMITS, DELTA, IFOLD, IPLOT, ILAST
    14.     C   SET LINE COUNTER
    15.     LC = 60
    16.     C
    17.     XSEE = .69315/(.5*DELTA/13.605)**2
    18.     C   READ INTEGRATION GRID DEFINITIONS.
    19.     420 READ(5,421) EVMIN, DELEV, EVMAX, LAST
    20.     421 FORMAT( 3E12.6, I6 )
    21.     I = 0
    22.     GO TO (450, 550), IFOLD
    23.     C   SIMPLE CURVE.....
  
```

```

24. 450 YMAX = 1.E-37
25. 500 I = I + 1
26. IF(I.GT.1000) GO TO 900
27. IF(I.GT.1) GO TO 505
28. EV(1) = EVMIN
29. GO TO 507
30. 505 EV(I) = EV(I-1) + DELEV
31. 507 XK = EV(I)/13.605
32. CALL CROSS(XK, CS(I))
33. YMAX = AMAX1(YMAX, CS(I))
34. IF(LC.LT.54) GO TO 520
35. 510 WRITE(6,511)
36. 511 FORMAT( 1H1, 39X 25 H SIMPLE CURVE - OMIDVAR - // 54X 2HEV, 19X,
37. 1 1HK, 18X, 2HCS )
38. CALL BCDCON(ARRAY)
39. WRITE(0,515)
40. 515 FORMAT(24HSIMPLE CURVE - OMIDVAR - 72X )
41. LC = 3
42. 520 WRITE(6,521) EV(I), XK, CS(I)
43. 521 FORMAT( 36X, 3E20.8 )
44. LC = LC + 1
45. IF(ABS(EV(I)-EVMAX)-.001) 700, 700, 500
46. C
47. C FOLDED CURVE.....
48. 550 YMAX = 1.E-37
49. 600 I = I + 1
50. IF(I.GT.1000) GO TO 900

```

```

51. IF(I.GT.1) GO TO 605
52. EV(1) = EVMIN
53. GO TO 607
54. 605 EV(I) = EV(I-1) + DELEV
55. 607 XK = EV(I)/13.605
56. XO = XK - LIMITS
57. XL = XK + LIMITS
58. NP = 1
59. REL = .01
60. CALL GAUSS(INIT, XO, XL, Y1, REL, NP, 1)
61. NP = 1
62. REL = .01
63. CALL GAUSS(INIT, XO, XL, Y2, REL, NP, 2)
64. CS(I) = Y1/Y2
65. YMAX = AMAX1(YMAX,CS(I))
66. IF(LC.LT.54) GO TO 620
67. 610 WRITE(6,611) DELTA, LIMITS
68. 611 FORMAT( 1H1, 9X, 25HFOLDED CURVE USING DELTA= , F10.5, 9H, LIMITS=
69. 1 F10.5, 12H - OMIIDVAR - // 54X, 2HEV, 19X, 1HK, 18X, 2HCS )
70. CALL BCDCON(ARRAY)
71. WRITE(0,615) DELTA, LIMITS
72. 615 FORMAT( 25HFOLDED CURVE USING DELTA= , F10.5, 8H LIMITS= , F10.5,
73. 1 12H - OMIIDVAR - 31X )
74. LC = 3
75. 620 WRITE(6,521) EV(I), XK, CS(I)
76. LC = LC + 1
77. IF(ABS(EV(I)-EVMAX)-.001) 700, 700, 600

```

```

78. C
79. C THIS GRID COMPLETE..
80. 700 GO TO(420, 710), LAST
81. C THIS FOLD COMPLETE. CHECK FOR PLOT.
82. 710 GO TO (720, 750), IPL0T
83. 720 IF(IFEND.GT.1) GO TO 730
84. CALL SETUP( 0.0, 0, 16)
85. IPEND = 2
86. IP = 1
87. 730 CALL ADF
88. CALL DGA(123,766,0,900, 13.45, 14.45, YMAX, 0.0 )
89. CALL OUTLIN
90. CALL DRG(5,7)
91. CALL SBLIN(5,9)
92. CALL SLLIN(7,9)
93. II=I-1
94. CALL DVR(II,1,EV,CS,1)
95. C... LABEL GRAPH
96. CALL CONX (1, XPT)
97. CALL CONY (1000, YPT)
98. CALL TSP (XPT, YPT, ARRAY, 96)
99. C CHECK FOR NEXT IFOLD
100. 750 GO TO (410, 760), ILAST
101. C THIS CURVE COMPLETE
102. 760 GO TO (400, 770), KLAST
103. C END OF JOB
104. 770 GO TO (780, 800), IP

```

```
105. C      CLOSE OUT PLOT ROUTINE
106.      780 CALL FINISH
107.      800 STOP
108.      900 WRITE(6,901)
109.      901 FORMAT(113H CHECK INPUT VALUE FOR EVMIN, EVMAX AND DELEV, ONE OF T
110.      THEM IS IN ERROR AND WILL CAUSE RESERVED STORAGE OVERFLOW. )
111.      IF(IPEND.EQ.1) STOP
112.      IP = 2
113.      GO TO 770
114.      END
END OF LISTING. 0 *DIAGNOSTIC* MESSAGE(S).
```

Q FOR GAUSS GAUSS
UNIVAC 1108 FORTRAN IV LEVEL 2201 0029 F46148
THIS COMPILATION WAS DONE ON 27 MAY 68 AT 11:58:07

SUBROUTINE GAUSS ENTRY POINT 000317

```
1. SUBROUTINE GAUSS(INIT, XO, XL, Y, REL, NP, IFUN)
2. DIMENSION AA(16), HH(16), YBAR(10), BYB(10)
3. IF(INIT) 1, 1, 2
4. 1 INIT = 1.
5. AA(1) = -.989400935
6. AA(2) = -.944575023
7. AA(3) = -.865631202
8. AA(4) = -.755404408
9. AA(5) = -.617876244
10. AA(6) = -.458016778
11. AA(7) = -.281603551
12. AA(8) = -.950125098E-01
13. AA(9) = -AA(8)
14. AA(10) = -AA(7)
15. AA(11) = -AA(6)
16. AA(12) = -AA(5)
17. AA(13) = -AA(4)
18. AA(14) = -AA(3)
19. AA(15) = -AA(2)
20. AA(16) = -AA(1)
21. HH(1) = .27152459E-01
```

22. HH(2) = .62253524E-01
 23. HH(3) = .95158512E-01
 24. HH(4) = .12462897
 25. HH(5) = .14959599
 26. HH(6) = .16915652
 27. HH(7) = .18260342
 28. HH(8) = .18945061
 29. HH(9) = HH(8)
 30. HH(10) = HH(7)
 31. HH(11) = HH(6)
 32. HH(12) = HH(5)
 33. HH(13) = HH(4)
 34. HH(14) = HH(3)
 35. HH(15) = HH(2)
 36. HH(16) = HH(1)
 37. NG = 16
 38. C
 39. 2 Y = 0.0
 40. XLGTH = XL - X0
 41. IF(XLGTH) 201, 105, 201
 42. 201 NPP = NP
 43. DO 103 K=1,10
 44. Y = 0.
 45. ENP = NP
 46. DO 200 L=1,NP

```

47. AREA = 0.0
48. AL = L
49. X1PX2 = (2.0*AL - 1.0)*XLGTH/ENP + 2.0*X0
50. X2MX1 = XLGTH/ENP
51. DO 100 J=1,NG
52. X = (X1PX2 + AA(J)*X2MX1)/2.0
53. CALL FOFX( X, FX, IFUN)
54. 100 AREA = AREA + HH(J)*FX
55. Y = Y + AREA
56. 200 CONTINUE
57. Y = XLGTH/(2.0*ENP)*Y
58. YBAR(K) = Y
59. IF(K-1) 104, 104, 144
60. 144 BYB(K-1) = ABS(YBAR(K-1) - Y)
61. IF(BYB(K-1) - REL*ABS(Y)) 105, 105, 104
62. 104 NP = 2*NP
63. 103 CONTINUE
64. DO 108 L=1,10
65. REL = 2.0*REL
66. DO 107 K=2,10
67. IF(BYB(K-1) - REL*ABS(YBAR(K))) 106, 106, 107
68. 107 CONTINUE
69. 108 CONTINUE
70. K = 10
71. 106 NP = (2**(K-1))*NPP

```


72. Y = YBAR(K)

73. 105 RETURN

74. END

END OF LISTING. 0 *DIAGNOSTIC* MESSAGE(S).

□ FOR FOFX,FOFX
UNIVAC 1108 FORTRAN IV LEVEL 2201 0029 F46148
THIS COMPILATION WAS DONE ON 27 MAY 68 AT 11:58:11

```
SUBROUTINE FOFX      ENTRY POINT 000033
1.  SUBROUTINE FOFX( X, FX, IFUN)
2.  C  EVALUATE ONE OF TWO FUNCTIONS FOR GAUSS.
3.  COMMON /FUN/ XSEE, E
4.  FX = EXP(-XSEE*(E-X)**2)
5.  GO TO (100, 200), IFUN
6.  100 CALL CROSS(X, CS)
7.  FX = FX*CS
8.  200 RETURN
9.  END

END OF LISTING.  0 *DIAGNOSTIC* MESSAGE(S).
```

9 FOR CROSS, CROSS
UNIVAC 1105 FORTRAN IV LEVEL 2201 0029 F46148
THIS COMPILATION WAS DONE ON 27 MAY 68 AT 11:56:13

```
SUBROUTINE CROSS      ENTRY POINT 000122
 1.  SUBROUTINE CROSS (E, CS )
 2.  COMMON  /SIGMA/ COE, POWER
 3.  C.
 4.  C... OMIDVAR
 5.  C
 6.  REAL NU
 7.  VALUE = E - 1.0
 8.  IF(VALUE) 100, 100, 200
 9.  100 CS = 0.0
10.  RETURN
11.  200 NU = 1.0/(SQRT(E)+1.0)
12.  F1 = 16.0*NU
13.  F2 = 3.0 - F1*NU
14.  F3 = 2.0*NU*ALOG(4.0*VALUE)
15.  CS = 6.0*NU*(1.0 + 3.0*(F2*COS(F3) + F1*SIN(F3)))/(F2**2 + F1**2)
16.  1  *VALUE**1.5/(TANH(3.14159265*NU)**.014)
17.  IF(POWER) 210, 220, 210
18.  210 CS = CS/VALUE**POWER
19.  220 RETURN
20.  END
```

END OF LISTING. 0 *DIAGNOSTIC* MESSAGE(S).

STEP 10: SIMTAB

This program is designed to fold a Gaussian function into any given function which has been prepared in table form. This program is identical to SIMCUR except the term CS(x) is interpolated from tabular data.

It is not necessary that the input be given in equal intervals. Within the program is an interpolation subroutine that can be as much as a ninth-order polynomial.

The input card formats are as follows:

First Card: FORTRAN format is (2I6)

Column

1-6 NL = number of points in the table (max 100)
7-12 KLAST = 1: return here for new table
 = 2: exit; all jobs finished

Table Cards: FORTRAN format is (6E12.6)

Column

1-12 XX(1) = first energy value
13-24 YY(1) = first cross section value
25-36 XX(2)
37-48 YY(2)
49-60 XX(3)
61-72 YY(3)

Continue with three pairs per card.

Next Card after Table: FORTRAN format is (2E12.6, 3I6)

Column

1-12 LIMITS
13-24 DELTA
25-30 IFOLD
31-36 IPLOT
37-42 ILAST

Next Card: FORTRAN format is (3E12.6, I6)

Column

1-12	EVMIN
13-24	DELEV
25-36	EVMAX
37-42	LAST

The last two cards are identical to cards two and three for the SIMCUR program.

A program listing follows.

Q FOR SIMTAB,SIMTAB
 UNIVAC 1103 FORTRAN IV LEVEL 2201 0029 F4G148
 THIS COMPILATION WAS DONE ON 27 MAY 68 AT 11:58:16

```

MAIN PROGRAM      ENTRY POINT 000000
1.  C      PLOT SIMPLE CURVE AND FOLD SIMPLE CURVE
2.  DIMENSION CS(1000), EV(1000), ARRAY(20)
3.  DIMENSION XX(100), YY(100)
4.  COMMON /SIGMA/ NL, XX, YY
5.  COMMON /FUN/ XSEE, XK
6.  DATA INIT/ -1/, IPEND/1/
7.  REAL LIMITS
8.  IP = 2
9.  C
10. ITAB = 0
11. 400 READ(5,406) NL, KLAST
12. 406 FORMAT( 2I6 )
13. READ(5,407) (XX(I), YY(I), I=1,NL )
14. 407 FORMAT(6E12.6 )
15. ITAB = ITAB + 1
16. DO 408 I=1,NL
17. 408 XX(I) = XX(I)/13.605
18. 401 FORMAT( 2E12.6,3I6)
19. 410 READ(5,401) LIMITS, DELTA, IFOLD, IPLOT, ILAST
20. C      SET LINE COUNTER
21. LC = 60
22. C

```

```

23.      XSEE = .69315/(.5*DELTA/13.605)**2
24.      C      READ INTEGRATION GRID DEFINITIONS.
25.      420 READ(5,421) EVMIN, DELEV, EVMAX, LAST
26.      421 FORMAT( 3E12.6, I6 )
27.      I = 0
28.      GO TO (450, 550), IFOLD
29.      C      SIMPLE CURVE.....
30.      450 YMAX = 1.E-37
31.      500 I = I + 1
32.      IF(I.GT.1000) GO TO 900
33.      IF(I.GT.1) GO TO 505
34.      EV(I) = EVMIN
35.      GO TO 507
36.      505 EV(I) = EV(I-1) + DELEV
37.      507 XK = EV(I)/13.605
38.      CALL CROSS(XK, CS(I))
39.      YMAX = AMAX1(YMAX, CS(I))
40.      IF(LC.LT.54) GO TO 520
41.      510 WRITE(6,511) ITAB
42.      511 FORMAT( 1H1, 39X 41H SIMPLE CURVE      SIGMA = FUNCTION OF TABLE I3
43.      1 // 54X 2HEV 19X 1HK 18X 2HCS )
44.      CALL BCDCON(ARRAY)
45.      WRITE(10,515) ITAB
46.      515 FORMAT(40HSIMPLE CURVE      SIGMA = FUNCTION OF TABLE I3, 53X )
47.      LC = 3
48.      520 WRITE(6,521) EV(I), XK, CS(I)
49.      521 FORMAT( 36X, 3E20.8 )

```

```

50. LC = LC + 1
51. IF((EV(I)+DELEV).LT.EVMAX) GO TO 500
*DIAGNOSTIC* THE TEST FOR EQUALITY BETWEEN NON-INTEGERS MAY NOT BE MEANINGFUL.
52. IF(EV(I).GE.EVMAX) GO TO 700
53. IF((I+1).GT.1000) GO TO 900
54. I = I + 1
55. EV(I) = EVMAX
56. GO TO 507
57. C
58. C FOLDED CURVE.....
59. 550 YMAX = 1.E-37
60. 600 I = I + 1
61. IF(I.GT.1000) GO TO 900
62. IF(I.GT.1) GO TO 605
63. EV(1) = EVMIN
64. GO TO 607
65. 605 EV(I) = EV(I-1) + DELEV
66. 607 XK = EV(I)/13.605
67. XO = XK - LIMITS
68. XL = XK + LIMITS
69. NP = 1
70. REL = .01
71. CALL GAUSS(INIT, XO, XL, Y1, REL, NP, 1)
72. NP = 1
73. REL = .01
74. CALL GAUSS(INIT, XO, XL, Y2, REL, NP, 2)
75. CS(I) = Y1/Y2

```



```

76.   YMAX = AMAX1(YMAX,CS(I))
77.   IF(LC.LT.54) GO TO 620
78.   610 WRITE(6,611) DELTA, LIMITS, ITAB
79.   611 FORMAT(1H1, 9X, 25HFOLDED CURVE USING DELTA= , F10.5, 9H, LIMITS
80.   1=, F10.5, 27H SIGMA = FUNCTION OF TABLE I3 //
81.   2 54X, 2HEV, 19X, 4HK, 18X, 2HCS )
82.   CALL BCDCON(ARRAY)
83.   WRITE(10,615) DELTA, LIMITS, ITAB
84.   615 FORMAT( 25HFOLDED CURVE USING DELTA= , F10.5, 8H LIMITS= , F10.5,
85.   1 27H SIGMA = FUNCTION OF TABLE I3 )
86.   LC = 3
87.   620 WRITE(6,521) EV(I), XK, CS(I)
88.   LC = LC + 1
89.   IF((EV(I)+DELEV).LT.EVMAX) GO TO 600
*DIAGNOSTIC* THE TEST FOR EQUALITY BETWEEN NON-INTEGERS MAY NOT BE MEANINGFUL.
90.   IF(EV(I).GE.EVMAX) GO TO 700
91.   IF((I+1).GT.1000) GO TO 900
92.   I = I + 1
93.   EV(I) = EVMAX
94.   GO TO 607
95.   C
96.   C THIS GRID COMPLETE..
97.   700 GO TO(420, 710), LAST
98.   C THIS FOLD COMPLETE. CHECK FOR PLOT.
99.   710 GO TO (720, 750), I PLOT
100.  720 IF(IPEND.GT.1) GO TO 730
101.  CALL SETUP( 0.0, 0, 16)

```

```

102.      IPEND = 2
103.      IP = 1
104.      730 CALL ADF
105.      XX1 = XX(1)*13.605
106.      XXNL = XX(NL)*13.605
107.      CALL DGA( 123, 766, 0, 900, XX1, XXNL, YMAX, 0.0 )
108.      CALL OUTLIN
109.      CALL DRG(5,7)
110.      CALL SBLIN(5,9)
111.      CALL SLLIN(7,9)
112.      II=I-1
113.      CALL DVR(II,1,EV,CS,1)
114.      C... LABEL GRAPH
115.      CALL CONX (1, XPT)
116.      CALL CONY (1000, YPT)
117.      CALL TSP (XPT, YPT, ARRAY, 96)
118.      C CHECK FOR NEXT IFOLD
119.      750 GO TO (410, 760), ILAST
120.      C THIS CURVE COMPLETE
121.      760 GO TO (400, 770), KLAST
122.      C END OF JOB
123.      770 GO TO (780, 800), IP
124.      C CLOSE OUT PLOT ROUTINE
125.      780 CALL FINISH
126.      800 STOP
127.      900 WRITE(6,901)
128.      901 FORMAT(113H CHECK INPUT VALUE FOR EVMIN, EVMAX AND DELEV, ONE OF T

```

```
129. THEM IS IN ERROR AND WILL CAUSE RESERVED STORAGE OVERFLOW. )
130. IF(IPEND.EQ.1) STOP
131. IP = 2
132. GO TO 770
133. END
END OF LISTING. 2 *DIAGNOSTIC* MESSAGE(S).
```

Q FOR GAUSS,GAUSS
UNIVAC 1108 FORTRAN IV LEVEL 2201 0029 F4614B
THIS COMPILATION WAS DONE ON 27 MAY 68 AT 11:58:20

SUBROUTINE GAUSS ENTRY POINT 000317

1. SUBROUTINE GAUSS(INIT, XO, XL, Y, REL, NP, IFUN)
2. DIMENSION AA(16), HH(16), YBAR(10), BYB(10)
3. IF(INIT) 1, 1, 2
4. 1 INIT = 1
5. AA(1) = -.989400935
6. AA(2) = -.944575023
7. AA(3) = -.865631202
8. AA(4) = -.755404408
9. AA(5) = -.617876244
10. AA(6) = -.458016778
11. AA(7) = -.281603551
12. AA(8) = -.950125098E-01
13. AA(9) = -AA(8)
14. AA(10) = -AA(7)
15. AA(11) = -AA(6)
16. AA(12) = -AA(5)
17. AA(13) = -AA(4)
18. AA(14) = -AA(3)
19. AA(15) = -AA(2)
20. AA(16) = -AA(1)
21. HH(1) = .27152459E-01
22. HH(2) = .62253524E-01

23. HH(3) = .95158512E-01
 24. HH(4) = .12462897
 25. HH(5) = .14959599
 26. HH(6) = .16915652
 27. HH(7) = .18260342
 28. HH(8) = .18945061
 29. HH(9) = HH(8)
 30. HH(10) = HH(7)
 31. HH(11) = HH(6)
 32. HH(12) = HH(5)
 33. HH(13) = HH(4)
 34. HH(14) = HH(3)
 35. HH(15) = HH(2)
 36. HH(16) = HH(1)
 37. NG = 16
 38. C
 39. 2 Y = 0.0
 40. XLGTH = XL - XO
 41. IF(XLGTH) 201, 105, 201
 42. 201 NPP = NP
 43. DO 103 K=1,10
 44. Y = 0.
 45. ENP = NP
 46. DO 200 L=1,NP
 47. AREA = 0.0
 48. AL = L

```

49. X1PX2 = (2.0*AL - 1.0)*XLGTH/ENP + 2.0*X0
50. X2MX1 = XLGTH/ENP
51. DO 100 J=1,NG
52. X = (X1PX2 + AA(J)*X2MX1)/2.0
53. CALL FOFX( X, FX, IFUN)
54. 100 AREA = AREA + HH(J)*FX
55. Y = Y + AREA
56. 200 CONTINUE
57. Y = XLGTH/(2.0*ENP)*Y
58. YBAR(K) = Y
59. IF(K-1) 104, 104, 144
60. 144 BYB(K-1) = ABS(YBAR(K-1) - Y)
61. IF(BYB(K-1) - REL*ABS(Y)) 105, 105, 104
62. 104 NP = 2*NP
63. 103 CONTINUE
64. DO 108 L=1,10
65. REL = 2.0*REL
66. DO 107 K=2,10
67. IF(BYB(K-1) - REL*ABS(YBAR(K))) 106, 106, 107
68. 107 CONTINUE
69. 108 CONTINUE
70. K = 10
71. 106 NP = (2**K-1)*NPP
72. Y = YBAR(K)
73. 105 RETURN
74. END

```

END OF LISTING. 0 *DIAGNOSTIC* MESSAGE(S).

© FOR FOFX,FOFX
UNIVAC 1108 FORTRAN IV LEVEL 2201 0029 F46148
THIS COMPILATION WAS DONE ON 27 MAY 68 AT 11:56:23

```

SUBROUTINE FOFX      ENTRY POINT 000033
1.  SUBROUTINE FOFX( X, FX, IFUN)
2.  C  EVALUATE ONE OF TWO FUNCTIONS FOR GAUSS.
3.  COMMON /FUN/ XSEE, E
4.  FX = EXP(-XSEE*(E-X)**2)
5.  GO TO (100, 200), IFUN
6.  100 CALL CROSS(X, CS)
7.  FX = .FX*CS
8.  200 RETURN
9.  END
END OF LISTING.  0 *DIAGNOSTIC* MESSAGE(S).
```

FOR CROSS, CROSS
UNIVAC 1108 FORTRAN IV LEVEL 2201 0029 F4G148
THIS COMPILATION WAS DONE ON 27 MAY 68 AT 11:58:26

SUBROUTINE CROSS ENTRY POINT 000034

```
1. SUBROUTINE CROSS (E,CS )  
2. DIMENSION XX(100), YY(100)  
3. COMMON /SIGMA/ NL, XX, YY  
4. IF(YY(1)) 10, 10, 17  
5. 10 IF(E-XX(2)) 15, 16, 17  
6. 15 CS = 0  
7. RETURN  
8. 16 CS = YY(2)  
9. RETURN  
10. 17 CS = TERP( XX, YY, NL, E, 3)  
11. IF(CS.LT.0.) CS = 0.0  
12. RETURN  
13. END
```

END OF LISTING. 0 *DIAGNOSTIC* MESSAGE(S).

Q FOR TERP, TERP
 UNIVAC 1108 FORTRAN IV LEVEL 2201 0029 F46148
 THIS COMPILATION WAS DONE ON 27 MAY 68 AT 11:58:29

FUNCTION TERP	ENTRY POINT	000267
1. FUNCTION TERP(X,Y,NL,ARG,IL)	TERP0010	
2. C-----	TERP0020	
3. C THIS FUNCTION DOES LAGRANGIAN INTERPOLATION OR	TERP0030	
4. C EXTRAPOLATION OF ILTH ORDER ON X AND Y FOR ARG	TERP0040	
5. C WHEN THE TABLES ARE EITHER INCREASING OR DECREASING	TERP0050	
6. C-----	TERP0060	
7. C X X ARRAY, INDEPENDENT VARIABLE	TERP0070	
8. C Y Y ARRAY, DEPENDENT VARIABLE	TERP0080	
9. C NL NUMBER OF ENTRIES IN TABLES OF X AND Y	TERP0090	
10. C ARG INDEPENDENT VARIABLE VALUE	TERP0100	
11. C IL NUMBER OF POINTS TO USE FOR INTERPOLATION	TERP0110	
12. C-----	TERP0120	
13. DIMENSION X(2),Y(2)	TERP0130	
14. C DIMENSION X(2),Y(2)	TERP0140	
15. C-----	TERP0150	
16. IF(NL-IL)97,98,99	TERP0160	
17. C NOT ENOUGH ENTRIES IN TABLES FOR THIS ORDER INTERPOLATION	TERP0170	
18. 97 IL=NL	TERP0180	
19. 98 L=1	TERP0190	
20. 60 TO 112	TERP0200	
21. 99 CONTINUE	TERP0210	

22.	IL2=IL/2	TERP0220
23.	IADD=MOD(IL,2)	TERP0230
24.	C CHECK IF TABLES IN INCREASING OR DECREASING SEQUENCE	TERP0240
25.	IF(X(1)-X(NL))100,100,101	TERP0250
26.	C INCREASING SEQUENCE	TERP0260
27.	100 ILOW=IL2+1	TERP0270
28.	IHI=NL-IL2-IADD	TERP0280
29.	IUSEL=1	TERP0290
30.	IUSEH=NL-IL+1	TERP0300
31.	IBEG=ILOW+1	TERP0310
32.	IEND=IHI-1	TERP0320
33.	LAST=IEND-IL2+1	TERP0330
34.	IADD=0	TERP0340
35.	60 TO 102	TERP0350
36.	C DECREASING SEQUENCE	TERP0360
37.	101 ILOW=NL-IL2	TERP0370
38.	IHI=IL2+IADD+1	TERP0380
39.	IUSEL=NL-IL+1	TERP0390
40.	IUSEH=1	TERP0400
41.	IBEG=IHI+1	TERP0410
42.	IEND=ILOW-1	TERP0420
43.	LAST=2	TERP0430
44.	IADD=1-IADD	TERP0440
45.	C CHECKS IF ARG IS SMALLER THAN TABLE VALUES	TERP0450
46.	102 IF(ARG-X(ILOW))103,104,105	TERP0460

47.	C	SMALLER THAN SMALLEST TABLE VALUE	TERP0470
48.		103 L=IUSEL	TERP0480
49.		GO TO 112	TERP0490
50.		104 TERP=Y(ILOW)	TERP0500
51.		GO TO 117	TERP0510
52.	C	CHECKS IF ARG IS GREATER THAN TABLE VALUES	TERP0520
53.		105 IF(X(IHI)-ARG)106,107,108	TERP0530
54.	C	ARG GREATER THAN TABLE VALUE	TERP0540
55.		106 L=IUSEH	TERP0550
56.		GO TO 112	TERP0560
57.		107 TERP=Y(IHI)	TERP0570
58.		GO TO 117	TERP0580
59.	C	SEARCHES X ARRAY TO BRACKET ARG	TERP0590
60.		106 DO 109 N=IBEG, IEND	TERP0600
61.		IF(IUSEL-1)1080,1080,1081	TERP0610
62.		1060 M=N	TERP0620
63.		GO TO 1082	TERP0630
64.		1081 M=N-L-N+1	TERP0640
65.		1082 IF(X(M)-ARG)109,110,111	TERP0650
66.		109 CONTINUE	TERP0660
67.		L=LAST	TERP0670
68.		GO TO 112	TERP0680
69.	C	EQUALS ARGUMENT, RETURN OK	TERP0690
70.		110 TERP=Y(M)	TERP0700
71.		GO TO 117	TERP0710

```

72. C EUREKA
73. 111 L=M-IL2+IADD
74. 112 CONTINUE
75. C INTERPOLATION SECTION
76. SUM=0.0
77. DO 115 I=1,IL
78. P=1.0
79. PK=1.0
80. INEL=I-1
81. DO 114 IP=1,IL
82. IF(IP-1)113,114,113
83. 113 INEL=IP-1
84. P=P*(ARG-X(INP))
85. PK=PK*(X(IN)-X(INP))
86. 114 CONTINUE
87. SUM=SUM+P*Y(IN)/PK
88. 115 CONTINUE
89. TERP=SUM
90. 117 RETURN
91. END

```

END OF LISTING. 0 *DIAGNOSTIC* MESSAGE(S).

10. OTHER COMPLEMENTARY ACTIVITIES

To promote a vigorous exchange of information on electron scattering between the theoretical and experimental communities, a city-wide series of colloquia was initiated with the support of Gulf General Atomic. The series has been known as CAMP (Colloquia on Atomic and Molecular Processes). During the contract period, the following CAMP colloquia have been of interest to this program:

- March 8, 1967 "Energetic Ions from Diatomic Molecules,"
Dr. Lee J. Keiffer, Joint Institute for Lab
Astrophysics, University of Colorado,
Boulder, Colorado
- March 14, 1967 "Theory of Near Adiabatic Collisional Transitions,"
Professor K. M. Watson, University of California,
Berkeley, Physics Department
- March 31, 1967 "Atomic Scattering Spectroscopy: Analysis of
Scattering of He^+ by Ne and Ar," Dr. Felix T.
Smith, Stanford Research Institute, Menlo Park,
California
- April 28, 1967 "Total Elastic and Inelastic Heavy Particle
Collisions in the Energy Range 10 to 1000 eV.
A: Elastic Scattering in the Alkali-Rare Gas
System; B: Ionization Due to Rare Gas Metastable
Collisions," Dr. Manfred Hollstein, Stanford
Research Institute, Menlo Park, California
- May 4, 1967 "The Importance of Polarization in Low Energy
Electron Molecular Collisions - An Application
to H_2 ," Dr. Neil F. Lane, Department of Physics,
Rice University, Houston, Texas
- October 16, 1967 "The Excitation and Spectroscopy of H-like Atoms,"
Dr. Hans Kleinpoppen, Joint Institute for Lab-
oratory Astrophysics, University of Colorado,
Boulder, Colorado
- November 3, 1967 "Low Energy Rotational Excitation Cross Sections
Derived from Spectroscopic Data," Dr. Marvin
Mittleman, Space Science Laboratory, University
of California, Berkeley, California

- December 11, 1967 "Proton H-Atom Collisions," Professor
M. R. C. McDowell, Goddard Space Flight
Center, Greenbelt, Maryland
- April 4, 1968 "Ionization Processes of Molecules at Low
Energies," Professor R. Stephen Berry,
Department of Chemistry, University of
Chicago, Chicago, Illinois
- May 17, 1968 "Polarization of Scattered Electrons,"
Professor E. Reichart, Department of
Physics, University of Mainz, Mainz, Germany

Probably the most significant activity this year was the Working Session on Electron H-Atom Collisions. The text of the notice and the program for the meeting are presented below.

WORKING SESSION ON ELECTRON H-ATOM COLLISIONS

The detailed experimental and theoretical study of electron hydrogen atom collisions has developed to the point where our group at Gulf General Atomic, in conjunction with the group at the University of California, San Diego, plan to spend two days in a "working session" in order to examine what has been done, what is being done, and what can be done to most effectively study (e-H) collisions. The days we have in mind are Monday and Tuesday, April 8 and 9.

In particular, we plan to examine resonance and threshold problems since these areas have received the most extensive study of late. We have invited R. Damburg and A. Temkin to help organize discussion during our first day and to give colloquia on topics of particular interest. We plan to have several other talks by J. C. Y. Chen and ourselves, but for the most part our program will be informal and will stress the broadest possible exchange of ideas. We hope to spend one day together in an informal meeting while the second day (or part of the day) we are setting aside for the exchange of thoughts on a more individual basis. This will occur both here and at the University.

For those who would like to join us, arrangements will be made at a local hotel. We plan to get together for dinner Monday evening. Since time is already short, from those who will join us, we would appreciate word as soon as possible.

J. William McGowan
James F. Williams
GULF GENERAL ATOMIC

WORKSHOP ON ELECTRON HYDROGEN-ATOM COLLISIONS

Monday, April 8, 1968

AM SESSION: La Salle Room, La Jolla Beach & Tennis Club

9:00 - 9:30 Business and Coffee

9:30 - 12:30 Elastic and Inelastic Electron Scattering

Chairman: Edward Gerjuoy

Review Experimental Measurements

J. William McGowan
Atomic Physics Lab
Gulf General Atomic

Excitation of the Hydrogen
Atom by Electron Impact

R. Damburg
Latvian Academy of
Science

Solutions of the Faddeev
Equation for the (e-H) System

J. C. Y. Chen
University of California
San Diego

Lunch
12:30 - 1:45

Scripps Institute of Oceanography
Cafeteria
After lunch, a visit to Scripps
Physiological Research Lab

PM SESSION: IGPP Building, University of California,
San Diego

2:00 - 5:00 Ionization Threshold Studies

Chairman: Kenneth M. Watson

Black Box Aspects of the Threshold
Law for Ionization

G. H. Wannier
University of Oregon

3:30 Coffee Break

An Approach to the Electron Atom
Ionization Threshold Behavior

A. Temkin
NASA-Goddard Space
Flight Center

Evening: La Valencia Hotel

Cocktail hour at 7:00
Dinner at 8:00

WORKSHOP ON ELECTRON HYDROGEN-ATOM COLLISIONS

Tuesday, April 9, 1968

AM SESSION: La Salle Room, La Jolla Beach & Tennis Club

9:00 - 12:00 Joint Experimental and Theoretical Workshop

Chairman: Marvin Mittleman

Possible Topics:

Polarization of Radiation

Polarized Electron and Atom Beams

Coincidence Experiments

Angular Correlation Experiments

The Application of Born Approximation

Lorentz Decay

Removal of Degeneracy

Definition of Threshold

Cascade of Radiation

Potential Resonances

12:00 Lunch at La Jolla Beach & Tennis Club Dining Room

PM SESSION: IGPP Building, University of California,
San Diego

2:00 Special Working Sessions

Visits to Gulf General Atomic and the University of California,
San Diego

NOTE: At 11:00 a.m. at Gulf General Atomic Professor Gregory H. Wannier
will be speaking on "Stark Ladders in Solids?"

REFERENCES

1. Fite, W. L., and R. T. Brackmann, "Collisions of Electrons with Hydrogen Atoms. II. Excitation of Lyman-Alpha Radiation," Phys. Rev. 112, 1151 (1958).
2. Burke, P. G., S. Ormonde, and W. Whitaker, "Low-Energy Electron Scattering by Atomic Hydrogen. I. The Close-Coupling Approximation," Proc. Phys. Soc. London 92, 319 (1967).
3. Chamberlain, G. E., S. J. Smith, and D. W. O. Heddle, "Excitation of the 2p State of Hydrogen by Electrons of Near Threshold Energy," Phys. Rev. Letters 12, 647 (1964).
4. Damburg, R. J., and M. K. Gailitis, "Calculations in the Vicinity of the 2s, 2p Threshold of the Cross Sections for the Excitation of Hydrogen Atoms by Electrons," Proc. Phys. Soc. London 82, 1068 (1963).
5. Taylor, A. J., and P. G. Burke, "Low-Energy Electron Scattering by Atomic Hydrogen. II. The Correlation Method," Proc. Phys. Soc. London 92, 336 (1967).
6. Damburg, R. J., and S. Geltman, "Excitation of $n = 2$ States in Hydrogen by Electron Impact," Phys. Rev. Letters 20, 485 (1968).
7. Long, R. L., D. M. Cox, and S. J. Smith, submitted for publication to NBS Journal of Research.
8. Fite, W. L., W. E. Kauppila, and W. R. Ott, "Polarization of Lyman-Alpha Radiation Emitted by H(2s) Atoms in Weak Electric Fields," Phys. Rev. Letters 20, 409 (1968).
9. Kleinpoppen, H, and E. Kraiss, Phys. Rev. Letters 20, 361 (1968).
10. Watanabe, K., E. C. Y. Inn, and M. Zelikoff, "Absorption Coefficients of Oxygen in the Vacuum Ultraviolet," J. Chem. Phys. 21, 1026 (1953).

11. Platzman, R. L., J. Phys. Radium 21, 853 (1960); "Some Remarks on the Nature of Ionization, Ionization Yields, and Isotope Effects in the Ionization of Molecules by Various Agencies," J. Chem. Phys. 38, 2775 (1963).
12. Burrows, K. M., and G. H. Dunn, "Isotope Effect in the Dissociative Excitation of $H_2(D_2)$," paper presented at Twentieth Annual Gaseous Electronics Conference, October 1967, San Francisco.
13. Vroom, D. H., and F. J. de Heer, F. O. M. Institute for Atomic and Molecular Physics, "Production of Excited Atoms by Impact of Fast Electrons on Molecular Hydrogen and Deuterium," submitted for publication.

APPENDIX I

ABSTRACTS OF PAPERS GIVEN
AT SCIENTIFIC MEETINGS

LYMAN-ALPHA PRODUCTION AND POLARIZATION IN He^+
COLLISIONS WITH H AND H_2 *

Robin A. Young, R. F. Stebbings,[†] and J. Wm. McGowan

Presented at 20th Annual Gaseous Electronics
Conference of the American Physical Society,
San Francisco, October 1967.

Measurements of the Lyman-alpha production from $\text{He}^+ + \text{H}(1s) \rightarrow \text{He}^+ + \text{H}(2p)$ collisions have been obtained over the energy range from 0.5 to 30 keV. At the lower ion energies the cross section remains large; this fact reflects the rotational interaction between states of the collision complex HeH^+ . A similar result had been reported by Stebbings *et al.* (1) for the $\text{H}^+ - \text{H}$ collision system. Also presented are measurements of the total cross section for Lyman-alpha production from $\text{He}^+ - \text{H}_2$ collisions. Some values of the polarization have been obtained for emission of Lyman-alpha from the collisions of He^+ , Ne^+ , and Ar^+ with atomic hydrogen.

* Work supported by the National Aeronautics and Space Administration, Goddard Space Flight Center, Contract NAS 5-11025.

[†] On leave from University College London, London, England.

-
1. R. F. Stebbings, R. A. Young, C. L. Oxley, and H. Ehrhardt, Phys. Rev. **138**, A1312 (1965).

THRESHOLD BEHAVIOR OF ELECTRON EXCITATION
FUNCTIONS IN ATOMIC HYDROGEN*

J. F. Williams, E. K. Curley, and J. Wm. McGowan

Presented at 20th Annual Gaseous Electronics
Conference of the American Physical Society,
San Francisco, October 1967.

The excitation function, for electron impact, of the (1s - 2p) transition in atomic hydrogen appears to be finite at the threshold. When electron energy distribution functions of from 240 to 100 meV (FWHM) are unfolded from the observed Lyman-alpha radiation versus electron energy curve, it appears that the excitation function reaches a significant value within several tens of meV of the threshold and then drops sharply to about 60% of its peak threshold value. A report is given of attempts made to observe the resonance in the 2p excitation function, which is predicted by Burke et al. (1) to appear just below the $n = 3$ level.

* Work supported by the National Aeronautics and Space Administration, Goddard Space Flight Center, Contract NAS-5-11025.

-
1. P. G. Burke, S. Ormonde, and W. Whitaker, Phys. Rev. Letters 17, 800 (1966).

(e-H) COMPOUND STATES REFLECTED IN THE H(2p) CHANNEL
IN THE VICINITY OF $n = 3$ *

J. William McGowan and James F. Williams

Presented at American Physical Society Meeting,
Los Alamos Scientific Laboratory, June 1968.

High resolution electron impact studies of the 2p excitation cross section of atomic hydrogen have been made in the vicinity of $n = 3$. Prominent resonance structure has been observed below and above $n = 3$. The structure below $n = 3$ qualitatively is in agreement with the predictions of Burke *et al.*, (1) but in detail there is some difference as to the breadth of the (e-H) resonances. Above $n = 3$ there is evidence that a shape resonance is present.

* Work supported by the National Aeronautics and Space Administration, Goddard Space Flight Center, Contract NAS-5-11025.

¹ P. G. Burke, S. Ormonde, and W. Whitaker, Proc. Phys. Soc. 92, 319 (1967).

COMPARISON OF THE CALCULATED AND OBSERVED RESONANCES
IN THE (e-H) ELASTIC SCATTERING CHANNEL
ABOVE 10.0 eV*

J. William McGowan and S. Ormonde[†]

Submitted to the Arnold Sommerfeld Centennial Memorial Meeting and International Symposium on the Physics of One and Two Electron Atoms, Munich, September 1968.

Recent measurements of the electron hydrogen atom elastic scattering cross section show a rather wide structure immediately below the $n = 2$ threshold. (1) This structure has been attributed to the 1D and 3S compound states of H^- , which have already been partially discussed in the literature. (2-4) Since the observed effect of these states on the differential cross section appears to be considerably larger than expected from what we know of the resonances in the 1S series, it was decided to compare the experiment with the results of a detailed close-coupling calculation of the resonances just below the $n = 2$ threshold. Preliminary results for the 1D resonance place it at an energy of 10.15 eV with width $\Gamma = 0.0073$ eV. When the energy distribution of the electron beam is folded into the calculated cross section, the agreement between theory and experiment is reasonably good. The effects of including higher hydrogenic states as well as taking into account the considerations of Damberg and Geltman (5) are presently being examined.

*Work supported by DASA and the Air Force Special Weapons Center, Contract AF29601-68-C-0052, and by the National Aeronautics and Space Administration, Contract NAS 5-11025.

[†]Quantum Systems, Incorporated, Albuquerque, New Mexico.

-
1. J. William McGowan, E. M. Clarke, and E. K. Curley, Phys. Rev. Letters **15**, 917 (1965); **17**, 66E (1966).
 2. M. K. Gailitis and R. Damburg, Proc. Phys. Soc. **82**, 192 (1963).
 3. J. C. Y. Chen, Phys. Rev. **156**, 150 (1967).
 4. A. J. Taylor and P. G. Burke, Proc. Phys. Soc. **92**, 336, (1967).
 5. R. J. Damburg and S. Geltman, Phys. Rev. Letters **20**, 485 (1968).

A DETAILED COMPARISON OF THE THEORETICAL AND
EXPERIMENTAL RESULTS FOR THE 2p ELECTRON-
IMPACT EXCITATION CROSS SECTION OF HYDROGEN*

J. William McGowan and J. F. Williams

Submitted to the Arnold Sommerfeld Centennial Memorial
Meeting and International Symposium on the Physics of
One and Two Electron Atom, Munich, September 1968.

At first glance one is satisfied with the agreement between theory and experiment in the threshold region of the 2p electron-impact excitation cross section of atomic hydrogen. However, when a detailed comparison is made in the region between the onset of the $n = 2$ level and the $n = 4$ level, one finds that there is much yet to be done with the theory. The measured value for the total cross section lies below the best theoretical value. For example, if we consider the interval between 0.2 and 1.5 eV above threshold, the measured cross section is only 80% of the value estimated by the correlation method. (1) Similar agreement between theory and experiment for 2s excitation was recently reported by Fite *et al.* (2) The shape resonance predicted in the 1P channel just above threshold and the finite threshold of excitation are approximately the magnitude suggested by the theory. However, following the first shape resonance are at least two other small structures which appear to be real and which may be part of a series of such shape resonances. Unfortunately, the calculations that have been performed thus far have not been done on a fine enough grid to identify in which channel these other resonances lie.

As predicted by the six-state approximation, (3) there are a number of resonances just below the onset of the $n = 3$ level. However, there is not good agreement between the theoretically predicted and the measured resonances. Provided the positions that have been predicted are correct, one is lead to the conclusion that the dominant resonance structure is in the 1P channel while less prominent structure appears in the 1S channel. The theory, however, predicts that the principle resonance will be in the 1D channel.

In our experimental results one of the most prominent features appears at the threshold of $n = 3$. This no doubt reflects a large shape resonance at the threshold of the $n = 3$ level. Part of the flux from this resonance will appear directly in the 2p channel while another portion of it will arrive

* Work supported by the National Aeronautics and Space Administration, Contract NAS 5-11025, and by Gulf General Atomic Incorporated private research funds.

there through cascade from the 3s and 3d states of the atom. Although detailed measurements of the resonance structure between $n = 3$ and $n = 4$ have not been completed, it is clear from our crude measurements that some measurable resonance structure does exist in this interval. One would hope that the calculations similar to those of Damburg and Geltman⁽⁴⁾ will eventually be able to correct for the incompleteness in the original close-coupling approximation calculations.

-
1. A. J. Taylor and P. G. Burke, Proc. Phys. Soc. 92, 336 (1967).
 2. W. L. Fite, W. E. Kauppila, and W. R. Ott, Phys. Rev. Letters 20, 409 (1968).
 3. P. G. Burke, S. Ormonde, and W. Whitaker, Proc. Phys. Soc. 92, 319 (1967).
 4. R. J. Damburg and S. Geltman, Phys. Rev. Letters 20, 485 (1968).

APPENDIX II
PAPERS RESULTING THIS YEAR FROM
THE PROGRAM

Faddeev Equations for Atomic Problems and Solutions for the (e,H) System*

James S. Ball†
Department of Physics,
University of California, Los Angeles, California

and

Joseph C. Y. Chen
Department of Physics and Institute for Pure and Applied Physical Sciences,
University of California, San Diego, La Jolla, California

and

David Y. Wong
Department of Physics,
University of California, San Diego, La Jolla, California
 (Received 1 April 1968)

Solutions of the Faddeev equations for Coulomb potentials are investigated. A method which is of practical use for solving the Faddeev equations below the three-particle breakup threshold is developed. As an example, the method is applied to the (e, H) system in which the H⁻ bound state and the lowest members of the resonances in both the singlet and the triplet $J=0$ series are calculated. The results are in good agreement with the experimental measurements and previous calculations which used conventional methods.

I. INTRODUCTION

The nonrelativistic three-body problem with two-body interactions has been formulated by Faddeev^{1,2} in a way that allows straightforward computations. For short-range forces, the Faddeev equations have been applied successfully to a number of problems.³⁻¹³ It is the purpose of this paper to show that the Faddeev equations are equally applicable to atomic problems as long as the total energy is below the three-body breakup threshold - for example, the calculation of three-body bound states and resonance energies and wave functions below the ionization energy. The significant advantage of the Faddeev equation over conven-

tional methods is that the wave functions are calculated systematically along with the energy levels. No trial wave function is needed in the computation. Although this paper only contains a few illustrative examples all dealing with the e-H problem, we believe that the Faddeev equation has a considerably wider range of applicability. A brief account of this work was presented recently at the Leningrad Conference.¹⁴

In Sec. II, we give a simple derivation of the Faddeev equation, and review the method of reduction with respect to angular momentum. The method of solution is presented in Sec. III and applied to the H⁻ problem in Sec. IV. A discussion of possible extensions is given in Sec. V.

II. THE FADDEEV EQUATIONS

A. Formal Derivation

The scattering matrix $T(s)$ for the three-particle system with two-body interactions is a solution of the equation

$$T(s) = V + VG_0(s)T(s), \quad (2.1)$$

$$\text{with } V = \sum_i V_i (V_i \equiv V_{jk}), \quad (2.2)$$

$$G_0(s) = (s - H_0)^{-1}, \quad (2.3)$$

where the three particles are labeled by i , j , and k , and $G_0(s)$ is the free three-particle Green's function. The "off-shell" scattering matrix $T_i(s)$ arising from the two-body potential V_i above is given by the Lippmann-Schwinger equation

$$T_i(s) = V_i + V_i G_0(s) T_i(s). \quad (2.4)$$

Since V_i acts only on two particles, the third particle is therefore left as a spectator in Eq. (2.4). Equation (2.4), in effect, is equivalent to the equation for two-particle scattering matrix; the presence of the spectator particle gives rise to merely a shift in the energy scale.

Now we decompose the three-particle scattering matrix $T(s)$ into three components

$$T(s) = T^{(1)}(s) + T^{(2)}(s) + T^{(3)}(s), \quad (2.5)$$

$$\text{where } T^{(i)}(s) = V_i + V_i G_0(s) T(s). \quad (2.6)$$

As it stands, Eq. (2.6) is a set of integral equations with each $T^{(i)}$ coupled to all three operators $T^{(j)}$, $j = 1, 2$, and 3 . The main difference between these equations and the Faddeev equations is that, in the latter, each $T^{(i)}$ is only coupled to two $T^{(j)}$'s with $j \neq i$, and as a result, the kernel of the integral equation is less singular. We give here a simple derivation of the Faddeev equations:

Define the expression

$$\Omega = T^{(i)}(s) - T_i(s) - \sum_{j \neq i} T_i(s) G_0(s) T^{(j)}(s). \quad (2.7)$$

One can readily show by utilizing Eqs. (2.4)–(2.6) that

$$\Omega = V_i + \sum_{j=1}^3 V_i G_0 T^{(j)} - V_i - V_i G_0 T_i - \sum_{j \neq i} V_i G_0 T^{(j)} - \sum_{j \neq i} V_i G_0 T_i G_0 T^{(j)} = V_i G_0 \Omega. \quad (2.8)$$

Since $V_i G_0(s)$ is not the identity operator, Eq. (2.8) implies that $\Omega = 0$ for each i . We then obtain for $T^{(i)}(s)$ the equations

$$T^{(i)}(s) = T_i(s) + \sum_{j \neq i} T_i(s) G_0(s) T^{(j)}(s), \quad i = 1, 2, 3, \quad (2.9)$$

which are the well-known Faddeev equations.¹ In the matrix form:

$$\begin{pmatrix} T^{(1)}(s) \\ T^{(2)}(s) \\ T^{(3)}(s) \end{pmatrix} = \begin{pmatrix} T_1(s) \\ T_2(s) \\ T_3(s) \end{pmatrix} + \begin{pmatrix} 0 & T_1(s) & T_1(s) \\ T_2(s) & 0 & T_2(s) \\ T_3(s) & T_3(s) & 0 \end{pmatrix} G_0(s) \begin{pmatrix} T^{(1)}(s) \\ T^{(2)}(s) \\ T^{(3)}(s) \end{pmatrix}. \quad (2.10)$$

This is a coupled set of integral equations in five variables. Since no approximation is made on this formal transformation, the solution of Eq. (2.10) yields $T^{(1)}$, $T^{(2)}$, and $T^{(3)}$ whose sum is the exact solution of the original equation (2.1).

The Faddeev equations can also be interpreted diagrammatically. Let us represent T_1 by the sum of the diagrams as shown in Fig. 1 and similarly for T_2 and T_3 . For the T 's with a superscript, we use the symbols shown in Fig. 2. The Faddeev equations are then given by Fig. 3. One can easily see that the iterative solution of the three equations in Fig. 3 using the equation in Fig. 1 reproduces all the diagrams in perturbation theory. Our formal derivation given earlier simply shows that the Eqs. in Fig. 3 are valid even if the perturbation series fails to converge. In the diagrammatic representation, it is physically evident that $T^{(1)}$ is that part of the full three-body T matrix where particles 2 and 3 undergo a final-state interaction. Since T_i already represent a complete sequence of two-body interactions, each $T^{(i)}$ can only couple to $T^{(j)}$, $j \neq i$. As mentioned earlier, this decoupling of $T^{(i)}$ from itself results in a less singular kernel as compared to the original equation (2.6). This is due to the fact that each T_i is associated with a δ function corresponding to the momentum conservation of the i th particle, and the decoupling removes the repeated δ functions.

B. Three-Body Kinematics

To reduce the Faddeev equations, a suitable set of basis variables must first be chosen. For this purpose, the momentum representation is adopted. Let the masses and asymptotic momenta of the three particles be denoted by m_1 , m_2 , and m_3 , and \vec{k}_1 , \vec{k}_2 , and \vec{k}_3 , respectively. An appropriate set of basis variables may be constructed by taking certain combinations of the momenta in the center-of-mass system of the three particles. For $T^{(1)}$, the suitable basis variables are the pair of independent momentum

$$T_1 = \frac{1}{2} \frac{1}{3} \frac{1}{2} \frac{1}{3} \dots = \frac{1}{2} + \frac{1}{3} + \frac{1}{2} + \dots$$

FIG. 1 Diagrams for the two-body scattering matrix T_i . The wavy lines represent the two-particle potential V_i .

$$T^{(1)} = \text{diagram} \quad T^{(2)} = \text{diagram} \quad T^{(3)} = \text{diagram}$$

FIG. 2 Symbols representing the three-body scattering matrix $T^{(j)}$ with a pair of particles undergoes a final-state interaction.

$$\text{diagram} = \text{diagram} + \text{diagram} + \text{diagram} + \dots$$

$$\text{diagram} = \text{diagram} + \text{diagram} + \text{diagram} + \dots$$

$$\text{diagram} = \text{diagram} + \text{diagram} + \text{diagram} + \dots$$

FIG. 3 Diagrammatical representation of the Faddeev equations. The gap between two diagrams represents a noninteracting three-body Green's function.

variables.³

$$\vec{p}_1 = [m_3 \vec{k}_2 - m_2 \vec{k}_3] / [2m_2 m_3 (m_2 + m_3)]^{1/2}, \quad \vec{q}_1 = [m_1 (\vec{k}_2 + \vec{k}_3) - (m_2 + m_3) \vec{k}_1] / [2m_1 (m_2 + m_3) (m_1 + m_2 + m_3)]^{1/2}, \quad (2.11)$$

and their conjugated pairs \vec{p}_2, \vec{q}_2 and \vec{p}_3, \vec{q}_3 which are obtained by a cyclic interchange of subscripts in Eqs. (2.11) are the appropriate sets for $T^{(2)}$ and $T^{(3)}$ respectively.

The nonrelativistic kinetic energy in the center-of-mass frame may be written in any pair of basis variables;

$$H_0 = p_1^2 + q_1^2 = p_2^2 + q_2^2 = p_3^2 + q_3^2. \quad (2.12)$$

Consequently, the corresponding state vector $|\vec{k}_1, \vec{k}_2, \vec{k}_3\rangle$ may be represented in several equivalent forms

$$|\vec{k}_1, \vec{k}_2, \vec{k}_3\rangle = |\vec{p}_1, \vec{q}_1\rangle_1 = |\vec{p}_2, \vec{q}_2\rangle_2 = |\vec{p}_3, \vec{q}_3\rangle_3, \quad (2.13)$$

where the extra subscript keeps track of the proper pair of basis variables.

These sets of basis momentum variables are linearly dependent on each other. The relations are summarized below.

$$\vec{p}_1 = \alpha_{12} \vec{p}_2 - \beta_{12} \vec{q}_2 = -\alpha_{13} \vec{p}_3 + \beta_{13} \vec{q}_3, \quad \vec{q}_1 = \beta_{12} \vec{p}_2 - \alpha_{12} \vec{q}_2 = -\beta_{13} \vec{p}_3 - \alpha_{13} \vec{q}_3, \quad (2.14a)$$

$$\vec{p}_2 = -\alpha_{21} \vec{p}_1 + \beta_{21} \vec{q}_1 = -\alpha_{23} \vec{p}_3 - \beta_{23} \vec{q}_3, \quad \vec{q}_2 = -\beta_{21} \vec{p}_1 - \alpha_{21} \vec{q}_1 = \beta_{23} \vec{p}_3 - \alpha_{23} \vec{q}_3, \quad (2.14b)$$

$$\vec{p}_3 = -\alpha_{32} \vec{p}_2 + \beta_{32} \vec{q}_2 = -\alpha_{31} \vec{p}_1 - \beta_{31} \vec{q}_1, \quad \vec{q}_3 = -\beta_{32} \vec{p}_2 - \alpha_{32} \vec{q}_2 = \beta_{31} \vec{p}_1 - \alpha_{31} \vec{q}_1, \quad (2.14c)$$

$$\text{where } \alpha_{ij} = [m_i m_j / (m_i + m_j)(m_j + m_k)]^{1/2}, \quad \beta_{ij} = (1 - \alpha_{ij}^2)^{1/2} \quad (2.15)$$

We will frequently interchange these basis momentum variables among different sets for convenience.

C. Separation of Angular Momentum

A separation of the angular momentum states in the Faddeev equations can be carried out using the relative angular momentum of two particles, which is combined with the angular momentum of the third particle in the over-all center-of-mass system.^{9,15} In this decoupling scheme, the state vector $|\vec{p}_i, \vec{q}_i\rangle_i$ may be expanded in terms of a set of orthonormal partial-wave states $|p_i l m_i, q_i L m_L\rangle_i$. Since the total angular momentum J is conserved, we may in general consider the states to be diagonal in J . These states are given by

$$|p q J M L\rangle_i = (-)^{L-l-M} (2J+1)^{\frac{1}{2}} \sum_{m_i m_L} \begin{pmatrix} J & l & L \\ -M & m_i & m_L \end{pmatrix} |p l m_i, q L m_L\rangle_i, \quad (2.16)$$

$$\text{with } |p l m_i, q L m_L\rangle_i = Y_{l m_i}(\hat{p}) Y_{L m_L}(\hat{q}) |\vec{p}, \vec{q}\rangle_i, \quad (2.17)$$

$$\langle p l m_i, q L m_L | p' l' m_i', q' L' m_L' \rangle_i = (p q)^{-2} \delta(p - p') \delta(q - q') \delta_{ll'} \delta_{LL'} \delta_{m_i m_i'} \delta_{m_L m_L'}, \quad (2.18)$$

where the Wigner $3j$ symbol is adopted for the Clebsch-Gordan coefficients.

The Faddeev equations [Eqs. (2.9)] may be written in this representation as

$$\Psi_{\alpha}^{(i)}(p, q, s) = \Phi_{\alpha}^{(i)}(p, q, s) + \frac{1}{4} \sum_{\alpha_j} \sum_{j \neq i} \int_0^{\infty} dp_j^2 \int_0^{\infty} dq_j^2 \mathcal{X}_j^{(i)}(p, q, \alpha_j) [\rho_j q_j / (\rho_j^2 + q_j^2 - s)] \times \Psi_{\alpha_j}^{(j)}(p_j, q_j, s), \quad (2.19)$$

$$\text{with } \Psi_{\alpha}^{(i)}(p, q, s) = {}_i \langle p, q, \alpha | T_i^{(i)}(s) | \vec{k}_1, \vec{k}_2, \vec{k}_3 \rangle, \quad (2.20)$$

$$\Phi_{\alpha}^{(i)}(p, q, s) = {}_i \langle p, q, \alpha | T_i(s) | \vec{k}_1, \vec{k}_2, \vec{k}_3 \rangle, \quad (2.21)$$

$$\mathcal{X}_j^{(i)}(p, q, \alpha_j) = {}_i \langle p, q, \alpha | T_i(s) | p_j, q_j, \alpha_j \rangle_j, \quad (2.22)$$

where for convenience the discrete quantum numbers (JML) are collectively denoted by α . The physical interpretation of the equations is straightforward. The quantity $\Psi_{\alpha_j}^{(j)}(p_j, q_j, s)$ represents the contribution to the three-particle scattering amplitude in which particles j and k ($j \neq k \neq i$) undergo final-state interaction with relative angular momentum l_j . The quantity $\Phi_{\alpha_j}^{(j)}(p_j, q_j, s)$ represents the scattering amplitude in which particle i acts as a spectator. The initial state which is denoted by $|\vec{k}_1, \vec{k}_2, \vec{k}_3\rangle$ is arbitrary. The quantity p is proportional to the magnitude of the relative momentum between particles j and k , and the quantity q is proportional to the magnitude of the momentum of particle i in the three-particle center-of-mass frame.

Utilizing Eqs. (2.16)–(2.18), we obtain for the kernel $\mathcal{X}_j^{(i)}$ [defined in Eq. (2.22)] the expression

$$\mathcal{X}_j^{(i)}(p, q, \alpha_j) = (-)^{L+L'-l-l'} \sum_{\substack{m_l, m_L \\ m_l', m_L'}} \begin{pmatrix} J & l & L \\ -M & m_l & m_L \end{pmatrix} \begin{pmatrix} J & l' & L' \\ -M & m_l' & m_L' \end{pmatrix} \times \int d\vec{p}_j d\vec{q}_j d\vec{p}_i d\vec{q}_i \langle \vec{p} \vec{q} | T_i(s) | \vec{p}_j \vec{q}_j \rangle_j (2J+1) Y_{lm_l}^*(\hat{p}_i) Y_{Lm_L}(\hat{q}_i) Y_{l'm_l'}(\hat{p}_j) \times Y_{L'm_L'}(\hat{q}_j). \quad (2.23)$$

Since T_i involves only two-body potential V_i [see Eq. (2.4)], the matrix element ${}_i \langle \vec{p} \vec{q} | T_i(s) | \vec{p}_j \vec{q}_j \rangle_j$ in Eq. (2.23) may be reduced to a two-particle matrix element. According to Eqs. (2.3), (2.12), and (2.13), we have

$${}_i \langle \vec{p} \vec{q} | T_i(s) | \vec{p}_j \vec{q}_j \rangle_j = {}_i \langle \vec{p} \vec{q} | T_i(s) | p_i, q_i \rangle_i = \delta(\vec{q} - \vec{q}_i) \langle \vec{p} | \tilde{T}_i(s - q^2) | \vec{p}_i \rangle, \quad (2.24)$$

$$\text{with } \delta(\vec{q} - \vec{q}_i) = 2q^{-1} \delta(q^2 - q_i^2) \delta(\cos \theta_{\vec{q}} - \cos \theta_{\vec{q}_i}) \delta(\varphi_{\vec{q}} - \varphi_{\vec{q}_i}), \quad (2.25)$$

where \tilde{T}_i is the two-particle scattering matrix in the Hilbert space of the two-particle states. We may make use of the decomposition

$$\langle \vec{p} | \tilde{T}_i(s - q^2) | \vec{p}_i \rangle = -\frac{1}{2\pi^2} \sum_{l=0}^{\infty} (2l+1) P_l(\cos \theta_{\vec{p} \vec{p}_i}) t_l^{(i)}(p, p_i; s - q^2), \quad (2.26)$$

where the scattering amplitude between particles j and k with angular momentum l is normalized according to the equation

$$t_l^{(i)}(p, p; p^2) = e^{i\delta_l} (\sin \delta_l) / p. \quad (2.27)$$

Here p^2 is the two-body center-of-mass energy.

When Eqs. (2.24)–(2.26) are utilized, the kernel in the Faddeev equations may be written as⁶

$$\mathcal{X}_j^{(i)}(p, q, \alpha_j) = \int_{-1}^1 d \cos \theta_{\vec{p}_j \vec{p}_j} A_{\alpha_j}(\theta_{\vec{p}_i \vec{p}_j}, \theta_{\vec{q}_i \vec{p}_j}, \theta_{\vec{q}_j \vec{p}_j}) \delta(q^2 - q_i^2) t_l^{(i)}(p, p_i; s - q^2) \quad (2.28)$$

$$\text{with } A_{\alpha\alpha'}(\theta_{\vec{q}_j, \vec{p}_j}) = \frac{(-)^{L+L'-l-l'+1}}{q} 16\pi^{\frac{1}{2}}(2l'+1)^{\frac{1}{2}} \delta_{JJ'} \delta_{MM'} \sum_{\bar{m}_l \bar{m}_L \bar{m}_{L'}} \begin{pmatrix} l & L & J \\ m_l & m_L & -m_{L'} \end{pmatrix} \begin{pmatrix} l' & L' & J' \\ 0 & \bar{m}_{L'} & -\bar{m}_{L'} \end{pmatrix} \\ \times Y_{l\bar{m}_l}^*(\theta_{\vec{p}_i, \vec{p}_j}, 0) Y_{L\bar{m}_L}^*(\theta_{\vec{q}_i, \vec{p}_j}, 0) Y_{L'\bar{m}_{L'}}(\theta_{\vec{q}_j, \vec{p}_j}, 0), \quad (2.29)$$

where $\theta_{\vec{q}_j, \vec{p}_j}$, for example, is the angle between momentum variables \vec{q}_j and \vec{p}_j . It should be noted that these angles are related through the relations between different sets of pair momentum variables [see Eqs. (2.14)].

The above result was derived for any angular momentum state J of the three-particle system. For convenience, we will consider explicitly only states corresponding to zero total angular momentum. For this $J=0$ case, $\alpha=(00l) \equiv l$, and Eq. (2.29) becomes

$$A_{ll'}(\theta_{\vec{q}_j, \vec{p}_j}) = \frac{2(-)^{l+l'}}{\pi q} (2l+1)^{\frac{1}{2}} (2l'+1)^{\frac{1}{2}} p_l(\cos\theta_{\vec{q}_i, \vec{p}_i}) p_{l'}(\cos\theta_{\vec{q}_j, \vec{p}_j}), \quad (2.30)$$

with $p_i^2 = p_j^2 + q_j^2 - q^2$ and

$$\cos\theta_{\vec{q}_i, \vec{p}_i} = (ij) \frac{[\alpha_{ij}^2(q_j^2 - q^2) + \beta_{ij}^2(\sigma^2 - p_j^2)]}{2\alpha_{ij}\beta_{ij}q p_i}, \quad (2.31)$$

$$\cos\theta_{\vec{p}_j, \vec{q}_j} = (ij) \frac{[\beta_{ij}^2 p_j^2 + \alpha_{ij}^2 q_j^2 - q^2]}{2\alpha_{ij}\beta_{ij} p_j q_j}, \quad (2.32)$$

where (ij) denotes that $(12) = (23) = (31) = 1$ and $(21) = (32) = (13) = -1$.

Substituting Eq. (2.28) with $A_{ll'}$ given by Eq. (2.30) back into Eq. (2.19), and integrating over the angles, we obtain for the Faddeev equations

$$\Psi_l^{(i)}(p, q, s) - \Phi_l^{(i)}(p, q, s) + \sum_{j \neq i} \sum_{l'=0}^{\infty} \int_0^{\infty} dq_j^2 \int_{L_{ij}} U_{ij} dp_j^2 \\ \times \frac{(-)^{l+l'} [(2l+1)(2l'+1)]^{\frac{1}{2}} P_l(\cos\theta_{\vec{p}_i, \vec{q}_i}) P_{l'}(\cos\theta_{\vec{p}_j, \vec{q}_j})}{4\pi\alpha_{ij}\beta_{ij}q(p_j^2 + q_j^2 - s)} \\ \times t_l^{(i)}(p, p_i; s - q^2) \Psi_{l'}^{(j)}(p_j, q_j, s), \quad i=1, 2, 3 \quad (2.33)$$

with $U_{ij} = (\alpha_{ij} q_j + q)^2 / \beta_{ij}^2$, $L_{ij} = (\alpha_{ij} q_j - q)^2 / \beta_{ij}^2$. (2.34)

It is clear that if $t_l^{(i)}(p, p_i; s - q^2)$ is expanded in a sum of terms separable in p and p_i , then the p dependence of $\Psi_l^{(i)}(p, q, s)$ becomes explicit (p does not appear in the kinematic functions or the limits of integrations), and the coupled integral equations in two variables [Eq. (2.33)] can be reduced to equations of one variable.^{10,12} We will consider the application of these equations to three-particle atomic systems in which the interaction proceeds through two-body Coulomb potentials between each pair of particles.

III. THE METHOD OF SOLUTION

A. Eigenfunction Expansion for "Off-Shell" Amplitude

As mentioned before, the partial-wave Faddeev equations of two variables may be reduced to equations of one variable if the "off-shell" two-body scattering amplitudes t_l are represented in sums of separable terms. In general, if the two-body potentials $V_l^{(i)}$ for a system are given, the two-body amplitude $t_l^{(i)}$ can be obtained from the solution of the Lippmann-Schwinger equation

$$t_l^{(i)}(p, p'; E) = V_l^{(i)}(p, p') + \pi^{-1} \int_0^{\infty} dp''^2 p'' V_l^{(i)}(p, p'') t_l^{(i)}(p'', p'; E) / (p''^2 - E). \quad (3.1)$$

Since the argument E is replaced by $(s - q^2)$ in the Faddeev equations, it is negative-definite provided the three-particle energy s is below the three-particle threshold ($s=0$). For negative values of E , the $(p''^2 - E)^{-1}$ term in Eq. (3.1) is nonsingular, and it is well known that the solution for $t_l^{(i)}$ can be expressed

in terms of eigenfunctions of the homogeneous portion of Eq. (3.1).

The solution $\phi_{nl}^{(i)}$ of the homogeneous Lippmann-Schwinger equation and the corresponding eigenvalues $\lambda_{nl}^{(i)}$ are defined by

$$\lambda_{nl}^{(i)}(E)\phi_{nl}^{(i)}(p, E) = \pi^{-1} \int_0^\infty dp'' \{p'' V^{(i)}(p, p'') / (p''^2 - E)\} \phi_{nl}^{(i)}(p'', E), \quad (3.2)$$

with the orthonormality property

$$\pi^{-1} \int_0^\infty dp'' p'' \phi_{nl}^{(i)}(p'', E) \phi_{ml}^{(i)}(p'', E) / (p''^2 - E) = \delta_{nm}. \quad (3.3)$$

Since $\phi_{nl}^{(i)}$ constitutes a complete set, the two-body amplitude $t_l^{(i)}$ can be expanded in the form

$$t_l^{(i)}(p, p'; E) = \sum_{n=0}^\infty C_{nl}^{(i)}(p', E) \phi_{nl}^{(i)}(p, E). \quad (3.4)$$

Substitution of (3.4) into Eq. (3.1) yields, with the help of Eqs. (3.2) and (3.3),

$$t_l^{(i)}(p, p'; E) = \sum_{n=0}^\infty \{\lambda_{nl}^{(i)}(E) / [1 - \lambda_{nl}^{(i)}(E)]\} \phi_{nl}^{(i)}(p, E) \phi_{nl}^{(i)}(p', E). \quad (3.5)$$

This is the desired representation for $t_l^{(i)}$ in the sums of separable terms. In momentum representation, the Coulomb potential is

$$V_l^{(i)}(p, p') = - (Z_i \mu_i)^{\frac{1}{2}} / \sqrt{2} p p' Q_l(p^2 + p'^2) / 2 p p', \quad (3.6)$$

where the Q_l 's are the Legendre functions of the second kind, μ_i is the reduced mass, and Z_i is the product of the charges (i. e., $Z_j Z_k$) of the two particles. For this potential the eigenfunction $\phi_{nl}^{(i)}$ and the eigenvalue $\lambda_{nl}^{(i)}$ are both known analytically.¹⁶ We have

$$\phi_{nl}^{(i)}(p, E) = [N_{nl}^{(i)}(E) p^l / (p^2 - E)^{l+1}] C_{n-l-1}^{l+1}[(p^2 + E) / (p^2 - E)], \quad n > l \quad (3.7)$$

$$\text{and } \lambda_{nl}^{(i)}(E) = -Z_i \mu_i^{\frac{1}{2}} / n \sqrt{-2E}, \quad (3.8)$$

where $n > l$ and the normalization constant is

$$N_{nl}^{(i)}(E) = [2^{4l+3} n(n-l-1)! / \Gamma(n+l+1)]^{\frac{1}{2}} l! (-E)^{(2l+3)/4}. \quad (3.9)$$

The $C_{m-1}^{l+1}(x)$'s in Eq. (3.7) are the Gegenbauer polynomials¹⁷

$$C_{m-1}^{l+1}(x) = \frac{\Gamma(m+2l+1)}{\Gamma(m)\Gamma(2l+3)} F\left(m+2l+1, 1-m; l+\frac{3}{2}; \frac{1}{2}(1-x)\right) = \sum_{\gamma=0}^{m-1} a_\gamma^{(l+1)}(m) \left(\frac{x-1}{2}\right)^\gamma, \quad (3.10)$$

$$\text{with } a_\gamma^{(l+1)}(m) = [2(m+2l+\gamma)(m-\gamma) / \gamma(2l+2\gamma+1)] a_{\gamma-1}^{(l+1)}(m), \quad (3.11)$$

where the recursion relation for the a 's starts with

$$a_0^{(l+1)}(m) = (m+2l)! / (2l+1)! (m-1)!. \quad (3.12)$$

B. Coupled Single-Variable Integral Equations

Utilizing the separable representation [Eq. (3.5)] for the off-shell two-particle amplitude, the p dependence of $\Psi_\alpha^{(i)}(p, q, s)$ can now be made explicit. Let us return to the Faddeev equations for total $J=0$. From Eq. (2.33), it is clear with the help of Eq. (3.5) that $\Psi_l^{(i)}(p, q, s)$ can be expressed as

$$\Psi_l^{(i)}(p, q, s) = \Phi_l^{(i)}(p, q, s) + \sum_n \{\lambda_{nl}^{(i)}(s - q^2) / [1 - \lambda_{nl}^{(i)}(s - q^2)]\} \phi_{nl}^{(i)}(p, s - q^2) \chi_{nl}^{(i)}(q, s). \quad (3.13)$$

Substituting Eq. (3.13) into Eq. (2.33), we obtain a set of coupled single-variable integral equations for $\chi_{nl}^{(i)}(q, s)$:

$$\chi_{nl}^{(i)}(q, s) = \eta_{nl}^{(i)}(q, s) + \sum_{n', l'; j \neq i} \int_0^\infty dq_j^2 \mathcal{K}_{nl, n'l'}^{(i, j)}(q, q_j; s) \chi_{n'l'}^{(j)}(q_j, s), \quad i=1, 2, 3 \quad (3.14)$$

$$\text{with } \eta_{nl}^{(i)}(q, s) = \sum_{l', j \neq i} \int_0^\infty dq_j^2 \int_{L_{ij}}^{U_{ij}} dp_j^2 \frac{(-)^{l+l'} [(2l+1)(2l'+1)]^{\frac{1}{2}}}{4\pi\alpha_{ij}\beta_{ij} q(p_j^2 + q_j^2 - s)} P_l(\cos\theta_{\vec{p}_i, \vec{q}_i}) P_{l'}(\cos\theta_{\vec{p}_j, \vec{q}_j}) \\ \times \phi_{nl}^{(i)}(p_i, s - q^2) \phi_{l'}^{(j)}(p_j, q_j), \quad (3.15)$$

$$\mathcal{K}_{nl, n'l'}^{(i, j)}(q, q_j; s) = \int_{L_{ij}}^{U_{ij}} dp_j^2 \frac{(-)^{l+l'} [(2l+1)(2l'+1)]^{\frac{1}{2}} P_l(\cos\theta_{\vec{p}_i, \vec{q}_i}) P_{l'}(\cos\theta_{\vec{p}_j, \vec{q}_j})}{4\pi\alpha_{ij}\beta_{ij} q(p_j^2 + q_j^2 - s) [1 - \lambda_{n'l'}^{(j)}(s - q_j^2)]} \\ \times \phi_{nl}^{(i)}(p_i, s - q^2) \lambda_{n'l'}^{(j)}(s - q_j^2) \phi_{n'l'}^{(j)}(p_j, s - q_j^2). \quad (3.16)$$

Equations (3.14) are the basic working equations. We will now examine their physical implications.

Let us first examine the singularities of the kernel \mathcal{K} given by Eq. (2.16). For negative values of s , two-particle bound states of the system (if they exist) play an important role in the analytic structure of the kernel \mathcal{K} . Denote the two-particle bound-state energy by $-\epsilon$. For each such two-particle state, there is a corresponding eigenvalue λ which equals to unity at $-\epsilon$. The denominator $1 - \lambda_{n'l'}^{(j)}(s - q^2)$ in the kernel then vanishes at $q^2 = s + \epsilon$ for $s > -\epsilon$, therefore creating a branch point for $\chi_{nl}^{(i)}(q, s)$ at $s = -\epsilon$. Three-particle bound states can only occur below the branch points. The region between the lowest and the next branch points is the energy region for purely elastic scattering of a particle by a two-particle system in its ground state. A single inelastic process occurs above the second threshold, and so forth. By solving the Faddeev equations, we can obtain bound-state and resonance energies and wave functions below the three-particle breakup threshold.

Now if there is no two-particle bound state between any pair of particles in the three-particle system, the behavior of the kernel \mathcal{K} becomes less complicated, since in this case the kernel is pure real below $s=0$. Again, Eqs. (3.14) can be solved in a straightforward manner for both the energies and wave functions of any possible three-particle bound states.

It should be noted, however, that if the total energy s is positive (i.e., above the three-particle breakup threshold), then there is a region $0 < q^2 < s$ where the two-particle energy $s - q^2$ is positive and the expansion for the off-shell two-particle amplitude [Eq. (3.5)] in general fails to converge. The method discussed above becomes unsuitable. This includes the problems of three-particle breakup such as, for example, the ionization of hydrogen atoms by electron impact.

We remark here that, for the Coulomb interaction, the two-body T matrix $t_l(p, p', E)$ is singular at $p^2 = E$, $p'^2 = E$ or $p = p'$ for all E . The first two regions are inaccessible below the three-particle threshold (ionization energy), because E is negative-definite while p and p' are positive. The region $p = p'$ is accessible but the kernel $\mathcal{K}_{nl, n'l'}(q, q_j; s)$ is already the result of an integration over p_j^2 . Since the singularity at $p = p'$ is only logarithmic, the kernel no longer contains such a logarithmic singularity. This, we believe, is the reason why the three particle atomic problem can be handled by the Faddeev equations without further modification, as long as the total energy is below the three-particle breakup threshold.

So far the initial states of the three-particle system are left unspecified. This is possible because the kernel of the integral equation is independent of the initial state, and the energy spectrum of the three-body system is determined entirely by the kernel. The specification of the initial state and the corresponding inhomogeneous terms are, however, of importance for the wave function of the scattering problem. We now show how this term may be calculated.

For a physical scattering process, one usually has an initial state consisting of two interacting subsystems; in the present case, a particle plus a two-particle subsystem in certain bound state. For definiteness, we consider an initial state consisting of particle 1 and a bound state of (2, 3) with energy s_0 and angular momentum l_0 . The corresponding inhomogeneous term takes the form [see Eqs. (2.21), (2.24), and (2.26)]

$$\Phi_{l_0}^{(1)}(p, q, s) = \frac{4}{q_0^2 - (s - s_0)} t_{l_0}^{(1)}(p, p_0, s - q_0^2) \delta(q^2 - q_0^2), \quad (3.17)$$

where p_0 and q_0 are the p and q of the initial state. Since $t_{l_0}^{(1)}$ has a pole at $s - q_0^2 = s_0$, $\Phi_{l_0}^{(1)}(p, q, s)$ can be rewritten as

$$\Phi_{l_0}^{(1)}(p, q, s) = \frac{4}{q_0^2 - (s - s_0)} \frac{1}{\pi q} [\delta(q^2 - s + s_0) / \lambda_{n_0 l_0}^{(1)'}(s_0)(s - q_0^2 - s_0)] \phi_{n_0 l_0}^{(1)}(p, s_0) \phi_{n_0 l_0}^{(1)}(p_0, s_0), \quad (3.18)$$

where λ' is the derivative of λ with respect to s .

Now multiply both sides of Eq. (2.33) by $(s - q_0^2 - s_0) / \phi_{n_0 l_0}^{(1)}(p_0, s_0)$ and then take the limit $q_0^2 - s - s_0$. It is easily seen that all the inhomogeneous terms vanish except for $\Phi_{l_0}^{(1)}$ and that the wave function of the initial (2,3) bound state $\phi_{n_0 l_0}^{(1)}(p_0, s_0)$ is factored out of the equation. Substitution of $\Phi_{l_0}^{(1)}$ from Eq. (3.18) into Eq. (3.15) gives an explicit inhomogeneous term $\eta_{nl}^{(i)}$. Equation (3.14) can now be solved by standard numerical methods. For s above the lowest branch point the kernel must be taken as the limit of s approaching the real axis from above. One can either use numerical methods for complex arithmetics or the Fredholm reduction given by Noyes¹⁸ and by Kowalski.¹⁹

C. Spin and Identical Particles

So far, we have not considered spin in this formulation of the Faddeev equations. For nonrelativistic atomic problems, there is no spin-orbit coupling and the effect of the spin simply appears as a multiplicative factor in the kernel⁸:

$$\chi_{nl, n'l'}^{(i,j)}(q, q_j; s) - \chi_{nl, n'l'S'}^{(i,j)}(q, q_j; s, S_0) = (-1)^{S_i + S_j + S_k + S_0} [(2S+1)(2S'+1)]^{\frac{1}{2}} \left\{ \begin{matrix} S_j & S_k & S \\ S_i & S_0 & S' \end{matrix} \right\} \times \chi_{nl, n'l'}^{(i,j)}(q, q_j, s), \quad (3.19)$$

where S_0 is the total spin of the three-particle system; S the spin of the pair (j, k) ; S' the spin of the pair (k, i) ; S_i , S_j , and S_k the spins of the individual particles; and $\left\{ \begin{matrix} S_j & S_k & S \\ S_i & S_0 & S' \end{matrix} \right\}$ denotes the $6j$ symbol. Of course, the T -matrix elements $\chi_{nl}^{(i)}$ should now carry an additional spin index S denoting the spin of the pair (j, k) .

As for identical particles, the statistics require that the two-body partial wave T matrix $t_l^{(i)}(p, p'; E, S)$ be identically zero for certain l . In particular, for two spin- $\frac{1}{2}$ identical fermions, t is zero for even l if $S=1$ and for odd l if $S=0$. As long as all the two-body T -matrix elements satisfy the requirement of statistics, the solution of the Faddeev equations also satisfies the statistic. The number of equations is reduced because some of the kernels become equivalent.

IV. APPLICATION TO THE (e, H) SYSTEM

It is well-known that for the (e, H) system, there exists only one three-particle bound state corresponding to the ground $^1S H^-$ state. All the other three-particle states are unstable. They correspond to the resonant states which may be generated in the laboratory in an electron-hydrogen (atom) scattering experiment.^{20,21} Theoretically it can be shown^{22,23} that associated with each excited two-particle threshold (corresponding to the excited states of H atom) there exist a number of resonances supported by a potential which asymptotically goes to zero primarily as r^{-2} . Reasonably accurate determinations of the position and the width of a few of the lower members of the resonances have been recently carried out both theoretically²⁴⁻²⁹ and experimentally.²¹ For the bound H^- state on the other hand, an accurate value for the H^- detachment potential has been known for some time. A calculation of this singlet H^- state and the lowest members of the resonances in both the singlet and the triplet $J=0$ series would therefore provide some insight into the feasibility of the method outlined in Sec. III.

A. The $^1S H^-$ Bound State

Since the $^1S H^-$ state has a zero total angular momentum (i.e., $J=0$), Eq. (3.4) may be used for the calculation of this state. One can readily show for singlet spin multiplicity that the electron-proton interaction amplitudes for electrons 1 and 2 must satisfy the relation

$$\chi_{nl}^{(1)}(q, s) = (-)^l \chi_{nl}^{(2)}(q, s), \quad (4.1)$$

and the electron-electron amplitude the relation

$$\chi_{nl}^{(3)}(q, s) = 0 \text{ for odd } l. \quad (4.2)$$

Equation (4.2) is simply the statement of the Pauli principle which excludes the possibility for two electrons in the singlet spin state to have odd parity. Equation (4.1) allows for the reduction of the coupled equations [Eq. (3.14)] into a pair of coupled equations. The spin factor for the kernel is unity in this case.

We write Eq. (3.14) in the matrix notation

$$\chi(q, s) = \underline{\eta}(q, s) + \int_0^\infty dq_j^2 \underline{\mathcal{K}}(q, q_j; s) \chi(q_j, s), \quad (4.3)$$

$$\text{with } \underline{\chi}^\dagger(q, s) = [\chi_0^{(1)}(q, s), \chi_0^{(3)}(q, s), \chi_1^{(1)}(q, s), \chi_1^{(3)}(q, s), \chi_2^{(1)}(q, s), \chi_2^{(3)}(q, s), \dots], \quad (4.4)$$

where each element $\chi_i^{(j)}(q, s)$ is a row with a dimension which equals the number of terms included in the off-shell two-particle amplitude $t_l^{(j)}$ [see Eq. (3.5)]. Equation (4.3) may be solved for $\chi(s)$ by digitizing the continuous variables q and q_j and inverting the matrix $[I - \underline{\mathcal{K}}]$

$$\underline{\chi}(s) = [I - \underline{\mathcal{K}}(s)]^{-1} \underline{\eta}(s). \quad (4.5)$$

To calculate the bound H^- state, we need to determine the pole in the inverse operator $[I - \underline{\mathcal{K}}(s)]^{-1}$. The pole may be located by locating the energy s at which the determinant of the $I - \underline{\mathcal{K}}(s)$ matrix is zero.

For Coulomb interactions, the matrix elements in $\underline{\mathcal{K}}$ may be obtained analytically since both the eigenfunctions $\phi_{nl}^{(i)}$ and eigenvalues $\lambda_{nl}^{(i)}$ of the homogeneous Lippmann-Schwinger equation [Eq. (3.2)] are known explicitly [see Eqs. (3.7) and (3.8)]. It can be shown that when these explicit expressions are utilized with the help of Eq. (3.10), all the integrals needed for the evaluation of the matrix element in $\underline{\mathcal{K}}$ can be expressed in terms of the basic integrals

$$I_n(q, q_i; s) \equiv \int \frac{(\sqrt{2}q + q_i)^2}{(\sqrt{2}q - q_i)^2} \frac{dp_i^2}{(p_i^2 + q_i^2 - s)^{n+1}}, \quad (4.6)$$

where we have made use of the large disparity between the electron and proton masses (i.e., $m_1/m_3 = m_2/m_3 \approx 0$). These integrals satisfy the recursion relation

$$I_{n+1} = [n/(n+1)] \{[(\xi + \zeta)^{n+1} - (\xi - \zeta)^{n+1}] / [(\xi + \zeta)^n - (\xi - \zeta)^n]\} [I_n / (\xi^2 - \zeta^2)], \quad n \geq 1, \quad (4.7)$$

$$\text{with } \xi = (2q^2 + 2q_i^2 - s), \quad \zeta = 2\sqrt{2}qq_i, \quad (4.8)$$

where the recursion relation for the I 's starts with

$$I_1 = 4\sqrt{2}qq_i / [(2q^2 + 2q_i^2 - s)^2 - 8q^2q_i^2]. \quad (4.9)$$

As discussed before, the three-particle bound states can only occur below the branch point corresponding to the elastic threshold. In this energy region $s < -1$ Ry (-13.605 eV), the matrix $[I - \underline{\mathcal{K}}]$ is pure real. After Eqs. (4.1) and (4.2) are utilized in Eqs. (4.3), the resultant matrix integral equations are then solved by matrix inversion [Eq. (4.5)]. By taking only the first term in the $t_l^{(j)}$ expansion [Eq. (3.5)], we found that the H^- state appears at -1.0516 Ry below the three-particle breakup threshold. This corresponds to a detachment potential of -0.0516 Ry (i.e., 0.702 eV) for H^- in comparison with the accurate value of -0.0555 Ry of Peheris.³⁰ The agreement is most remarkable in view of the fact that only a single $1s$ term in the $t_l^{(j)}$ expansion is used in the calculation. This then implies that all the remaining terms contribute less than 7%.

To demonstrate that all the remaining terms in the $t_l^{(j)}$ expansion contribute less than 7% is, however, a somewhat difficult task. The expansion converges in an oscillatory manner and involves large cancellations. For example, the addition of the $2s$ term pushes the H^- state up very close to the elastic threshold. The $2s$ term effect is cancelled by the $3s$ term. The net result due to the inclusion of the $2s$ and $3s$ terms is to move the H^- state down to -1.061 Ry. On the other hand, the addition of $2p$ and $3p$ terms would lower further the H^- state to -1.064 Ry, and the addition of a $3d$ and $4s$ terms then pushes the H^- state up to -1.063 Ry. It is clear from the numerical result that the oscillations become smaller for higher terms in the $t_l^{(j)}$ expansion. However, our results seem to converge to a value lower than the accepted value. This is probably due to systematic errors in our numerical calculations. We will return to the convergence problem in Sec. V. Perhaps it is worthwhile to note that there is a substantial continuum component in each term of the $t_l^{(j)}$ expansion because this is a Stieltjes function expansion, so that the symbols $1s$, $2s$, $2p$, etc. should be interpreted accordingly.

Recently, a calculation of the H^- bound state has been carried out by Vesselova.³¹ In this calculation the two-body interaction amplitude between the electrons $t_l^{(j)}$ was taken to be zero. As a test of our program we have considered the $t_l^{(j)} = 0$ case and obtained, as expected, an energy spectrum which is simply the superposition of two sets of hydrogenic levels.

B. The Resonant H^- States

As the total energy s of the system moves above the elastic threshold, we encounter the electron-hydrogen scattering problem. The corresponding matrix $(I - \mathfrak{K})$ now becomes complex and contains branch points arising from bound states of H atom. These branch points must be treated properly in solving Eq. (4.3) for resonant states and in calculating the complex poles in $(I - \mathfrak{K})^{-1}$. As an example, we will determine the two lowest $J=0$ resonances with singlet and triplet spin states in the elastic region. We choose this example for simplicity since in the elastic energy region the branch point of concern is reduced to just the one associated with the ground hydrogen state.

For the calculation of the singlet $J=0$ resonances, one may again solve Eq. (4.3) numerically. Due to the presence of the branch points, it is difficult to maintain a desired accuracy by the standard numerical method of complex integration. However, the accuracy may be significantly improved by the Fredholm reduction method^{18,19} in which the branch points are removed from the matrix to be inverted. For the present problem, the only branch point of concern is that associated with the ground H state in $\chi_0^{(1)}(q, s)$ [Eq. (4.4)]. We will now show how such a method may be adopted for the present problem.

Write for $\underline{\chi}(q, s)$ the expression

$$\underline{\chi}(q, s) = u(s) \underline{\Upsilon}(q, s) \quad (4.10)$$

where $u(s) = \chi(\sqrt{s_0}, s)$ and

$$\underline{\Upsilon}^\dagger(s) = [\tau_0^{(1)\dagger}(q, s), \tau_0^{(3)\dagger}(q, s), \tau_1^{(1)\dagger}(q, s), \tau_1^{(3)\dagger}(q, s), \tau_2^{(1)\dagger}(q, s), \tau_2^{(3)\dagger}(q, s), \dots] \quad (4.11)$$

where $s_0 \equiv s + 1$, $u(s_0)$ is a scalar function, and the $\tau_j^{(i)}(q, s)$'s are columns with elements $\tau_{nl}^{(i)}(q, s)$. For the purpose of calculating resonance poles, we may replace Eq. (4.3) by

$$u(s) \underline{\Upsilon}(q, s) = \mathfrak{K}_{10}^{(1)}(q, \sqrt{s_0}, s) + u(s) \int_0^\infty dq_j^2 \mathfrak{K}(q, q_j, s) \underline{\Upsilon}(q_j, s) \quad (4.12)$$

where we have replaced $\eta(q, s)$ [see Eq. (4.3)] by $\mathfrak{K}_{10}^{(1)}(q, s_0; s)$ since poles in $\chi(s)$ are independent of the inhomogeneous term $\eta(q, s)$ [see Eq. (4.5)]. The symbol $\mathfrak{K}_{10}^{(1)}$ stands for $\mathfrak{K}_{10, nl}^{(1, i)}$ where i, n , and l are the suppressed indices of Υ . This quantity $\mathfrak{K}_{10}^{(1)}(q, s_0; s)$ in Eq. (4.12) is chosen to make the kernel of the integral equation for Υ nonsingular at $q^2 = s_0$. By definition of u , $\tau_{10}^{(1)}(\sqrt{s_0}, s)$ is normalized to unity. Solving Eq. (4.12) for $u(s)$ at $q^2 = s_0$, we obtain

$$u(s) = \mathfrak{K}_{10, 10}^{(1, 1)}(\sqrt{s_0}, \sqrt{s_0}; s) / \left(1 - \sum_{\substack{j, n, l \\ n > l}} \int_0^\infty dq_j^2 \mathfrak{K}_{10, nl}^{(l, j)}(\sqrt{s_0}, q_j; s) \tau_{nl}^{(j)}(q_j, s) \right). \quad (4.13)$$

Substitution of $u(s)$ from Eq. (4.13) back into Eq. (4.12) yields

$$\underline{\Upsilon}(q, s) = \frac{\mathfrak{K}_{10}^{(1)}(q, \sqrt{s_0}, s)}{\mathfrak{K}_{10, 10}^{(1, 1)}(\sqrt{s_0}, \sqrt{s_0}; s)} + \int_0^\infty dq_j^2 \left\{ \mathfrak{K}(q, q_j; s) - \frac{\mathfrak{K}_{10}^{(1)}(q, \sqrt{s_0}; s)}{\mathfrak{K}_{10, 10}^{(1, 1)}(\sqrt{s_0}, \sqrt{s_0}; s)} \mathfrak{K}_{10}^{(1)\dagger}(\sqrt{s_0}, q_j; s) \right\} \underline{\Upsilon}(q_j, s). \quad (4.14)$$

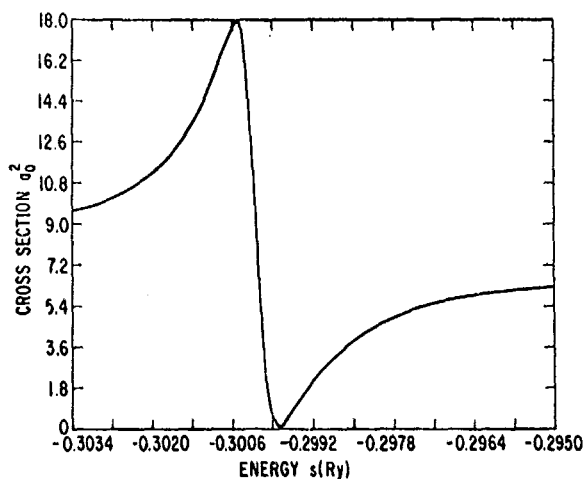
Now, the kernel does not have a pole at $q_j^2 = s_0$, and Eq. (4.14) contains no branch point for $s < -0.25$ Ry. It may be solved in a straightforward manner for $\underline{\Upsilon}(q, s)$. Having obtained $\underline{\Upsilon}(q, s)$, $u(s)$ can be calculated by evaluating the principal part integral in Eq. (4.13), and the poles of $u(s)$ are then poles of χ .

Unlike the case for the bound state, retaining only the $1s$ term in the $t_j^{(i)}$ expansion [Eq. (3.5)] fails to give any resonance. A resonance pole is found when either the $2s$ or the $2p$ term is included in the $t_j^{(i)}$ expansion. This is expected since the H^- resonances are closed-channel resonances²² lying very close to the excitation threshold. The positions of the pole obtained in the $1s-2s$ and $1s-2p$ expansions are at -0.286 and -0.291 Ry below the three-particle breakup threshold, respectively. The position of the lowest H^- resonance in the $J=0$ singlet series has been found to be at -0.2973 Ry both experimentally²¹ and theoretically.²²⁻²⁹ This seems to indicate that neither the $2s$ nor the $2p$ term alone is sufficiently attractive to lower the pole to -0.2973 Ry. From these results one may also conclude that the $2p$ term is more attractive than the $2s$ term.

The combined effect of the $2s$ and $2p$ terms, on the other hand, is much too attractive. The pole is lowered in the $1s-2s-2p$ approximation to -0.326 Ry. It requires the $3s$ term to push the pole up to -0.3004 Ry. The addition of the $3p$ and $3d$ terms move the pole further up to -0.298 Ry, which is closer to the value of -0.2973 Ry calculated in the closed-coupling approximation with correlated wave functions. Though there is a definite indication of convergence towards the value of -0.2973 Ry, the convergence is again oscillatory and not rapid. It is perhaps worthwhile to emphasize that the present calculation is term-by-term exact. No variational or stationary parameters were used in the calculation.

The calculated width for the lowest $J=0$ singlet resonance in the $1s-2s-2p-3s$ approximation is 0.0025 Ry (0.034 eV) which is in reasonable agreement with previous calculations.^{24, 25, 28, 29} The measured width for this resonance is 0.043 eV.²¹ In Fig. 4 the profile of the elastic scattering cross section in the neigh-

FIG. 4 Energy dependence of the singlet $J=0$ elastic scattering cross section in the neighborhood of the resonance in the $1s-2s-2p-3s$ approximation.



borhood of the $J=0$ singlet resonance is given. It is seen that the interference between direct and resonance scattering is important. Due to the absence of other channels, the cross section actually dips through zero at $s = -0.2997$ Ry.

For the triplet case, the electron-proton interaction amplitudes for electrons 1 and 2 must satisfy, instead of Eq. (4.1), the relation

$$\chi_{nl}^{(1)}(q, s) = (-)^{l+1} \chi_{nl}^{(2)}(q, s), \quad (4.15)$$

and the electron-electron interaction must satisfy, instead of Eq. (4.2), the relation

$$\chi_{nl}^{(3)}(q, s) = 0, \quad \text{for even } l. \quad (4.16)$$

Equation (4.16) is again the statement of the Pauli principle which excludes the possibility for two electrons in the triplet spin state to have even parity. Equation (4.15) allows for the reduction of Eq. (3.14) into a different pair of coupled equations for the triplet case. The spin factor for the kernel is again unity.

The behavior of the solution for the triplet case is similar in nature to the singlet case. We obtain in the $1s-2s-2p-3s-3p$ approximation a resonance pole at -0.257 Ry below the three-particle breakup threshold with a width of $\sim 2 \times 10^{-5}$ Ry (2.72×10^{-4} eV) which are in reasonable agreement with the previously calculated values.^{25,29}

V. CONCLUDING REMARKS

The method presented in Sec. III provides a practical way of solving the Faddeev equation for Coulomb potentials below three-particle breakup threshold. It is seen, from the example in Sec. IV, that by retaining only a few leading terms in the series a reasonably accurate value is obtained. The interesting problem is then to investigate the convergence of the remaining terms in the series. This is, however, a somewhat difficult task, since, as was pointed out in Sec. IV, the expansion converges in an oscillatory manner and involves large cancellations. The net sum of all the terms, considered as a whole, constitutes, nevertheless, a small correction. It is then feasible that a perturbation scheme in which the sum of the contribution of the remaining terms is treated as a perturbation may be developed. In this concluding section, we outline such a perturbative scheme.

Let us consider the problem of determining the poles in the inverse operator in Eq. (4.5) by examining the energy dependence of the determinant $\text{Det}\{I - \mathcal{K}(s)\}$. We can partition the matrix as

$$I - \mathcal{K}(s) = \underline{B} + \underline{\mathcal{E}} = \underline{B}\{I + \underline{B}^{-1}\underline{\mathcal{E}}\}, \quad (5.1)$$

where \underline{B} is a square matrix consisting of elements obtained in a truncated expansion including the leading terms in the series and $\underline{\mathcal{E}}$ is the remainder. Utilizing the relation between the determinant and the trace of the logarithm of the corresponding matrix,

$$\text{Det } \underline{A} = \exp\{\text{Tr}(\ln \underline{A})\}, \quad (5.2)$$

we have

$$\text{Det}\{I - \mathcal{K}(s)\} = \text{Det } \underline{B} \exp\{\text{Tr}[\ln(1 + \underline{B}^{-1}\underline{\mathcal{E}})]\} = \text{Det } \underline{B} \{1 + \text{Tr} \underline{B}^{-1}\underline{\mathcal{E}} - \frac{1}{2} \text{Tr}(\underline{B}^{-1}\underline{\mathcal{E}}\underline{B}^{-1}\underline{\mathcal{E}}) + \dots\}. \quad (5.3)$$

Defining $\underline{C} = \underline{B}^{-1}$, we have

$$\text{Det}\{I - \underline{K}(s)\} = \text{Det}\underline{B} \left[1 + \sum_{\alpha=m+1}^n \epsilon_{\alpha\alpha} - \sum_{\alpha=1}^m \sum_{\beta=1}^m \sum_{\gamma=m+1}^n c_{\alpha\beta} \epsilon_{\beta\gamma} \epsilon_{\gamma\alpha}^{-\frac{1}{2}} \sum_{\alpha=m+1}^n \sum_{\lambda=m+1}^n \epsilon_{\lambda\alpha} \epsilon_{\alpha\lambda} + \frac{1}{2} \left(\sum_{\alpha=m+1}^n \epsilon_{\alpha\alpha} \right)^2 + \dots \right], \quad (5.4)$$

where ϵ_{ij} and c_{ij} are the elements of matrices \underline{G} and \underline{C} respectively, n is the order of the matrix while m is the order of the submatrix corresponding to the truncated expansion. This then provides a systematic way of investigating the convergence problem.

*This research was supported in part by the Advanced Research Projects Agency (Project DEFENDER) and was monitored by the U.S. Army Research Office - Durham under Contract DA-31-124-ARO-D-257, by the U.S. Atomic Energy Commission, and by NASA under contract NAS 5-9321 through Gulf General Atomic Inc.

†Alfred P. Sloan Fellow.

¹L. D. Faddeev, *Zh. Eksperim. i Teor. Fiz.* **39**, 1459 (1960) [English transl.: *Soviet Phys. - JETP* **12**, 1014 (1961)]; *Dokl. Akad. Nauk SSSR* **138**, 565 (1961) [English transl.: *Soviet Phys. - Doklady* **6**, 384 (1961)]; *Dokl. Akad. Nauk SSSR* **145**, 301 (1962) [English transl.: *Soviet Phys. - Doklady* **7**, 600 (1963)].

²L. D. Faddeev, *Mathematical Problems of the Quantum Theory of Scattering for a Three-Particle System* (Steklov Mathematical Institute, Leningrad, 1965), No. 69. [English transl.: H. M. Stationary Office (Harwell, 1964)].

³C. Lovelace, *Phys. Rev.* **135**, B1225 (1964).

⁴R. L. Omnès, *Phys. Rev.* **134**, B1358 (1964); R. L. Omnès and V. A. Alessandrini, *Phys. Rev.* **136**, B1137 (1964); V. A. Alessandrini and R. L. Omnès, *Phys. Rev.* **137**, B681 (1965); **139**, B167 (1965).

⁵R. Aaron, R. D. Amado and Y. Y. Yam, *Phys. Rev.* **140**, B1291 (1965).

⁶M. Bander, *Phys. Rev.* **138**, B322 (1965).

⁷J. L. Basdevant, *Phys. Rev.* **138**, B892 (1965).

⁸A. Ahmadzadeh and J. A. Tjon, *Phys. Rev.* **139**, B1085 (1965).

⁹R. E. Kreps and P. Nath, *Phys. Rev.* **152**, 1475 (1966).

¹⁰D. Y. Wong and G. Zambotti, *Phys. Rev.* **154**, 1050 (1967).

¹¹T. A. Osborn, private communication.

¹²J. S. Ball and D. Y. Wong, to be published.

¹³J. R. Fulco and D. Y. Wong, to be published.

¹⁴J. S. Ball, J. C. Y. Chen, and D. Y. Wong, in

Proceedings of the Fifth International Conference on the Physics of Electronic and Atomic Collisions (Nauka, Leningrad, 1967), p. 20.

¹⁵The same results for the partial wave reduction are also obtained by T. Osborn and H. P. Noyes, *Phys. Rev. Letters* **17**, 215 (1966).

¹⁶H. A. Bethe and E. E. Salpeter, *Quantum Mechanics of One- and Two-Electron Atoms* (Academic Press Inc., New York, 1957).

¹⁷Bateman Manuscript Project - *Higher Transcendental Functions* edited by A. Erdélyi et al.; (McGraw-Hill Book Co., Inc., New York, 1953), Vol. I, p. 175.

¹⁸H. P. Noyes, *Phys. Rev. Letters* **15**, 538 (1965).

¹⁹K. L. Kowalski, *Phys. Rev. Letters* **15**, 798 (1965).

²⁰G. J. Schulz, *Phys. Rev. Letters* **13**, 583 (1964); H. Kleinpoppen and V. Raihle, *Phys. Rev. Letters* **18**, 24 (1965); J. W. McGowan, E. M. Clarke, and E. K. Curley, *Phys. Rev. Letters* **15**, 917 (1965); **17**, 66 (1966).

²¹J. W. McGowan, *Phys. Rev.* **156**, 165 (1967).

²²M. Gailitis and R. Damburg, *Proc. Phys. Soc. (London)* **82**, 192 (1963).

²³P. G. Burke, *Advan. Phys.* **14**, 521 (1965); M. H. Mittleman, *Phys. Rev.* **147**, 73 (1966).

²⁴P. G. Burke and H. M. Schey, *Phys. Rev.* **126**, 149 (1962).

²⁵P. G. Burke and A. J. Taylor, *Proc. Phys. Soc. (London)* **88**, 549 (1966).

²⁶T. F. O'Malley and S. Geltman, *Phys. Rev.* **137**, A1344 (1965); A. K. Bhatia, A. Temkin, and J. F. Perkins, *Phys. Rev.* **153**, 177 (1967).

²⁷E. Høloien and J. Midtdal, *J. Chem. Phys.* **45**, 2209 (1966).

²⁸J. C. Y. Chen, *Phys. Rev.* **156**, 150 (1967).

²⁹J. C. Y. Chen and M. Rotenberg, *Phys. Rev.* **166**, 7 (1968).

³⁰C. L. Pekeris, *Phys. Rev.* **112**, 1649 (1958); **115**, 1216 (1959).

³¹A. M. Veselova, *Phys. Letters* **11**, 594 (1967).

H(2p) EXCITATION RESONANCES IN (e-H) SYSTEM NEAR THRESHOLD*

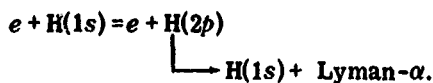
J. F. Williams† and J. William McGowan

Gulf General Atomic Incorporated, John Jay Hopkins Laboratory for Pure and Applied Science,
San Diego, California

(Received 5 August 1968)

High-resolution electron-impact measurements reveal that just above the threshold for excitation of the 2p level of atomic hydrogen there is a complicated resonance structure, part of which had not previously been predicted or observed.

In this note we discuss our recent measurements of the resonance structure found in the total cross section for the production of Lyman- α from the reaction



The observed structure is associated with the temporary formation of one or more H^- compound states in the (2s)², (2p)², or (2s, 2p) doubly excited configurations. These "potential" resonances are of the same configurations as the resonances previously studied in the elastic channel below the first inelastic threshold.¹

It has previously been observed, both theoretically²⁻⁴ and experimentally,⁵ that the excitation cross section does not follow what is normally considered Wigner's law. The most recent calculations have demonstrated that near threshold there is at least one resonance. However, a major point of this report will be to show that the resonance structure in the threshold region is more complicated than has been suggested thus far by theory. In the paper which follows, a par-

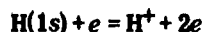
tial explanation of this observation is given by Marriott and Rotenberg.⁶ In a subsequent experimental paper, the details of our experimental technique, our total cross-section measurements, and our measurements of the resonances below and above the $n=3$ level will be discussed.

A modulated rectangular beam of H atoms (more than 85% pure) is crossed with a rectangular beam of electrons with an energy distribution (the width of the Gaussian energy distribution at half-maximum) of 0.07 eV. Electrons from a 127° electron-energy selector enter a magnetic and electric-field free region, cross the modulated H-atom beam from below, and then pass into a collector in which a crossed electric field can be applied to collect all the electrons in the beam. When this field is removed the electrons pass through the collector region into a second, rotatable, electrostatic energy analyzer which measures the energy and angular distribution of the electrons. Photons from the interaction of the electron and hydrogen atoms are detected at an angle of 54.5° with respect to the direction of the electrons. At this angle the observed signal

is proportional to the total $2p$ -excitation cross section.⁷

Ions from the interaction region are accelerated along the atomic-beam axis into a Paul mass filter. As in previous experiments^{1, 6} the linear extrapolation of the ionization efficiency curve to its energy axis is used as a calibration reference point for the electron energy scale. As has already been shown, this point is approximately 0.03 eV above the real ionization threshold.⁶

For each experimental run, data were collected automatically over a period which often exceeded 100 h. The instrument was programmed to step through a prescribed energy interval which in this experiment is usually 0.90 eV taken in 0.015-eV steps. The residence time for each energy step was normally 60 sec. The data were collected digitally, i.e., for each energy interval, the signal plus background, the background, and the electron current were recorded on punched tape to be processed later by the computer. Every 12 to 15 h the process was interrupted and an ionization efficiency curve for the collision



was taken to make sure that the electron energy scale for excitation remained constant. Through all of our experiments the ionization reference point remained constant to within ± 0.015 eV.

Because particular attention was to be focused upon the details of the structure which appeared in our excitation curves, it was necessary to make certain that none of the structure observed was due to radiation from the collisions of the electrons with H_2 molecules residual in our H-atom beam or with H_2 which formed part of the background gas. It has already been recognized⁷ that the oxygen gas filter which is normally placed in front of the Lyman- α detector, although transparent to Lyman- α , also passes some molecular radiation. However, it has now been verified by our experiments that the electron energy threshold for production of this molecular radiation is in the vicinity of 11.3 eV, well above the range of interest for this report. Consequently, such radiation cannot have affected our results.

In Fig. 1(a), we give a comparison of our data with the earlier low-resolution experimental results of Chamberlain, Smith, and Heddle⁵ and with two calculations on this system, both by Taylor and Burke.⁴ In Fig. 1(b), the results of Taylor and Burke are shown as modified by folding into their correlation calculation our experimental electron energy distribution. The experi-

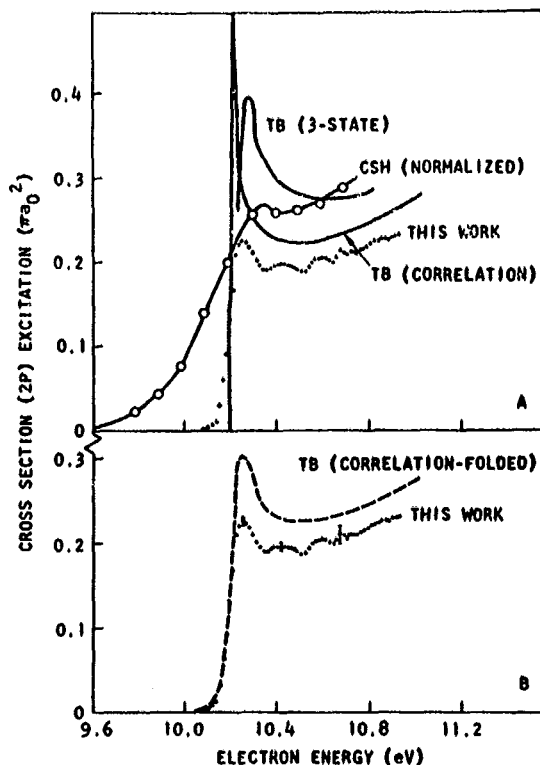


FIG. 1. (a) Our data for the excitation of $\text{H}(2p)$ (this work), together with earlier measurements by Chamberlain, Smith, and Heddle (CSH) of the Lyman- α excitation cross section (for radiation observed at 90° to the direction of the bombarding electrons). Also shown are two theoretical calculations: the three-stage close-coupling calculations of Taylor and Burke [TB (3 state)] and the three-state-plus-correlation calculation of Taylor and Burke [TB (correlation)]. (b) Comparison of our data with the calculated cross section of Taylor and Burke into which has been folded our experimental energy distribution 0.07 eV.

mental data reported here have been normalized to the Born approximation at high energies by a procedure to be discussed in detail in a later paper.⁹ The results of Chamberlain, Smith, and Heddle are also normalized to theory near threshold in the manner given by Burke, Taylor, and Ormonde.⁴

The sharp rise in the excitation cross section at threshold has been predicted by Damburg and Gailitis⁸ from a close-coupling approximation calculation which includes the lowest three states of the H atom, i.e., the $1s$, $2s$, and $2p$ states. Subsequent three-state close-coupling calculations by Taylor and Burke,³ shown as TB (3-state) in Fig. 1(a), have used a finer energy grid to show that within 0.03 eV of the threshold, there is a sharp resonance in the 1P channel of

the temporary H^- doubly excited compound state. A modified calculation, in which the interaction potential contains an additional term to describe the electron-electron interaction (correlation), shown as TB (correlation) in Fig. 1(a), lowers the total cross-section value, shifts the position of the resonance closer to threshold, and considerably reduces its width.

The results of Chamberlain, Smith, and Heddle using an electron beam with a resolution of 0.35 eV, and observing Lyman- α emitted at 90° to the direction of the electron beam, show that the cross section near threshold is finite as predicted. By assuming various shapes for the excitation cross section into which they folded their known electron-energy distribution, they were able to suggest that the cross section near threshold contained a peak. Subsequently, Burke, Taylor, and Ormonde⁴ theoretically identified this peak and showed that their calculations were consistent with the measurements. With our measurements, which have been made with an electron-energy resolution of 0.07 eV, the predicted sharp onset at threshold and the 1P potential resonance near threshold are clearly defined. Now, however, our data reveal the presence of second and third maxima which have not previously been reported. This second maximum is statistically real, its height being approximately twice the rms error, while the third maximum is not yet statistically sound although its presence has been observed in all our data.

In Fig. 1(b) we show our data in comparison with the three-state close-coupling-plus-correlation calculation of Taylor and Burke³ into which we have folded our electron energy distribution. The agreement at threshold and over the first peak is good, thus giving credence to the calculated position of the resonance at 10.214 eV; however, the discrepancy in widths is large enough so that we suggest that the width of their resonance should be slightly in excess of the suggested 0.015 eV.¹⁰

What is the second peak which appears in our data? One possible explanation is that there is more than one potential resonance in the 1P channel. Another possible explanation, which is discussed in the following paper by Marriott and Rotenberg,⁶ is that the second peak is part of the first resonance and is not really a separate resonance at all.

One possible explanation for the conjectured third peak is that it, too, is part of a series of potential resonances. Another, and perhaps a more reasonable explanation, is that this is structure which appears in some channel other than the 1P .

It is with pleasure that we acknowledge the help of Professor E. M. Clarke who participated in the early stages of this work and of E. K. Curley who has continuously assisted our program.

*Work supported in part by the National Aeronautics and Space Administration under Contract No. NAS5-11025 and in part by Gulf General Atomic Private Research Funds.

†Gulf General Atomic Associate Scientist.

¹J. Wm. McGowan, E. M. Clarke, and E. K. Curley, *Phys. Rev. Letters* **15**, 917 (1965), and **17**, 66(E) (1966); J. Wm. McGowan, *Phys. Rev.* **156**, 165 (1967).

²R. Damburg and M. K. Gailitis, *Proc. Phys. Soc. (London)* **82**, 1068 (1963).

³A. J. Taylor and P. G. Burke, *Proc. Phys. Soc. (London)* **92**, 336 (1967).

⁴P. G. Burke, A. J. Taylor, and S. Ormonde, *Proc. Phys. Soc. (London)* **92**, 345 (1967).

⁵G. Chamberlain, S. Smith, and D. W. D. Heddle, *Phys. Rev. Letters* **12**, 647 (1964).

⁶R. Marriott and M. Rotenberg, following Letter [*Phys. Rev. Letters* **12**, 722 (1968)].

⁷W. L. Fite and R. T. Brackmann, *Phys. Rev.* **112**, 1151 (1958).

⁸J. Wm. McGowan and E. M. Clarke, *Phys. Rev.* **167**, 43 (1968).

⁹J. Wm. McGowan, J. F. Williams, and E. K. Curley, to be published.

¹⁰J. Macek and P. G. Burke, *Proc. Phys. Soc. (London)* **92**, 351 (1967).